Identification of Synthetic Lethal Gene Interactions with REV3 in Lung Cancer Cells

---

Dissertation

zur

Erlangung der naturwissenschaftlichen Doktorwürde (Dr.sc.nat.)

vorgelegt der

Mathematisch-naturwissenschaftlichen Fakultät

der

Universität Zürich

von

Ilya Kotov

aus

Russland

Promotionskomitee

Prof. Dr. Massimo Lopes (Vorsitz)

Prof. Dr. med. Rolf Stahel

Dr. Thomas Marti (Supervisor)

Prof. Dr. Jonathan Hall

Zürich, 2013

Table of Contents

1. Summary

Polymerase ζ (zeta) is the only known translesion synthesis polymerase, of which the knockout causes embryonic lethality in mice. This fact suggests that apart from its function in post-replication repair it plays a special, yet to be identified, role in mammalian development.

It is known that inhibition of REV3, the catalytic subunit of the translesion polymerase ζ, reduces the formation of resistance and increases the sensitivity of human cells to cisplatin. Surprisingly, recent findings of our laboratory revealed that inhibition of REV3 *per se* reduces cell growth of mesothelioma, lung- and breast cancer cells whereas normal cells are less affected.

The purpose of my PhD thesis was to identify genes whose inhibition will not only reduce but completely abolish cancer cell growth in a REV3-deficient background, i.e. to investigate synthetic lethal interactions with REV3 in human lung cancer cells. This was done to identify cancer-specific alterations that might be responsible for the observed differential REV3 *per se* effect. Additionally, the discovery of such genes could provide a rationale for a new combinational therapy. Finally, these results could also give us insights into the cellular function of REV3.

Using a whole-genome siRNA library we performed sets of global screens to identify targets whose inhibition preferentially affects viability of REV3-deficient A549 cells. The top confirmed hit was RRM1, the large subunit of ribonucleotide reductase (RNR), a critical enzyme of *de novo* nucleotide synthesis.

Treatment with the RNR-inhibitor hydroxyurea (HU) synergistically increased the fraction of REV3-deficient cells containing single stranded DNA (ssDNA) as indicated by increased staining of replication protein A (RPA). However, this increase was not accompanied by accumulation of the DNA damage marker γH2AX suggesting a role of REV3 in tolerance of replication stress (RS). Consistent with a role of REV3 in DNA replication, increased RPA staining was confined to S-phase cells. Additionally, we found genes related to RS to be significantly enriched among the top hits of the synthetic lethality screen further corroborating the importance of REV3 for replication under conditions of RS. These data outline a novel function of mammalian REV3 that could serve as a molecular basis of the observed REV3 cancer-specific *per se* effect as well as its indispensability during embryonic development.

2. Introduction

2.1. Translesion synthesis

Translesion DNA synthesis (TLS) is a specialized process of copying damaged DNA template that allows avoiding replication fork breakdown and subsequent chromosomal instability. This process doesn't repair the DNA damage but rather allows tolerating it, very often leading to occurrence of mutations. TLS is carried out by translesion polymerases that include 7 polymerases from four families – X, Y, A and B families [1]. X family of polymerases consists of three polymerases - DNA polymerase beta (Polβ, POLB), TLS polymerase lambda (Polλ, POLL) and TLS polymerase mu (Polμ, POLM). All four polymerases in the Y family are translesion polymerases including REV1 (REV1L), polymerase Eta (Polη, POLH), polymerase Iota (Polι, POLI) and polymerase Kappa (Polκ, POLK) [2]. Translesion polymerases of the A family are represented by polymerase theta (Polθ, POLQ) and polymerase nu (Polv, POLN). The only member of the B-family that is involved in TLS is polymerase zeta (Polζ), which consists of two subunits – catalytic subunit REV3 (REV3L) and structural subunit REV7 (MAD2L2, MAD2B). The choice of polymerases recruited for TLS is heavily dependent on the nature of DNA damage and is briefly discussed below [1].

Activation of DNA damage tolerance mechanisms is commonly thought to be mediated by PCNA modifications [3, 4]. Monoubiquitination of PCNA is carried out by RAD6-RAD18 complex and initiates TLS. The polymerases of Y-family can start the DNA damage bypass by binding to monoubiquitinated PCNA via ubiquitin-interacting domains such as the UBM, the UBZ and the PCNA interacting peptide box (PIP) [5, 6]. Alternatively, Fanconi anemia FA-ID complex [7-9] and Rad9-Rad1-Hus1 (9-1-1) complex can play a role in exchange of replicative polymerases by TLS polymerases [10].

In yeast RAD5/Ubc13/Mms2 can polyubiquitinate monoubiquitinated PCNA. PCNA polyubiquitination can trigger template switching and recombination-assisted error-free DNA damage bypass [11, 12]. Rad5 has two homologues in human, HLTF and SHPRH, both of which can polyubiqutinate PCNA *in vitro* [13, 14]. The potentially mutagenic switch to TLS appears to be controlled by deubiquitinating enzyme USP1 and the protein Elg1 (ATAD5) [15] [16, 17].

Although initially proposed to function in S-phase [18], the growing body of evidence supports a role of TLS polymerases in post-replicative repair (PRR) outside of S-phase. Thus, depletion of REV3 in mouse embryonic fibroblasts (MEFs) didn't affect replication-dependent TLS across UV-adducts, but completely abolished post-replicative repair of [6-4] photoproducts [19]. Additionally, expression of both subunits of polymerase zeta – REV3 and REV7 is the highest during G2/M phase suggesting a function of TLS in this cell cycle phase [20]. REV1 that interacts with several TLS polymerases appears to be important for bypass of blocking lesions during replication, while PCNA is required for the post-replicative gap filling in chicken DT40 cells, indicating differential role of REV1 and PCNA in replicative and post-replicative TLS.

TLS can be performed using one and two translesion polymerases. Some types of lesions can be bypassed by a single TLS polymerase. For example, UV-induced cis-syn cyclobutane pyrimidine dimers (CPDs) are bypassed by Polη in an error-free way *in vivo* [21]. Similarly, it was shown that several TLS polymerases are capable of replicating over abasic sites [22]. But for efficient TLS-mediated bypass of other lesions the so-called two-polymerase mechanism is employed. In this process, the first TLS polymerase inserts a nucleotide opposite the lesion and the second one efficiently extends from it. The choice of the first polymerase is dictated by the type of the DNA damage that has to be bypassed. Due to its unique ability to extend from the nucleotides inserted opposite the lesions, DNA Polζ very often functions as the second polymerase in the two polymerase mechanism and therefore plays a very important role in TLS across a wide variety of DNA lesions in mammalian cells [23]. Main types of DNA lesions and the polymerases that are known to be employed for their bypass are summarized in the Table 1.

Replication of undamaged template by TLS polymerases is error-prone with the error rate ranging from 10^{-1} to 10^{-3} [24]. For comparison the error rate of the conventional replicative polymerases from the A, B and C families is between 10^{-6} and 10^{-8} which is further decreased by accessory proteins like PCNA and RPA and mismatch repair (MMR) down to 10^{-8}-10^{-10} [25]. The low fidelity of TLS polymerases is the result of lacking exonuclease activity and a more open and less constrained catalytic site that allows accommodation of DNA lesions and unconventional base pairs [26]. Therefore, even in the absence of DNA damage, excessive activity of TLS polymerases leads to

mutagenesis and can lead to occurrence of cancer [27]. The same is true for the TLS bypassing of DNA lesions, which can be carried out in error-free manner *in vitro*, but results of *in vivo* experiments show that this process is very often the main source of mutability. This makes TLS, and especially REV3 as an essential member of it, highly relevant for tumorigenesis and cancer treatment [1].

REV3L was found to be overexpressed in human gliomas and its expression level was reversely correlated with their sensitivity to cisplatin [28]. Conversely, human REV3L gene is located at the chromosome 6q21 within the FRA6F CFS that was reported to be frequently deleted in human tumors [29]. Moreover, REV3 is less expressed in colon carcinomas compared to the normal adjacent tissues and was proposed to play a tumor-suppressor role [30].

Besides tumorigenesis, TLS synthesis is also associated with the outcome of cancer therapy including sensitivity to chemotherapeutic agents and occurrence of resistance. TLS allows bypass of various lesions that are formed as a result of DNA modification by chemotherapeutic drugs thus decreasing sensitivity of the tumor. For instance, REV3L suppression sensitized both chemosensitive lymphoma and chemoresistant non-small-cell lung cancer to cisplatin treatment [31]. On the other hand, TLS due to its error-prone, mutagenic nature facilitates acquirement of tumor chemoresistance [32] thereby deteriorating response to treatment. Taken together, these two arguments strongly support the rationale for complementing traditional chemotherapy with REV3 targeting.

DNA lesion	Insertion	Extension	Outcome
Apurinic/ apyrimidinic (AP) site	TLS Pol κ	TLS Pol κ	Mutagenic
	TLS Pol θ	TLS Pol θ	Mutagenic
	TLS Pol η	TLS Pol η	Mutagenic
	TLS Pol λ	TLS Pol λ	Unknown
	TLS Pol μ	Unknown	Mutagenic
	TLS Pol ι	Unknown	Mutagenic
	REV1	Unknown	Accurate
7, 8-dihydro-8-oxoguanine (8-oxo-G)	TLS Pol ι	TLS Pol ι	Mutagenic
	TLS Pol μ	N/A	Mutagenic
	TLS Pol λ	N/A	Accurate (+PCNA and RPA)
	TLS Pol η	N/A	Mutagenic (+PCNA and RPA)
Thymine glycol (Tg)	TLS Pol θ		Mutagenic
	TLS Pol ν	TLS Pol ν	Accurate (5S-Tg); Mutagenic (5R-Tg)
	TLS Pol λ	TLS Pol λ	Mutagenic
	TLS Pol κ	TLS Pol ζ	Accurate
(6-4) photoproduct	TLS Pol ι	TLS Pol θ	Mutagenic
	TLS Pol ι	Unknown	Mutagenic
	TLS Pol η	Unknown	Mutagenic
	TLS Pol μ	Unknown	Accurate
	Unknown	TLS Pol ζ	Accurate
Cyclobutane pyrimidine dimer (CPD)	TLS Pol μ	TLS Pol μ	Mutagenic
	TLS Pol η	TLS Pol η	Accurate
	TLS Pol ι	TLS Pol ζ	Mutagenic
	TLS Pol κ	TLS Pol ζ	Mutagenic
	Unknown	TLS Pol ζ	Mutagenic
Benzo[α]pyrene-guanine (BP-G)	TLS Pol η	TLS Pol ζ	Accurate
	TLS Pol κ	TLS Pol ζ	Mutagenic
CDDP Intrastrand-crosslinks	Pol β	Pol β	Unknown
	TLS Pol η	TLS Pol η	Mutagenic
	TLS Pol κ	TLS Pol ζ	Mutagenic
	TLS Pol η	TLS Pol ζ	Accurate
CDDP Interstrand-crosslink (ICL)	Recombination independent ICL repair including NER, REV1 and TLS Pol ζ		Mutagenic
	Recombination dependent ICL repair including NER, REV1 and TLS Pol ζ		Mutagenic

Table 1.1. TLS opposite DNA lesions by mammalian one and two-polymerase mechanism. Reproduced from [1]

2.2. Synthetic lethality

The idea about existence of synthetic lethal gene interaction originated in the field of Drosophila genetics and is almost a century old [33], However, the precise term “synthetic lethal” was introduced only two decades later [34]. Synthetic lethality is a type of genetic interaction where the co-occurrence of two genetic events results in organismal or cellular death [35, 36]. In other words, two genes are synthetic lethal when the single mutants are viable but simultaneous disruption of both genes results in killing of the cell. Similarly, when the double gene knockout doesn’t cause cell death but impairs cellular fitness the gene interaction is called synthetic sickness. Synthetic sickness is often considered together with the synthetic lethality under the common term synthetic sickness/lethality (SSL). This type of interaction can be viewed as a particular case of gene buffering. Within the course of evolution, living organisms developed several ways to perform the same function in order to maintain homeostasis in the face of diverse genetic and environmental challenges. This functional redundancy allows cells to tolerate disruption of certain genes making thereby SSL a feature of genetic robustness [36, 37].

Simplicity of gene knockdown in yeast allowed the genome-wide scale quantitative mapping of genetic interactions [38]. Resulting networks can be used for functional gene annotation, because the genes that are connected with SSL interaction, i.e. buffering each other, very often act in the same pathway and tend to cluster together in the network [35, 39]. SSL are significantly evolutionary conserved. Thus, the data of genetic interactions for two yeast species *S. cerevisiae* and *S. pombe* indicate that this organisms share approximately 30% of their genetic interactions [40, 41]. Although several studies found that as few as 1% of interactions are conserved between yeast and *C. elegans*, questioning the general conservation of synthetic lethality between evolutionary distant organisms [42, 43]. Similarly, the few studies that used yeast genetic interactions to predict interactions in mammalian cells suggest that conservation is rather limited [36, 44, 45]. This also implies the difficulty of direct transfer of the SSL interactions from model organisms to mammalian and human cells and supports the need of direct investigation of genetic interactions in these cells.

Discovery of RNA interference (RNAi) made it possible to perform efficient silencing of target genes in mammalian cells. Even though overexpression of genes can also result in SSL, wide spreading of loss-of-function genetic screens was facilitated by the rapid development of RNAi technology [36, 46]. Another advantage of loss-of-function screens is their ability to be translated to medical practice since the absolute majority (if not all) of the drugs used in the clinic are inhibitors of a certain function.

Cancer cells harbor multiple mutations in their genome, many of which affect DDR and lead to genomic instability but can be tolerated because of the redundant function of some of the DNA repair pathways [47]. Targeting the genes that carry out the function of the gene disturbed by a mutation is an attractive approach to cancer therapy [48]. The idea of using SSL for targeting tumors is based on the assumption that there are pathways, disruption of which by itself can be tolerated but become lethal when combined with cancer-specific mutations, i.e. a synthetic lethal interaction [1,49].

Cancer cells are often adapted to oncogene overexpression/activation or tumor suppressor deletion/inactivation which makes them more vulnerable to some stimuli than normal cells. This phenomenon is often defined as oncogene addiction and denotes the genetic changes that are directly associated with oncogenic transformation. A major problem in tumor therapy is that most oncogenes and tumor suppressors are not druggable meaning that they are difficult to target by a small molecule. The new genetic network of cancer cells should also carry some changes not directly caused by the oncogene but occurred as a result of genetic rewiring. In contrast to oncogene addiction, these changes lead to so called non-oncogene addiction that represent promising approach to the cancer therapy [50].

Currently the biggest success of the synthetic lethality concept for cancer treatment is the SSL interaction between BRCA1/2 and PARP1. Upon PARP inhibition, spontaneous single-strand breaks are not repaired and subsequently result in collapsed replication forks, triggering HR-dependent repair as evidenced by gamma-H2AX and RAD51 foci formation. It was shown that BRCA2-deficient cells, as a result of their deficiency in HR, are strongly dependent on PARP1 function and therefore are sensitive to PARP inhibitors. BRCA1 and BRCA1 are often mutated in breast cancer making these tumors

ideal target of therapy with PARP-inhibitors [51, 52]. In a clinical trial, the PARP inhibitor olaparib had few of the adverse effects of conventional chemotherapy and demonstrated antitumor activity in cancers associated with the BRCA1 or BRCA2 mutation [53].

SSL interactions among DDR genes seem to be quite common. Thus, following the example of BRCA1/2 and PARP1, deficiencies in mismatch repair proteins were found to be SSL with DNA polymerases: MSH2 with DNA polymerase β (POLB) and MLH1 with polymerase γ (POLG). Both SSL resulted in the accumulation of 8-oxoG oxidative DNA lesions and appeared to be caused by formation of DNA breaks [54].

A recent study gives another example of synthetic lethality between the genes related to replication and repair. Silencing of DNA pol λ (POLL) induced replication fork stress and slowed down S phase progression in different human cancer cell lines. Moreover, the absence of DNA pol λ is specifically lethal in the cells with non-functional S-phase checkpoint suggesting a SSL interaction between pol λ and Chk1. Mechanistically, this synthetic lethal interaction indicates that DNA pol λ not only protects cells from oxidative DNA damage, but also functions in rescuing stalled replication forks [55].

Besides targeting DDR genes, an intriguing approach for selective killing of cancer cells based on SSL is to target common oncogenes. Lately there were several publications in which RNA interference technology was successfully used to identify vulnerabilities of cancers driven by RAS oncogene. One study found many processes involved in the buffering of RAS-induced transformation. Most notably, RAS mutant cells were hypersensitive to inhibition of polo-like kinase 1 (PLK1) [56]. In a similar effort, a screen in isogenic colorectal carcinoma cell line HCT116 identified the transcription factor SNAIL2 to be SSL with RAS [57]. Another two bigger screens determined SSL of RAS with STK33 [58] and TBK1 [59]. The latter kinase was known to activate NF-κB pathway, which in turn was shown to be essential for RAS transformed cells [60, 61]. Confirming the screen results, NF-κB signaling was required for progression of RAS-driven lung adenocarcinoma in a mouse model [62].

Oncogenes that are known to induce excessive RS, e.g. Myc and Cyclin E, are supposed to be SSL with the genes that allow the cell to cope with RS [63]. Examples of such genes are Chk1 and ATR that were demonstrated to be essential in tumors with

high levels of RS [64]. Since RS is a rather common phenomenon, genes with a SSL interaction with RS are considered a promising target for cancer therapy and identification of such gene interactions will be an interesting direction for future research.

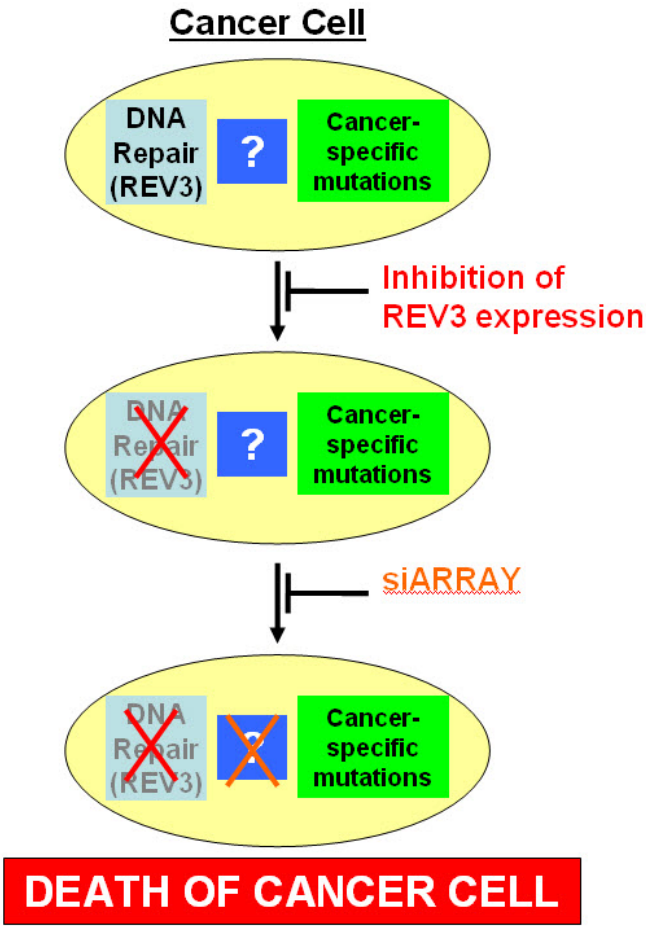

Figure 1.1. Concept of synthetic lethality applied to cancer cells deficient for DNA damage. Loss-off-function RNAi screen (siARRAY) can be used to identify SSL interactions with the targeted DDR gene (REV3).

2.3. Nucleotide synthesis

The ability to replicate itself is a fundamental property of the living cell. Cells require four deoxyribonucleotides to replicate and repair its DNA. As replication progresses, nucleotide pools have to be constantly replenished, i.e. nucleotides have to be synthesized from glucose and aminoacids. Deoxynucleotides synthesis can be divided in two main pathways: *de novo* and salvage synthesis. In the *de novo* pathway ribonucleotides are first synthesized from other metabolites that are subsequently reduced to deoxyribonucleotides (dNs). The last transformation is performed by the enzyme ribonucleotide reductase (RNR) and is thought to be limiting for the whole *de novo* synthesis pathway. During this process, the four ribonucleotides ADP, CDP, GDP and UDP are reduced to form their deoxy-counterparts three of which dADP, dCDP, dGDP after phosphorylation by nucleoside diphosphate kinase can be directly used for DNA synthesis. Another substrate of DNA replication, dTTP cannot be obtained in this way, but has to be synthesized from reduced forms of dCDP or dUTP, making dTTP synthesis also strongly dependent on the function of RNR. The central role of this enzyme in the *de novo* pathway allows fine regulation and balancing of the different nucleotide pools but at the same time requires tight control of its function. This is accomplished by many mechanisms such as regulation of mRNA expression, posttranslational modifications of the protein and allosteric regulation of its catalytic activity that will be described later in a more detail [65].

As an alternative to the *de novo* pathway, cells can obtain nucleotides by phosphorylation of nucleosides catalyzed by specialized kinases. Such transformation is often called salvage synthesis and the corresponding enzymes – salvage kinases, because activity of this pathway is not necessary for the survival of mammalian cells in culture. This pathway is intended to recycle the nucleosides obtained in the process of DNA degradation and nucleosides that enter the cell by a process of facilitated diffusion. The extracellular deoxyribonucleosides (dNs) originate from liver biosynthesis [66], degradation of DNA in apoptotic cells [67] and food digestion. Deoxycytidine kinase (dCK) and thymidine kinase 1 (TK1) are the salvage kinases that are rate limiting for the metabolic flux of the pathway. dCK phosphorylates dC to produce deoxycytidine monophosphate (dCMP), a precursor of dCTP and dTTP pools. Although with the lower

efficacy dCK can also phosphorylate dA and dG [68]. TK1 phosphorylates thymidine to produce dTMP that can be used for synthesis of dTTP required for DNA replication [67].

Even though the salvage pathway is not essential for the cell, it seems to play an important role in cancer and in certain tissues. Thus, it was shown that purine salvage enzyme activities were higher in human intestinal and breast carcinomas than compared to that of normal tissues [69].

Besides, this pathway is particularly important in hematopoietic tissue because it contributes both to induction and to prevention of replication stress (RS) during development. $dCK^{-/-}$ mice have severe developmental abnormalities affecting T cell, B cell and erythroid lineage [70]. TK1 knockout leads to slightly abnormal lymphoid structures and elevated levels of micronucleated erythrocytes [71]. Intriguingly, dCTP pool depletion, RS and hematopoietic defects induced by dCK inactivation are almost completely reversed by a concomitant TK1 knockout. In this case endogenous thymidine has a novel biological activity of RS inducer through TK1-mediated dCTP pool depletion [72].

The dominant role of RNR in regulation of dNTP pool sizes and composition has long been recognized [81]. The mammalian RNR consists of two homodimeric subunits, i.e. large subunit R1 and small subunit R2. The R1 subunit (RRM1, 90 kDa) carries the active site, whereas the small R2 protein (RRM2, 45 kDa) contains an iron center generating a tyrosyl free radical that is essential for catalysis [65, 73]. An additional mammalian RNR protein, p53R2, was identified in 2000 [73, 74]. Like the homologous R2 protein, p53R2 contains a tyrosyl free radical and forms an active RNR complex with R1 protein. The tyrosyl free radical of both the R2 and the p53R2 proteins is specifically destroyed by RNR inhibitor hydroxyurea [73, 75]. Expression of p53R2 is controlled by the tumor suppressor p53 and strongly increases after DNA damage allowing a moderate (less than two fold) expansion of nucleotide pools in G_0/G_1 cell phases, where the pools are about 5% that of the size of the pools in S-phase [73].

Reduction of NDPs by mammalian RNR is strongly regulated by nucleoside triphosphate allosteric effectors. There are three types of allosteric sites present on the large subunit – activity, substrate specificity and hexamerization sites. The activity site changes

overall activity of the enzyme by binding ATP or dATP (activity correspondingly increases and decreases). In addition to controlling activity, the allosteric mechanism also regulates the substrate specificity and ensures the enzyme produces an equal amount of each dNTP for DNA synthesis. Binding of ATP or dATP to the allosteric site induces reduction of CDP and UDP; dGTP induces reduction of ADP; and dTTP induces reduction of GDP[76]. Interestingly, upon allosteric regulation not only catalytic properties of the enzyme change but it also undergoes multistep oligomerization. According to a model, nucleotide binding to the specificity site (s-site) drives formation of an active $R1_2R2_2$ dimer, ATP or dATP binding to the adenine site (a-site) drives formation of a tetramer, $mR1_{4a}$, which isomerizes to an inactive form, $mR1_{4b}$, and ATP binding to the hexamerization site (h-site) drives formation of an active $R1_6R2_6$ hexamer [77, 78]. Later X-ray structural studies confirmed formation of the hexamer in the presence of physiological dATP concentrations [79]. Mutations affecting allosteric control sites lead to both unbalanced dNTP pools and increased mutation rates [76].

RNR activity varies greatly during the cell cycle. It is highest in S-phase contributing to nucleotide pool expansion in this cell phase and barely detectable in resting G_0 cells. The regulation is mainly mediated by targeting the small subunit of RNR. Whereas R1 levels remain relatively constant and high through the mammalian cell cycle, R2 fluctuates cyclically and is controlled by both protein synthesis and degradation [81]. The transcription of R2 is mainly regulated by the E2F transcription factor. As a number of other genes, R2 transcription is repressed by E2F in a cycle-specific manner. In the beginning of S-phase the repression is released by activating the region upstream of the R2 gene [80]. Upon exit from S-phase the R2 levels are reduced by selective protein degradation. In detail, cell cycle regulator Cdh1 is phosphorylated late in S phase leading to its release from anaphase-promoting complex (APC), a cell cycle dependent ubiquitin ligase. APC in turn recognizes a specific peptide sequence on the R2 protein leading to its ubiquitination and subsequent proteosomal degradation. The depletion of the R2 protein stops the nucleotide synthesis in G_2, but residual dNTP remain as shown in studies with synchronized cells [81]. Apart from RNR, APC also controls other nucleotide synthesis enzymes. Thymidylate kinase and thymidine kinase are recognized and targeted for degradation by APC during the transition from mitosis to the early G1

phase and after mitotic exit, respectively, showing that that down-regulation of dTTP pool size by the APC pathway during mitosis and the G1 phase is an essential means to maintain a balanced dNTP pool and to avoid genetic instability [82]. A recent publication uncovers another universal mechanism of RNR regulation by cyclin F. During G_2, following CDK-mediated phosphorylation of Thr33, RRM2 is degraded via cyclin F. After DNA damage, cyclin F is downregulated in an ATR-dependent manner to allow accumulation of RRM2 [83].

Because of the low levels of nucleotide pools outside of S phase of the cell cycle the importance of dNTP pool expansion after DNA damage has long been speculated and thought to be mediated by p53R2 [74]. Although, unlike in yeast where nucleotide pools raise by some 6- to 8-fold as a result of DNA-damaging events [84], mammalian cells don't respond to DNA damage induction with a major dNTP pool expansion suggesting existence of other mechanism supporting nucleotide supply to the sites of DNA damage. Indeed, compartmentalization of RNR was shown to play major role in this process and is dependent on a histone acetyl transferase Tip60. RRM1 was shown to physically interact and being recruited to sites of DNA damage by Tip60. Disruption of Tip60-RRM1 interaction leads to hypersensitivity to DNA damage which supports the role of Tip60 in nucleotide supplementation to the sites of DNA repair during G1 phase [85].

Nucleotide concentrations are critical for the fidelity of normal replication process. Increased or decreased nucleotide concentrations as well as nucleotide pool imbalances lead to increased replication error rate and mutagenesis. The likelihood of a mismatched nucleotide to force a replication error, whether through misinsertion or a next-nucleotide effect, was shown to be strongly dependent on the concentrations of correct and incorrect nucleotides [81, 86]. Asymmetry of dNTP pools are naturally occurring in most of the living organisms and therefore can be an important factor contributing to replication mutagenesis. For deoxynucleosides-triphosphate (dNTP), the concentrations in dividing mammalian cells are: dATP, 24 +/- 22 µM; dGTP, 5.2 +/- 4.5 µM; dCTP, 29 +/- 19 µM and dTTP 37 +/- 30 µM [87]. For synchronized S-phase HeLa cells this concentration are estimated to be: dATP 60 µM, dTTP 60 µM, dCTP 30 µM, dGTP 10 µM [88]. According to this data, dGTP seems to be always underrepresented in dNTP pools constituting only 6% of the total. *In vitro* replication experiments showed that

change from equimolar to *in vivo* dNTP concentrations didn't cause increase in replication error rate [89], suggesting that natural dNTP pool asymmetries are not strongly mutagenic [81]. In contrast, strong dNTP pool imbalances caused by different amino acid substitutions in yeast R1 increased substitution and insertion-deletion rates by 10- to 300-fold. But the locations of the mutations in the CAN1 gene in a strain with elevated dTTP and dCTP concentrations were completely different from those in a strain with elevated dATP and dCTP concentrations [90]. Therefore imbalanced dNTP pools reduce genome stability in a manner that is highly dependent on the nature and degree of the imbalance.

The increased mutagenesis due to increased concentrations of four dNTPs found in cell-free extracts [89] can be relevant for cancer cells because an elevated rate on nucleotide synthesis in tumors has long been recognized. Change of nucleotide metabolism by oncogenes has been best demonstrated for Myc and it was shown that nucleotide metabolic genes are enriched among c-Myc targets [91]. c-MYC depletion in melanoma cells resulted in the repression of several genes encoding enzymes rate-limiting for dNTP metabolism including thymidylate synthase (TS), inosine monophosphate dehydrogenase 2 (IMPDH2) and phosphoribosyl pyrophosphate synthetase 2 (PRPS2). This repression resulted in reduction in the amounts of deoxyribonucleoside triphosphates (dNTPs) and inhibition of proliferation. On the other hand, overexpression of C-MYC in normal melanocytes enhanced expression of the above enzymes and increased individual dNTP pools [92]. Similarly, up-regulation of RRM2 expression mediated by another oncogene KRAS is essential for the proliferation of colorectal cancer cell lines [93]. This phenomenon appear to be rather common in cancer cells, since a study including a large samples size found that concentrations of the 4 dNTPs in tumor cells are on average 6-11 fold over normal cells, and for the 4 NTPs, tumor cells also have concentrations 1.2-5 fold over the normal cells [87].

If an oncogene increases replication rate but doesn't activate the nucleotide synthesis to a sufficient extent this can cause RS and subsequent genomic instability. Thus, aberrant activation of Rb-E2F pathway by HPV-16 E6/E7 or cyclin E oncogenes significantly decreased the cellular concentrations of dNTPs. Exogenously supplied nucleosides rescued the RS and DNA damage and dramatically decreased oncogene-induced

transformation. And expression of c-myc increased transcription of nucleotide biosynthesis genes, alleviated nucleotide deficiency and also rescued the replication-induced DNA damage [94]. This study provides a model of oncogene-induced genomic instability in the early stages of cancer development.

A recent finding provides a link between nucleotide synthesis and oncogene-induced senescence. It shows that oncogene-induced repression of RRM2 leads to decreased dNTP concentrations and subsequent senescence-associated cell-cycle exit. Consistently, RRM2 downregulation is both necessary and sufficient for senescence [95]. It was shown that anchorage-independent growth of cells transformed with v-fms, v-src, A-raf, v-fes, c-myc, and ornithine decarboxylase was markedly enhanced when RRM2 was overexpressed. Therefore, RRM2 cooperates with a variety of activated oncogenes to support the transformation and its overexpression increases the malignant potential of cells [96, 97]. Altogether these data indicate that overexpression of RRM2 observed in many tumors can serve as a tool to overcome the barrier of oncogene-induced senescence in early tumorigenesis.

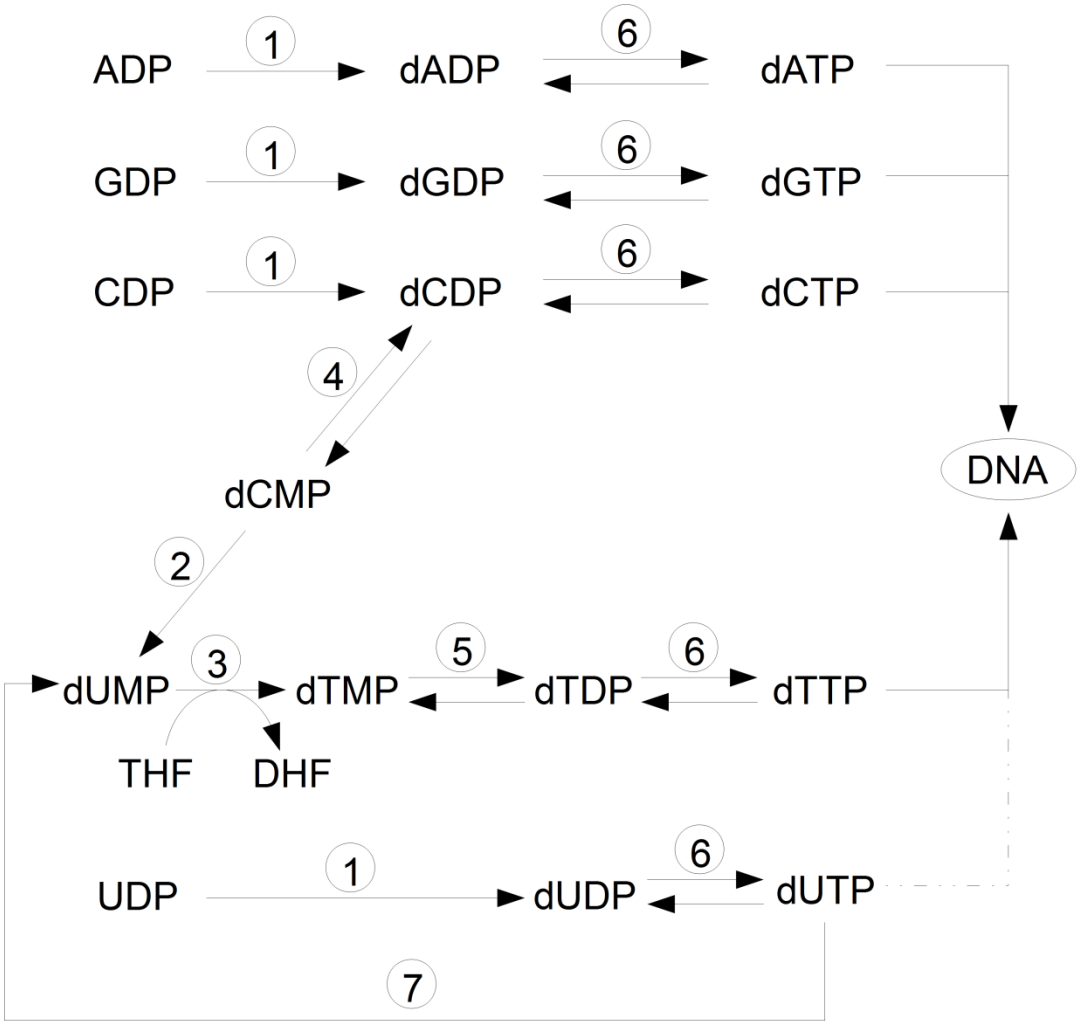

Figure 1.2. De novo pathway of deoxyribonucleotide synthesis. Allosterically regulated enzymes:(1) ribonucleotide reductase, (2) dCMP deaminase. Not regulated: (3) dTMP synthase, (4) (d)CMP kinase, (5) thymidylate kinase, (6) nucleoside diphosphate kinase, (7) dUTPase. Abbreviations used: THF, tetrahydrofolate; DHF, dihydrofolate. Adapted from [65].

2.4. Replication stress

DNA replication stress (RS) is defined as inefficient DNA replication that causes DNA replication forks to progress slowly or stall [98]. Even though not fully understood, RS and RS-induced DNA damage are thought to be caused by multiple factors. These include dNTP pools imbalances and altered frequency of origin initiation, DNA damage lesions that block replication fork and inhibition of DNA replication by drugs. Also the difficult-to-replicate regions are especially prone to RS due to their secondary structure, chromatin organization or their intrinsic topological complexity that makes them difficult to unwind. Some replication proteins bound to DNA are able to pause the replication thus causing RS [99].

There are many proteins that participate in stabilization and restart of stalled replication forks as well as restart of collapsed forks. Most of these proteins are known by their well-defined functions in homologous recombination (HR) repair and/or DNA damage checkpoint signaling. In this introduction I will only shortly introduce some major players of the RS response [100].

The cell response to RS is mainly orchestrated by ATR even though ATM seems to play a certain role. Thus, thymidine that induces RS by depleting cellular dCTP pools induces DNA damage response that depends on both ATM and ATR, ATM playing a role in HRR-mediated rescue of replication forks impaired by thymidine treatment [101].

Several types of DNA damage and replication interference such as DNA breaks, adducts, crosslinks and inhibition of DNA polymerases activate ATR-ATRIP kinase signaling [102]. It is widely accepted nowadays that ATR activation is triggered by single-stranded DNA (ssDNA), which is commonly formed during DNA replication and repair. When generated, ssDNA is immediately coated by replication protein A (RPA) complex. ATRIP is mediating ATR recruitment by binding RPA-ssDNA complex and allowing the ATRIP-ATR complex to be localized to the sites of DNA damage and stalled replication forks [102, 103].

RPA not only recruits ATR but is also a target of ATR-mediated phosphorylation. It was shown that RPA2 is phosphorylated by ATR primarily in the late S and G_2 phases. Cells carrying mutations in RPA2, a target of ATR-mediated phosphorylation, had low rate of

DNA synthesis and higher levels of ssDNA upon RS. After mitosis these cells also had a broader DNA distribution and were prone to apoptosis [104]. Apart from ATR-Chk1 pathway, DNA-dependent protein kinase (DNA-PK) appears to be indispensable for RS response signaling. DNA-PKcs mutant cells fail to arrest replication following stress, and mutations in RPA32 phosphorylation sites targeted by DNA-PK catalytic subunit increase the proportion of cells in mitosis, impair ATR signaling to Chk1 and confer a G_2/M arrest defect [105]. These data corroborate an important role of RPA phosphorylation by ATR and DNA-PK in response to RS.

In addition to ssDNA, double-stranded DNA (dsDNA) adjacent to ssDNA is required for ATR activation [106]. The two main regulators of ATR are the Rad17-RFC complex and the Rad9-Rad1-Hus1 (9-1-1) complex. Rad17-RFC complex functions to recruit the clamp-shaped 9-1-1 complex onto DNA in the presence of ssDNA-dsDNA junctions [102, 107]. The recruitment of Rad17-RFC and 9-1-1 complexes is largely independent from recruitment of ATR-ATRIP by RPA-ssDNA [108]. In human cells, besides RPA, Rad17-RFC and 9-1-1, full activation of ATR also requires topoisomerase II binding protein 1 (TOPBP1). TOPBP1 functions in both the initiation of DNA replication and activation of the checkpoint, but how it is regulated upon DNA damage is not fully understood [102]. ATR phosphorylates RAD17, which recruits Claspin to be phosphorylated by ATR. Phosphorylated RAD17-Claspin (along with TIM and Tipin) promotes ATR phosphorylation/activation of Chk1 [100]. In yeast, expression of a mutant allele of MEC1 leads to destabilization of DNA polymerases at stalled forks [109]. These activation mechanisms constitute the intra-S checkpoint that is activated upon induction of RS [110].

Chk1 is a critical G2/M checkpoint protein transducing the signal upon induction of DNA strand breaks but is also required for normal proliferation [111, 122]. Chk1 appears to have two distinct functions in two phases of the unperturbed cell cycle: S phase and mitosis [122]. During unperturbed S phase, Chk1 controls the progress of DNA replication. Inhibition of Chk1 activity leads to increased replication-associated DNA strand breaks [112], impaired replication fork progression, and increased fork stalling [113, 114, 122]. An important function of the ATR–Chk1 pathway is also associated with common fragile sites (CFS) where several proteins involved in the Chk1 signaling,

including TOPBP1, BRCA1, CLASPIN and CHK1, are required for preventing fork collapse [102, 115].

Several studies in yeast support the critical role of ATR-Chk1 pathway in RS response and protection of replication forks at specific loci in the genome during unperturbed S phase [102]. Thus, Chk1 homologue Rad53 was shown to be indispensable for stabilization of stalled forks induced by nucleotide depletion [116]. In the absence of Rad53, Exo1 exonuclease is recruited to stalled forks counteracting reversed fork accumulation by generating ssDNA intermediates [117]. Consistently, deletion of Exo1 rescues the fork instability induced by RAD53 mutation [118]. The yeast ATR homolog Rad3 phosphorylates histone H2A during S phase at natural replication fork barriers, ribosomal DNA (rDNA) repeats and heterochromatin in centromeres and telomeres [102, 119]. Besides that, ATR-Chk1 signaling regulates licensing of replication origins, that are available in excess provided sufficient amount of Mcm2-7 complexes [120]. Thus, ATR and Chk1 suppress origin firing in response to replication blocks and during normal S phase by inhibiting the cyclin-dependent kinase Cdk2 [113, 121].

Chk1 knockout mice are not viable [111], but the essential function seems to be related to mitosis and not associated with DNA damage checkpoint and replication control. Unlike mice with a targeted Chk1 mutation of S345, S317 mutants are viable, but had deficient G2/M checkpoint activation, impaired efficient progression of DNA replication forks, and increased fork stalling [122]. S345 phosphorylation initiated at the centrosome during unperturbed mitosis is independent of codon 317 status and mechanistically distinct from the ordered and sequential phosphorylation of serine residues on Chk1 induced by DNA damage [122].

The physiological importance of ATR is highlighted by the fact that ATR knockout is lethal in mice [123, 124]. However, there is a hypomorphic mutation in humans that causes Seckel syndrome. Homozygous mutation introduces a splicing defect that reduces the abundance of ATR to almost undetectable, yet the remaining protein is sufficient for viability. Viable ATR-Seckel mice show high levels of RS during embryogenesis, which is reduced in postnatal life. In spite of this decrease, adult Seckel mice show accelerated aging, which is further aggravated in the absence of p53. This

study suggests that RS contributes to the onset of aging in postnatal life, and this is balanced by the replicative stress–limiting role of the checkpoint proteins ATR and p53 [125].

Mutations in many DNA repair and cell cycle associated genes cause age-related diseases. Werner syndrome, Cockayne syndrome, trichothiodystrophy, dyskeratosis congenital and ataxia-telangiectasia are examples of such diseases [126]. RS was suggested to play an important role in aging based on the premature aging phenotypes observed in eukaryotes harboring mutations in RecQ helicases [98]. Mutations in RecQ helicases WRN, BLM and RECQL4 all cause genome instability and the premature aging syndromes called Werner, Bloom Rothmund–Thomson syndromes respectively [127, 128]. Moreover, RS induced by reduced Mcm2 expression results in severe stem/progenitor cell deficiency, premature aging and cancer [129]. Since premature aging phenotype can be a result of stem and progenitor cells attrition, it was speculated that stem cells might be particularly vulnerable to RS [130].

Homologous recombination (HR) pathway plays a major role in restarting stalled and collapsed forks and therefore is essential for RS tolerance [100, 131]. Apart from the core HR proteins (RAD51, RAD54, BRCA1/2, BLM), PARP-1 mediated recruitment of MRN complex (MRE11, RAD50 and NBS1) appears to be important for RS-induced HR [132]. Interestingly, PARP activity is also required for effective fork reversal that limits DSB formation upon RS induced by the topoisomerase I poison camptothecin [133].

At stalled forks, HR carries our template switching of a blocked replicating strand to the undamaged sister chromatid where DNA synthesis and a second template switch result in the bypass of the blocking lesion. At collapsed forks, when the one-ended double stranded break is formed, process called break-induced repair (BIR) takes place. In BIR, HR mediates strand invasion of the 3’-end of when the one-ended double stranded break into sister chromatids that is used as a new template [100]. Apart from their role in the fork restart, recent studies identify repair-independent function of HR and Fanconi anemia proteins BRCA2, BRCA1 and FANCD2 in direct stabilization of stalled replication forks by protecting them from degradation by MRE11 [134, 135].

The growing body of evidence suggests that many oncogenes induce RS playing an important role in cancer development and progression. First, DNA damage response (DDR) markers such as phosphorylated kinases ATM and Chk2, and phosphorylated histone H2AX, p53 and 53bp foci were found in multiple tumor samples. This DDR appeared to be associated with oncogene-induced RS, to occur early stages in tumorigenesis and to represent an anti-cancer barrier [136, 137]. Further, oncogene-induced senescence was identified to be associated with signs of RS including prematurely terminated DNA replication forks and DNA double-strand breaks and could be suppressed by inhibiting the DNA double-strand break response kinase ataxia telangiectasia mutated (ATM) [138, 139].

The molecular basis of RS still remains largely under-investigated, although there are several reports addressing this issue. One study [94] found that transformation by HPV-16 E6/E7 or cyclin E oncogenes significantly slowed down replication fork progression but also decreased cellular nucleotide levels. Interestingly, exogenous supplementation of nucleosides rescued the RS and DNA damage induced by these oncogenes, suggesting that nucleotide deficiency represents an important factor contributing to oncogene-induced RS and genomic instability. In another study [140], Cyclin E overexpression caused increased firing of replication origins, impaired replication fork progression and DNA damage that activated RAD51-mediated recombination. Additionally, inhibition of transcription completely abolished induction of RAD51 foci by Cyclin E and reduced numbers of Cyclin E-induced 53BP1 foci indicating that interference between replication and transcription underlies the activation of HR upon oncogene-induced RS. A very recent study investigated structural basis of RS induced by Cyclin E and Cdc25A [141]. Overexpression of these oncogenes slowed down replication forks and induced fork reversal, but was not associated with chromosomal breakage or DDR activation unless arrested in G2/M or undergo premature mitotic entry.

The genomic instability of cancers is widely acknowledged [142] and RS is increasingly seen as one of the factors contributing to its development [143, 144]. Already in the early studies, it was hypothesized that genomic instability arising from DDR induced by RS can facilitate later transformation events such as loss of p53 [136, 137]. Later it was found that common fragile sites are preferentially targeted by oncogene-induced RS,

supporting the idea that RS is especially harmful for the regions that are intrinsically difficult for replication [145]. In these regions the forks stall and break more often than anywhere else in genome, potentially leading to highly mutagenic DSBs. Consistently with this hypothesis, RS was shown to induce γH2AX-positive micronuclei comprising of aggregated DSBs [146].

An established mediator of DSB repair 53bp1 was known to form distinct nuclear bodies in normally proliferating mammalian cells. A role of 53bp1 in shielding chromosomal fragile sites from RS-induced breakage was identified recently [147]. 53bp1 nuclear bodies represent therefore under-replicated chromosomal lesions that are transferred to the daughter cells through mitosis. 53bp1 was shown to protect DNA ends from excessive resection in G1, and thereby favors repair by nonhomologous end-joining (NHEJ) as opposed to homologous recombination (HR). But during S phase, BRCA1 antagonizes 53bp1 to promote HR [148]. Conversely, fragile site loci are often linked with BLM-associated DNA ultra-fine bridges even as cells traverse mitosis. These loci are often induced after partial inhibition of DNA replication, i.e. after RS, and are covered with by Fanconi anaemia proteins FANCD2 and FANCI [149], suggesting that sister-chromatid homology is used to facilitate replication of fragile sites. These data indicate that fragile sites cannot be replicated in time by conventional machinery and subsequently rescued either by HR or NHEJ.

Until recently there was no direct evidence that chromosomal instability can be directly caused by RS. But in 2011 a publication came out that investigated this issue and showed that sites of chromosome breakage correlate with replication fork locations. Moreover, ssDNA can be detected prior to chromosome breakage, suggesting that ssDNA accumulation is the common precursor to DSB at collapsed replication forks [150]. Following this line, it was demonstrated that DNA lesions induced by RS can trigger mitotic aberration, chromosomal missegregation and tetraploidy development [151]. The most recent study aimed to identify the genes suppressing chromosomal instability by searching for the DNA regions for which copy-number variation negatively correlates to the ploidy of the tumors. It found three genes on chromosome 18q, silencing of which lead to RS, chromosome abnormalities and chromosome missegregation [152].

Frequently induced in tumors, RS is increasingly considered as an attractive target for cancer therapy. It was proposed that ATR and Chk1 inhibitors can be employed for selective killing of tumors with high levels of RS [63]. There were several studies investigating this possibility. Thus, it was demonstrated that the reduced level of ATR expression in the mice carrying ATR-Seckel mutation completely prevented the development of Myc-induced pancreatic tumors and lymphomas, both of which have high levels of RS. Moreover, Chk1 inhibitors were highly efficient in killing Myc-driven lymphomas, but not pancreatic adenocarcinomas initiated by K-Ras mutation showing no detectable evidence of RS response [64]. Similarly, ATR inhibition was particularly toxic for the cells overexpressing cyclin E [153]. Investigation of sensitivity of melanoma cell lines to Chk1 inhibition revealed that it was correlated to the level of endogenous DNA damage indicating level of RS [154]. These data support the model of the dual role of ATR-Chk1 signaling in the cancer progression: suppressive in the early lesions and necessary for the survival of full malignancies with the high levels of RS [155].

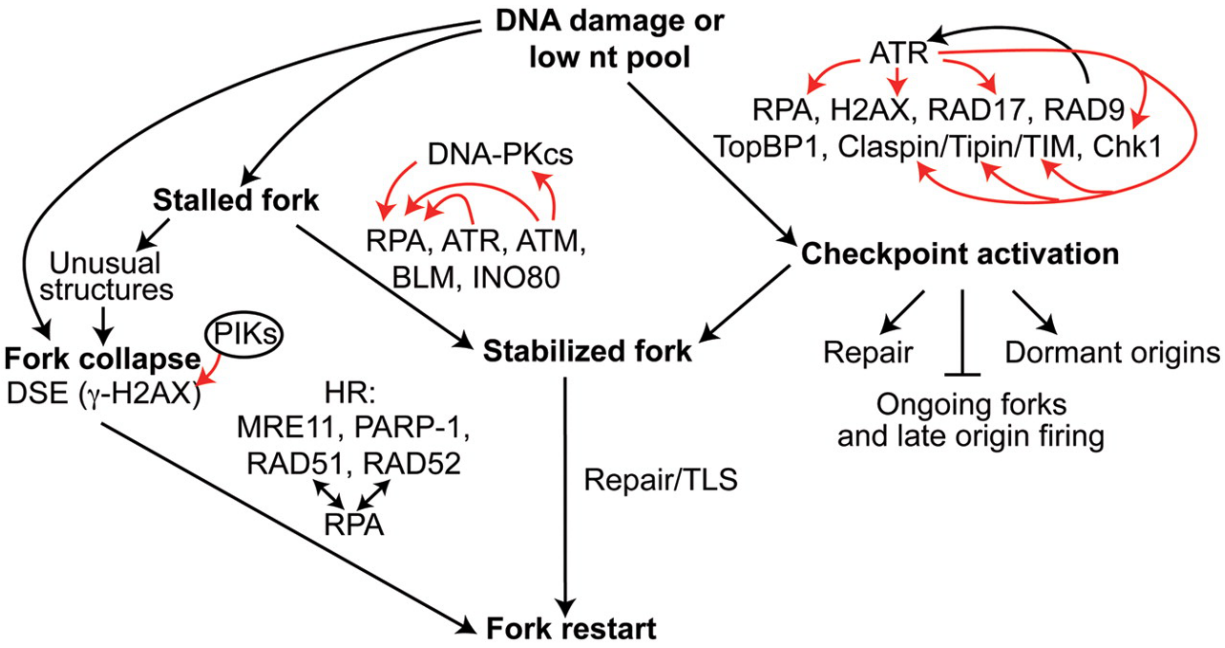

Figure 1.3. Key proteins and pathways in the replication stress response network. Black arrows/bars indicate activation/suppression pathways or interactions between proteins; red arrows indicate some of the known phosphorylation events by indicated kinases. Note that several proteins, such as RPA and ATR, have roles in more than one pathway in this network. Adapted from [100].

2.5 References

1. Knobel, P.A. and T.M. Marti, *Translesion DNA synthesis in the context of cancer research.* Cancer Cell Int, 2011. **11**: p. 39.
2. Ohmori, H., et al., *The Y-family of DNA polymerases.* Mol Cell, 2001. **8**(1): p. 7-8.
3. Kannouche, P.L., J. Wing, and A.R. Lehmann, *Interaction of human DNA polymerase eta with monoubiquitinated PCNA: a possible mechanism for the polymerase switch in response to DNA damage.* Mol Cell, 2004. **14**(4): p. 491-500.
4. Watanabe, K., et al., *Rad18 guides poleta to replication stalling sites through physical interaction and PCNA monoubiquitination.* EMBO J, 2004. **23**(19): p. 3886-96.
5. Bienko, M., et al., *Ubiquitin-binding domains in Y-family polymerases regulate translesion synthesis.* Science, 2005. **310**(5755): p. 1821-4.
6. Guo, C., et al., *Ubiquitin-binding motifs in REV1 protein are required for its role in the tolerance of DNA damage.* Mol Cell Biol, 2006. **26**(23): p. 8892-900.
7. Wang, W., *Emergence of a DNA-damage response network consisting of Fanconi anaemia and BRCA proteins.* Nat Rev Genet, 2007. **8**(10): p. 735-48.
8. Hicks, J.K., et al., *Differential roles for DNA polymerases eta, zeta, and REV1 in lesion bypass of intrastrand versus interstrand DNA cross-links.* Mol Cell Biol, 2010. **30**(5): p. 1217-30.
9. Mirchandani, K.D., R.M. McCaffrey, and A.D. D'Andrea, *The Fanconi anemia core complex is required for efficient point mutagenesis and Rev1 foci assembly.* DNA Repair (Amst), 2008. **7**(6): p. 902-11.
10. Sabbioneda, S., et al., *The 9-1-1 checkpoint clamp physically interacts with polzeta and is partially required for spontaneous polzeta-dependent mutagenesis in Saccharomyces cerevisiae.* J Biol Chem, 2005. **280**(46): p. 38657-65.
11. Andersen, P.L., F. Xu, and W. Xiao, *Eukaryotic DNA damage tolerance and translesion synthesis through covalent modifications of PCNA.* Cell Res, 2008. **18**(1): p. 162-73.
12. Chang, D.J. and K.A. Cimprich, *DNA damage tolerance: when it's OK to make mistakes.* Nat Chem Biol, 2009. **5**(2): p. 82-90.
13. Unk, I., et al., *Human SHPRH is a ubiquitin ligase for Mms2-Ubc13-dependent polyubiquitylation of proliferating cell nuclear antigen.* Proc Natl Acad Sci U S A, 2006. **103**(48): p. 18107-12.
14. Unk, I., et al., *Human HLTF functions as a ubiquitin ligase for proliferating cell nuclear antigen polyubiquitination.* Proc Natl Acad Sci U S A, 2008. **105**(10): p. 3768-73.
15. Lee, K.Y., et al., *Human ELG1 regulates the level of ubiquitinated proliferating cell nuclear antigen (PCNA) through Its interactions with PCNA and USP1.* J Biol Chem, 2010. **285**(14): p. 10362-9.
16. Ulrich, H.D., *Deubiquitinating PCNA: a downside to DNA damage tolerance.* Nat Cell Biol, 2006. **8**(4): p. 303-5.
17. Huang, T.T., et al., *Regulation of monoubiquitinated PCNA by DUB autocleavage.* Nat Cell Biol, 2006. **8**(4): p. 339-47.
18. Friedberg, E.C., A.R. Lehmann, and R.P. Fuchs, *Trading places: how do DNA polymerases switch during translesion DNA synthesis?* Mol Cell, 2005. **18**(5): p. 499-505.

19. Jansen, J.G., et al., *Mammalian polymerase zeta is essential for post-replication repair of UV-induced DNA lesions.* DNA Repair (Amst), 2009. **8**(12): p. 1444-51.
20. Bhat, A., et al., *Rev3, the catalytic subunit of Polzeta, is required for maintaining fragile site stability in human cells.* Nucleic Acids Res, 2013.
21. McCulloch, S.D., et al., *Preferential cis-syn thymine dimer bypass by DNA polymerase eta occurs with biased fidelity.* Nature, 2004. **428**(6978): p. 97-100.
22. Choi, J.Y., et al., *Translesion synthesis across abasic lesions by human B-family and Y-family DNA polymerases alpha, delta, eta, iota, kappa, and REV1.* J Mol Biol, 2010. **404**(1): p. 34-44.
23. Shachar, S., et al., *Two-polymerase mechanisms dictate error-free and error-prone translesion DNA synthesis in mammals.* Embo J, 2009. **28**(4): p. 383-93.
24. Kunkel, T.A., *DNA replication fidelity.* J Biol Chem, 2004. **279**(17): p. 16895-8.
25. Fortune, J.M., et al., *RPA and PCNA suppress formation of large deletion errors by yeast DNA polymerase delta.* Nucleic Acids Res, 2006. **34**(16): p. 4335-41.
26. Boudsocq, F., et al., *Investigating the role of the little finger domain of Y-family DNA polymerases in low fidelity synthesis and translesion replication.* J Biol Chem, 2004. **279**(31): p. 32932-40.
27. Albertella, M.R., A. Lau, and M.J. O'Connor, *The overexpression of specialized DNA polymerases in cancer.* DNA Repair (Amst), 2005. **4**(5): p. 583-93.
28. Wang, H., et al., *REV3L confers chemoresistance to cisplatin in human gliomas: the potential of its RNAi for synergistic therapy.* Neuro Oncol, 2009. **11**(6): p. 790-802.
29. Morelli, C., et al., *Cloning and characterization of the common fragile site FRA6F harboring a replicative senescence gene and frequently deleted in human tumors.* Oncogene, 2002. **21**(47): p. 7266-76.
30. Brondello, J.M., et al., *Novel evidences for a tumor suppressor role of Rev3, the catalytic subunit of Pol zeta.* Oncogene, 2008. **27**(47): p. 6093-101.
31. Doles, J., et al., *Suppression of Rev3, the catalytic subunit of Pol{zeta}, sensitizes drug-resistant lung tumors to chemotherapy.* Proc Natl Acad Sci U S A, 2010. **107**(48): p. 20786-91.
32. Xie, K., et al., *Error-prone translesion synthesis mediates acquired chemoresistance.* Proc Natl Acad Sci U S A, 2010. **107**(48): p. 20792-7.
33. Bridges, C.B., *The Origin of Variations in Sexual and Sex-Limited Characters.* The American Naturalist, 1922. **56**(642): p. 51-63.
34. Dobzhansky, T., *Genetics of Natural Populations. Xiii. Recombination and Variability in Populations of Drosophila Pseudoobscura.* Genetics, 1946. **31**(3): p. 269-90.
35. Boone, C., H. Bussey, and B.J. Andrews, *Exploring genetic interactions and networks with yeast.* Nat Rev Genet, 2007. **8**(6): p. 437-49.
36. Nijman, S.M., *Synthetic lethality: general principles, utility and detection using genetic screens in human cells.* FEBS Lett, 2011. **585**(1): p. 1-6.
37. Hartman, J.L.t., B. Garvik, and L. Hartwell, *Principles for the buffering of genetic variation.* Science, 2001. **291**(5506): p. 1001-4.
38. Costanzo, M., et al., *The genetic landscape of a cell.* Science, 2010. **327**(5964): p. 425-31.
39. Fiedler, D., et al., *Functional organization of the S. cerevisiae phosphorylation network.* Cell, 2009. **136**(5): p. 952-63.

40. Roguev, A., et al., *Conservation and rewiring of functional modules revealed by an epistasis map in fission yeast.* Science, 2008. **322**(5900): p. 405-10.
41. Dixon, S.J., et al., *Significant conservation of synthetic lethal genetic interaction networks between distantly related eukaryotes.* Proc Natl Acad Sci U S A, 2008. **105**(43): p. 16653-8.
42. Tischler, J., B. Lehner, and A.G. Fraser, *Evolutionary plasticity of genetic interaction networks.* Nat Genet, 2008. **40**(4): p. 390-1.
43. Byrne, A.B., et al., *A global analysis of genetic interactions in Caenorhabditis elegans.* J Biol, 2007. **6**(3): p. 8.
44. Conde-Pueyo, N., et al., *Human synthetic lethal inference as potential anti-cancer target gene detection.* BMC Syst Biol, 2009. **3**: p. 116.
45. McLellan, J., et al., *Synthetic lethal genetic interactions that decrease somatic cell proliferation in Caenorhabditis elegans identify the alternative RFC CTF18 as a candidate cancer drug target.* Mol Biol Cell, 2009. **20**(24): p. 5306-13.
46. Mullenders, J. and R. Bernards, *Loss-of-function genetic screens as a tool to improve the diagnosis and treatment of cancer.* Oncogene, 2009. **28**(50): p. 4409-20.
47. Jackson, S.P. and J. Bartek, *The DNA-damage response in human biology and disease.* Nature, 2009. **461**(7267): p. 1071-8.
48. Hartwell, L.H., et al., *Integrating genetic approaches into the discovery of anticancer drugs.* Science, 1997. **278**(5340): p. 1064-8.
49. Kaelin, W.G., Jr., *The concept of synthetic lethality in the context of anticancer therapy.* Nat Rev Cancer, 2005. **5**(9): p. 689-98.
50. Luo, J., N.L. Solimini, and S.J. Elledge, *Principles of cancer therapy: oncogene and non-oncogene addiction.* Cell, 2009. **136**(5): p. 823-37.
51. Bryant, H.E., et al., *Specific killing of BRCA2-deficient tumours with inhibitors of poly(ADP-ribose) polymerase.* Nature, 2005. **434**(7035): p. 913-7.
52. Farmer, H., et al., *Targeting the DNA repair defect in BRCA mutant cells as a therapeutic strategy.* Nature, 2005. **434**(7035): p. 917-21.
53. Fong, P.C., et al., *Inhibition of poly(ADP-ribose) polymerase in tumors from BRCA mutation carriers.* N Engl J Med, 2009. **361**(2): p. 123-34.
54. Martin, S.A., et al., *DNA polymerases as potential therapeutic targets for cancers deficient in the DNA mismatch repair proteins MSH2 or MLH1.* Cancer Cell, 2010. **17**(3): p. 235-48.
55. Zucca, E., et al., *Silencing of human DNA polymerase lambda causes replication stress and is synthetically lethal with an impaired S phase checkpoint.* Nucleic Acids Res, 2013. **41**(1): p. 229-41.
56. Luo, J., et al., *A genome-wide RNAi screen identifies multiple synthetic lethal interactions with the Ras oncogene.* Cell, 2009. **137**(5): p. 835-48.
57. Wang, Y., et al., *Critical role for transcriptional repressor Snail2 in transformation by oncogenic RAS in colorectal carcinoma cells.* Oncogene, 2010. **29**(33): p. 4658-70.
58. Scholl, C., et al., *Synthetic lethal interaction between oncogenic KRAS dependency and STK33 suppression in human cancer cells.* Cell, 2009. **137**(5): p. 821-34.
59. Barbie, D.A., et al., *Systematic RNA interference reveals that oncogenic KRAS-driven cancers require TBK1.* Nature, 2009. **462**(7269): p. 108-12.

60. Mayo, M.W., et al., *Requirement of NF-kappaB activation to suppress p53-independent apoptosis induced by oncogenic Ras.* Science, 1997. **278**(5344): p. 1812-5.
61. Chien, Y., et al., *RalB GTPase-mediated activation of the IkappaB family kinase TBK1 couples innate immune signaling to tumor cell survival.* Cell, 2006. **127**(1): p. 157-70.
62. Meylan, E., et al., *Requirement for NF-kappaB signalling in a mouse model of lung adenocarcinoma.* Nature, 2009. **462**(7269): p. 104-7.
63. Toledo, L.I., M. Murga, and O. Fernandez-Capetillo, *Targeting ATR and Chk1 kinases for cancer treatment: a new model for new (and old) drugs.* Mol Oncol, 2011. **5**(4): p. 368-73.
64. Murga, M., et al., *Exploiting oncogene-induced replicative stress for the selective killing of Myc-driven tumors.* Nat Struct Mol Biol, 2011. **18**(12): p. 1331-5.
65. Reichard, P., *Interactions between deoxyribonucleotide and DNA synthesis.* Annu Rev Biochem, 1988. **57**: p. 349-74.
66. Fustin, J.M., et al., *Rhythmic nucleotide synthesis in the liver: temporal segregation of metabolites.* Cell Rep, 2012. **1**(4): p. 341-9.
67. Arner, E.S. and S. Eriksson, *Mammalian deoxyribonucleoside kinases.* Pharmacol Ther, 1995. **67**(2): p. 155-86.
68. Sabini, E., et al., *Structural basis for substrate promiscuity of dCK.* J Mol Biol, 2008. **378**(3): p. 607-21.
69. Camici, M., et al., *Purine salvage enzyme activities in normal and neoplastic human tissues.* Cancer Biochem Biophys, 1990. **11**(3): p. 201-9.
70. Toy, G., et al., *Requirement for deoxycytidine kinase in T and B lymphocyte development.* Proc Natl Acad Sci U S A, 2010. **107**(12): p. 5551-6.
71. Choi, O., et al., *A deficiency in nucleoside salvage impairs murine lymphocyte development, homeostasis, and survival.* J Immunol, 2012. **188**(8): p. 3920-7.
72. Austin, W.R., et al., *Nucleoside salvage pathway kinases regulate hematopoiesis by linking nucleotide metabolism with replication stress.* J Exp Med, 2012. **209**(12): p. 2215-28.
73. Hakansson, P., A. Hofer, and L. Thelander, *Regulation of mammalian ribonucleotide reduction and dNTP pools after DNA damage and in resting cells.* J Biol Chem, 2006. **281**(12): p. 7834-41.
74. Tanaka, H., et al., *A ribonucleotide reductase gene involved in a p53-dependent cell-cycle checkpoint for DNA damage.* Nature, 2000. **404**(6773): p. 42-9.
75. Guittet, O., et al., *Mammalian p53R2 protein forms an active ribonucleotide reductase in vitro with the R1 protein, which is expressed both in resting cells in response to DNA damage and in proliferating cells.* J Biol Chem, 2001. **276**(44): p. 40647-51.
76. Jordan, A. and P. Reichard, *Ribonucleotide reductases.* Annu Rev Biochem, 1998. **67**: p. 71-98.
77. Kashlan, O.B., et al., *A comprehensive model for the allosteric regulation of mammalian ribonucleotide reductase. Functional consequences of ATP- and dATP-induced oligomerization of the large subunit.* Biochemistry, 2002. **41**(2): p. 462-74.
78. Kashlan, O.B. and B.S. Cooperman, *Comprehensive model for allosteric regulation of mammalian ribonucleotide reductase: refinements and consequences.* Biochemistry, 2003. **42**(6): p. 1696-706.

79. Fairman, J.W., et al., *Structural basis for allosteric regulation of human ribonucleotide reductase by nucleotide-induced oligomerization.* Nat Struct Mol Biol, 2011. **18**(3): p. 316-22.
80. Chabes, A.L., S. Bjorklund, and L. Thelander, *S Phase-specific transcription of the mouse ribonucleotide reductase R2 gene requires both a proximal repressive E2F-binding site and an upstream promoter activating region.* J Biol Chem, 2004. **279**(11): p. 10796-807.
81. Mathews, C.K., *DNA precursor metabolism and genomic stability.* FASEB J, 2006. **20**(9): p. 1300-14.
82. Ke, P.Y., et al., *Control of dTTP pool size by anaphase promoting complex/cyclosome is essential for the maintenance of genetic stability.* Genes Dev, 2005. **19**(16): p. 1920-33.
83. D'Angiolella, V., et al., *Cyclin F-mediated degradation of ribonucleotide reductase M2 controls genome integrity and DNA repair.* Cell, 2012. **149**(5): p. 1023-34.
84. Chabes, A., et al., *Survival of DNA damage in yeast directly depends on increased dNTP levels allowed by relaxed feedback inhibition of ribonucleotide reductase.* Cell, 2003. **112**(3): p. 391-401.
85. Niida, H., et al., *Essential role of Tip60-dependent recruitment of ribonucleotide reductase at DNA damage sites in DNA repair during G1 phase.* Genes Dev, 2010. **24**(4): p. 333-8.
86. Kunz, B.A., et al., *International Commission for Protection Against Environmental Mutagens and Carcinogens. Deoxyribonucleoside triphosphate levels: a critical factor in the maintenance of genetic stability.* Mutat Res, 1994. **318**(1): p. 1-64.
87. Traut, T.W., *Physiological concentrations of purines and pyrimidines.* Mol Cell Biochem, 1994. **140**(1): p. 1-22.
88. Zhang, X. and C.K. Mathews, *Natural DNA precursor pool asymmetry and base sequence context as determinants of replication fidelity.* J Biol Chem, 1995. **270**(15): p. 8401-4.
89. Martomo, S.A. and C.K. Mathews, *Effects of biological DNA precursor pool asymmetry upon accuracy of DNA replication in vitro.* Mutat Res, 2002. **499**(2): p. 197-211.
90. Kumar, D., et al., *Mechanisms of mutagenesis in vivo due to imbalanced dNTP pools.* Nucleic Acids Res, 2011. **39**(4): p. 1360-71.
91. Liu, Y.C., et al., *Global regulation of nucleotide biosynthetic genes by c-Myc.* PLoS One, 2008. **3**(7): p. e2722.
92. Mannava, S., et al., *Direct role of nucleotide metabolism in C-MYC-dependent proliferation of melanoma cells.* Cell Cycle, 2008. **7**(15): p. 2392-400.
93. Yoshida, Y., et al., *KRAS-mediated up-regulation of RRM2 expression is essential for the proliferation of colorectal cancer cell lines.* Anticancer Res, 2011. **31**(7): p. 2535-9.
94. Bester, A.C., et al., *Nucleotide deficiency promotes genomic instability in early stages of cancer development.* Cell, 2011. **145**(3): p. 435-46.
95. Aird, K.M., et al., *Suppression of nucleotide metabolism underlies the establishment and maintenance of oncogene-induced senescence.* Cell Rep, 2013. **3**(4): p. 1252-65.
96. Fan, H., et al., *The mammalian ribonucleotide reductase R2 component cooperates with a variety of oncogenes in mechanisms of cellular transformation.* Cancer Res, 1998. **58**(8): p. 1650-3.

97. Fan, H., C. Villegas, and J.A. Wright, *Ribonucleotide reductase R2 component is a novel malignancy determinant that cooperates with activated oncogenes to determine transformation and malignant potential.* Proc Natl Acad Sci U S A, 1996. **93**(24): p. 14036-40.
98. Burhans, W.C. and M. Weinberger, *DNA replication stress, genome instability and aging.* Nucleic Acids Res, 2007. **35**(22): p. 7545-56.
99. Hyrien, O., *Mechanisms and consequences of replication fork arrest.* Biochimie, 2000. **82**(1): p. 5-17.
100. Allen, C., et al., *More forks on the road to replication stress recovery.* J Mol Cell Biol, 2011. **3**(1): p. 4-12.
101. Bolderson, E., et al., *ATM is required for the cellular response to thymidine induced replication fork stress.* Hum Mol Genet, 2004. **13**(23): p. 2937-45.
102. Flynn, R.L. and L. Zou, *ATR: a master conductor of cellular responses to DNA replication stress.* Trends Biochem Sci, 2011. **36**(3): p. 133-40.
103. Zou, L. and S.J. Elledge, *Sensing DNA damage through ATRIP recognition of RPA-ssDNA complexes.* Science, 2003. **300**(5625): p. 1542-8.
104. Vassin, V.M., et al., *Human RPA phosphorylation by ATR stimulates DNA synthesis and prevents ssDNA accumulation during DNA-replication stress.* J Cell Sci, 2009. **122**(Pt 22): p. 4070-80.
105. Liu, S., et al., *Distinct roles for DNA-PK, ATM and ATR in RPA phosphorylation and checkpoint activation in response to replication stress.* Nucleic Acids Res, 2012. **40**(21): p. 10780-94.
106. MacDougall, C.A., et al., *The structural determinants of checkpoint activation.* Genes Dev, 2007. **21**(8): p. 898-903.
107. Ellison, V. and B. Stillman, *Biochemical characterization of DNA damage checkpoint complexes: clamp loader and clamp complexes with specificity for 5' recessed DNA.* PLoS Biol, 2003. **1**(2): p. E33.
108. Zou, L., D. Cortez, and S.J. Elledge, *Regulation of ATR substrate selection by Rad17-dependent loading of Rad9 complexes onto chromatin.* Genes Dev, 2002. **16**(2): p. 198-208.
109. Cobb, J.A., et al., *Replisome instability, fork collapse, and gross chromosomal rearrangements arise synergistically from Mec1 kinase and RecQ helicase mutations.* Genes Dev, 2005. **19**(24): p. 3055-69.
110. Budzowska, M. and R. Kanaar, *Mechanisms of dealing with DNA damage-induced replication problems.* Cell Biochem Biophys, 2009. **53**(1): p. 17-31.
111. Liu, Q., et al., *Chk1 is an essential kinase that is regulated by Atr and required for the G(2)/M DNA damage checkpoint.* Genes Dev, 2000. **14**(12): p. 1448-59.
112. Syljuasen, R.G., et al., *Inhibition of human Chk1 causes increased initiation of DNA replication, phosphorylation of ATR targets, and DNA breakage.* Mol Cell Biol, 2005. **25**(9): p. 3553-62.
113. Maya-Mendoza, A., et al., *Chk1 regulates the density of active replication origins during the vertebrate S phase.* EMBO J, 2007. **26**(11): p. 2719-31.
114. Petermann, E., et al., *Chk1 requirement for high global rates of replication fork progression during normal vertebrate S phase.* Mol Cell Biol, 2006. **26**(8): p. 3319-26.
115. Arlt, M.F., et al., *Common fragile sites as targets for chromosome rearrangements.* DNA Repair (Amst), 2006. **5**(9-10): p. 1126-35.

116. Lopes, M., et al., *The DNA replication checkpoint response stabilizes stalled replication forks.* Nature, 2001. **412**(6846): p. 557-61.
117. Cotta-Ramusino, C., et al., *Exo1 processes stalled replication forks and counteracts fork reversal in checkpoint-defective cells.* Mol Cell, 2005. **17**(1): p. 153-9.
118. Segurado, M. and J.F. Diffley, *Separate roles for the DNA damage checkpoint protein kinases in stabilizing DNA replication forks.* Genes Dev, 2008. **22**(13): p. 1816-27.
119. Rozenzhak, S., et al., *Rad3 decorates critical chromosomal domains with gammaH2A to protect genome integrity during S-Phase in fission yeast.* PLoS Genet, 2010. **6**(7): p. e1001032.
120. Ge, X.Q., D.A. Jackson, and J.J. Blow, *Dormant origins licensed by excess Mcm2-7 are required for human cells to survive replicative stress.* Genes Dev, 2007. **21**(24): p. 3331-41.
121. Shechter, D., V. Costanzo, and J. Gautier, *ATR and ATM regulate the timing of DNA replication origin firing.* Nat Cell Biol, 2004. **6**(7): p. 648-55.
122. Wilsker, D., et al., *Essential function of Chk1 can be uncoupled from DNA damage checkpoint and replication control.* Proc Natl Acad Sci U S A, 2008. **105**(52): p. 20752-7.
123. Brown, E.J. and D. Baltimore, *Essential and dispensable roles of ATR in cell cycle arrest and genome maintenance.* Genes Dev, 2003. **17**(5): p. 615-28.
124. de Klein, A., et al., *Targeted disruption of the cell-cycle checkpoint gene ATR leads to early embryonic lethality in mice.* Curr Biol, 2000. **10**(8): p. 479-82.
125. Murga, M., et al., *A mouse model of ATR-Seckel shows embryonic replicative stress and accelerated aging.* Nat Genet, 2009. **41**(8): p. 891-8.
126. Kipling, D., et al., *What can progeroid syndromes tell us about human aging?* Science, 2004. **305**(5689): p. 1426-31.
127. Bachrati, C.Z. and I.D. Hickson, *RecQ helicases: suppressors of tumorigenesis and premature aging.* Biochem J, 2003. **374**(Pt 3): p. 577-606.
128. Larizza, L., I. Magnani, and G. Roversi, *Rothmund-Thomson syndrome and RECQL4 defect: splitting and lumping.* Cancer Lett, 2006. **232**(1): p. 107-20.
129. Pruitt, S.C., K.J. Bailey, and A. Freeland, *Reduced Mcm2 expression results in severe stem/progenitor cell deficiency and cancer.* Stem Cells, 2007. **25**(12): p. 3121-32.
130. Ruzankina, Y., A. Asare, and E.J. Brown, *Replicative stress, stem cells and aging.* Mech Ageing Dev, 2008. **129**(7-8): p. 460-6.
131. Sonoda, E., et al., *Rad51-deficient vertebrate cells accumulate chromosomal breaks prior to cell death.* EMBO J, 1998. **17**(2): p. 598-608.
132. Bryant, H.E., et al., *PARP is activated at stalled forks to mediate Mre11-dependent replication restart and recombination.* EMBO J, 2009. **28**(17): p. 2601-15.
133. Ray Chaudhuri, A., et al., *Topoisomerase I poisoning results in PARP-mediated replication fork reversal.* Nat Struct Mol Biol, 2012. **19**(4): p. 417-23.
134. Schlacher, K., et al., *Double-strand break repair-independent role for BRCA2 in blocking stalled replication fork degradation by MRE11.* Cell, 2011. **145**(4): p. 529-42.

135. Schlacher, K., H. Wu, and M. Jasin, *A distinct replication fork protection pathway connects Fanconi anemia tumor suppressors to RAD51-BRCA1/2.* Cancer Cell, 2012. **22**(1): p. 106-16.
136. Gorgoulis, V.G., et al., *Activation of the DNA damage checkpoint and genomic instability in human precancerous lesions.* Nature, 2005. **434**(7035): p. 907-13.
137. Bartkova, J., et al., *DNA damage response as a candidate anti-cancer barrier in early human tumorigenesis.* Nature, 2005. **434**(7035): p. 864-70.
138. Bartkova, J., et al., *Oncogene-induced senescence is part of the tumorigenesis barrier imposed by DNA damage checkpoints.* Nature, 2006. **444**(7119): p. 633-7.
139. Di Micco, R., et al., *Oncogene-induced senescence is a DNA damage response triggered by DNA hyper-replication.* Nature, 2006. **444**(7119): p. 638-42.
140. Jones, R.M., et al., *Increased replication initiation and conflicts with transcription underlie Cyclin E-induced replication stress.* Oncogene, 2012.
141. Neelsen, K.J., et al., *Oncogenes induce genotoxic stress by mitotic processing of unusual replication intermediates.* J Cell Biol, 2013. **200**(6): p. 699-708.
142. Hanahan, D. and R.A. Weinberg, *Hallmarks of cancer: the next generation.* Cell, 2011. **144**(5): p. 646-74.
143. Negrini, S., V.G. Gorgoulis, and T.D. Halazonetis, *Genomic instability--an evolving hallmark of cancer.* Nat Rev Mol Cell Biol, 2010. **11**(3): p. 220-8.
144. Halazonetis, T.D., V.G. Gorgoulis, and J. Bartek, *An oncogene-induced DNA damage model for cancer development.* Science, 2008. **319**(5868): p. 1352-5.
145. Tsantoulis, P.K., et al., *Oncogene-induced replication stress preferentially targets common fragile sites in preneoplastic lesions. A genome-wide study.* Oncogene, 2008. **27**(23): p. 3256-64.
146. Xu, B., et al., *Replication stress induces micronuclei comprising of aggregated DNA double-strand breaks.* PLoS One, 2011. **6**(4): p. e18618.
147. Lukas, C., et al., *53BP1 nuclear bodies form around DNA lesions generated by mitotic transmission of chromosomes under replication stress.* Nat Cell Biol, 2011. **13**(3): p. 243-53.
148. Callen, E., et al., *53BP1 Mediates Productive and Mutagenic DNA Repair through Distinct Phosphoprotein Interactions.* Cell, 2013. **153**(6): p. 1266-80.
149. Chan, K.L., et al., *Replication stress induces sister-chromatid bridging at fragile site loci in mitosis.* Nat Cell Biol, 2009. **11**(6): p. 753-60.
150. Feng, W., et al., *Replication stress-induced chromosome breakage is correlated with replication fork progression and is preceded by single-stranded DNA formation.* G3 (Bethesda), 2011. **1**(5): p. 327-35.
151. Ichijima, Y., et al., *DNA lesions induced by replication stress trigger mitotic aberration and tetraploidy development.* PLoS One, 2010. **5**(1): p. e8821.
152. Burrell, R.A., et al., *Replication stress links structural and numerical cancer chromosomal instability.* Nature, 2013. **494**(7438): p. 492-6.
153. Toledo, L.I., et al., *A cell-based screen identifies ATR inhibitors with synthetic lethal properties for cancer-associated mutations.* Nat Struct Mol Biol, 2011. **18**(6): p. 721-7.
154. Brooks, K., et al., *A potent Chk1 inhibitor is selectively cytotoxic in melanomas with high levels of replicative stress.* Oncogene, 2013. **32**(6): p. 788-96.
155. Bartek, J., M. Mistrik, and J. Bartkova, *Thresholds of replication stress signaling in cancer development and treatment.* Nat Struct Mol Biol, 2012. **19**(1): p. 5-7.

3. Inhibition of REV3 expression induces persistent DNA damage and growth arrest in cancer cells

3.1. Contribution statement

Statement of contribution to the paper “Inhibition of REV3 expression induces persistent DNA damage and growth arrest in cancer cells” by Knobel PA, Kotov IN, Felley-Bosco E, Stahel RA, Marti TM (Neoplasia, 2011 Oct;13(10):961-70).

My experimental contribution to the paper is limited to the data presented in the Table 1, i.e. the microscopic quantitation of senescence in cancer cells (untreated, shSCR and shREV3) performed using SA-β-galactosidase staining. I also participated in the discussion of the content and editing of the manuscript.

NEOPLASIA
www.neoplasia.com

Volume 13 Number 10 October 2011 pp. 961–970 961

Inhibition of *REV3* Expression Induces Persistent DNA Damage and Growth Arrest in Cancer Cells[1,2]

Philip A. Knobel, Ilya N. Kotov, Emanuela Felley-Bosco, Rolf A. Stahel and Thomas M. Marti

Laboratory of Molecular Oncology, Clinic and Polyclinic of Oncology, University Hospital Zurich, Zurich, Switzerland

Abstract

REV3 is the catalytic subunit of DNA translesion synthesis polymerase ζ. Inhibition of *REV3* expression increases the sensitivity of human cells to a variety of DNA-damaging agents and reduces the formation of resistant cells. Surprisingly, we found that short hairpin RNA–mediated depletion of *REV3 per se* suppresses colony formation of lung (A549, Calu-3), breast (MCF-7, MDA-MB-231), mesothelioma (IL45 and ZL55), and colon (HCT116 +/−p53) tumor cell lines, whereas control cell lines (AD293, LP9-hTERT) and the normal mesothelial primary culture (SDM104) are less affected. Inhibition of *REV3* expression in cancer cells leads to an accumulation of persistent DNA damage as indicated by an increase in phospho-ATM, 53BP1, and phospho-H2AX foci formation, subsequently leading to the activation of the ATM-dependent DNA damage response cascade. *REV3* depletion in p53-proficient cancer cell lines results in a G_1 arrest and induction of senescence as indicated by the accumulation of p21 and an increase in senescence-associated β-galactosidase activity. In contrast, inhibition of *REV3* expression in *p53*-deficient cells results in growth inhibition and a G_2/M arrest. A small fraction of the p53-deficient cancer cells can overcome the G_2/M arrest, which results in mitotic slippage and aneuploidy. Our findings reveal that *REV3* depletion *per se* suppresses growth of cancer cell lines from different origin, whereas control cell lines and a mesothelial primary culture were less affected. Thus, our findings indicate that depletion of REV3 not only can amend cisplatin-based cancer therapy but also can be applied for susceptible cancers as a potential monotherapy.

Neoplasia (2011) 13, 961–970

Introduction

Screening in *Saccharomyces cerevisiae* for mutants defective in UV-induced mutagenesis revealed the so-called reversionless phenotype (REV), which is characterized by a diminished frequency of mutations reverting a specific marker gene deficiency [1]. Two genes that confer this phenotype when absent are *Rev3* and *Rev7*, the catalytic and the structural subunits of the DNA translesion synthesis (TLS) polymerase ζ (Pol ζ), respectively [2,3]. The mammalian *REV3L* gene (hereafter *REV3*) encodes a ~350-kDa protein (REV3) consisting of a large C-terminal DNA polymerase subunit, which misses the characteristic proofreading activity present in other B-family DNA polymerases (reviewed in Waters et al. [4]). REV3 interacts through a specific binding domain with REV7, but no additional protein-protein interaction sites were identified. Deletion of *REV3* is embryonically lethal around midgestation [5–8], whereas overexpression of *REV3* leads to increased spontaneous mutation rates [9], confirming that *REV3* expression has to be tightly regulated to maintain genomic integrity. Conversely, one study found that *REV3* expression was downregulated in colon carcinomas compared with that in adjacent normal tissue [10], whereas another study found that *REV3* expression was elevated in human glioma tissues resected before therapy compared with that in normal brain tissues [11].

Abbreviations: TLS, DNA translesion synthesis; Pol ζ, DNA translesion synthesis polymerase ζ; *REV3*, the mammalian *REV3L* gene; MEF, mouse embryonic fibroblast; DDR, DNA damage response; DSBs, DNA double-strand breaks; ATM, ataxia-telangiectasia mutated; γH2AX, phosphorylated H2AX; P-Chk2, phosphorylated Chk2; AN, aneuploid nondividing; AD, aneuploid dividing

Address all correspondence to: Thomas M. Marti, PhD, Laboratory of Molecular Oncology, Clinic and Polyclinic of Oncology, University Hospital Zurich, Häldeliweg 4, CH-8044 Zurich, Switzerland. E-mail: thomas.marti@usz.ch

[1]This study was funded by support from the Cancer League Zurich and the Sassella Foundation to T.M.M. and from the Seroussi Foundation and the Foundation for Applied Cancer Research Zurich to R.A.S. The authors have declared that no competing interests exist.

[2]This article refers to supplementary materials, which are designated by Figures W1 to W6 and are available online at www.neoplasia.com.

Received 16 June 2011; Revised 23 August 2011; Accepted 26 August 2011

DOI 10.1593/neo.11828

Pol ζ belongs to the functional group of TLS DNA polymerases, which are characterized by a less-stringent active site and a lower processivity compared with the high-fidelity replicative DNA polymerases (reviewed in Waters et al. [4]). TLS polymerases contribute to the maintenance of the genomic integrity by allowing DNA replication to continue in the presence of DNA adducts, which otherwise could lead to DNA replication fork breakdown and subsequent gross chromosomal instability. Pol ζ is the major extender from mismatches formed when incorrect nucleotides are inserted opposite DNA adducts, thereby contributing to mutation formation on the nucleotide level. Recently, it was shown that REV3 is involved not only in DNA damage tolerance but also in DNA repair mechanisms, for example, interstrand cross-link repair [12–14], homologous recombination [15], and nonhomologous end-joining as indicated by the deficiency of *REV3*-deleted B cells in class switching of immunoglobulin genes [16].

The unique function of REV3 is highlighted by the fact that the *REV3* depletion increases sensitivity and decreases mutagenesis induced by UV light, cisplatin, and other mutagens in human and mouse fibroblasts [15,17,18]. In addition, depletion of *REV3* sensitizes mouse B-cell lymphomas and lung adenocarcinomas to cisplatin [19,20]. Although disruption of mouse *REV3* leads to embryonic lethality, it is possible to generate *REV3*-deleted mouse embryonic fibroblasts (MEFs) in a p53-deficient background [21]. Spontaneous chromosomal instability was observed in *REV3*-deleted MEFs and *REV3*-deleted cell lines [16,22,23].

DNA damage induction results in the activation of an evolutionarily conserved signal cascade known as DNA damage response (DDR) (reviewed in d'Adda di Fagagna [24]). Induction of DNA double-strand breaks (DSBs) results in recruitment and activation of ataxia-telangiectasia mutated (ATM). Activated ATM phosphorylates the histone variant H2AX at serine 139 (γH2AX) near DNA DSBs, subsequently leading to an accumulation of DDR proteins at DSBs, which can be visualized by immunofluorescence microscopy as distinct foci. Once ATM activation reaches a certain threshold, checkpoint kinase Chk2 is phosphorylated, resulting in the accumulation of p53, leading to the accumulation of the cyclin-dependent kinase inhibitor p21. Prolonged activation of p21 after DNA damage is associated with a terminal proliferation arrest, i.e., senescence.

While investigating how inhibition of *REV3* expression affects cisplatin-induced mutagenesis, we observed that depletion of *REV3 per se* reduces cancer cell growth, whereas growth of control cells is less affected. Suppression of *REV3* expression in cancer cells leads to the accumulation of persistent DNA damage independent of the p53 status. In p53-proficient cancer cells, inhibition of *REV3* expression results in the activation of the ATM-dependent DDR cascade, leading to senescence induction. In p53-deficient cancer cells, depletion of *REV3* results in a G_2/M arrest and increases the fraction of aneuploid cells. In contrast, inhibition of REV3 expression in control cell lines and a mesothelial primary culture neither reduces colony formation nor activates the DDR cascade.

Materials and Methods

Cell Lines and Culture

All cell lines used in this study were authenticated by DNA fingerprinting (Microsynth, Balgach, Switzerland). SDM104 was maintained as described previously [25]. All other cell lines were maintained in high-glucose Dulbecco modified Eagle medium (DMEM; Sigma-Aldrich, St Louis, MO) supplemented with 2 mM L-glutamine, 1 mM sodium pyruvate, 10% fetal calf serum, and 1% (wt/vol) penicillin/streptomycin. All cells were grown at 37°C in a humidified atmosphere containing 5% CO_2. Additional details can be found in Supplemental Materials and Methods.

Vector Production and Transduction

Replication-deficient lentiviral particles were produced, titrated, and used for transduction as described previously [26,27]. Additional details can be found in Supplemental Materials and Methods.

Plasmid Transfection

Cells were transfected using Lipofectamine 2000 (Invitrogen, Carlsbad, CA) according to the manufacturer's instructions with pSuperior.puro containing either scrambled control short hairpin RNA (shSCR) or three distinct short hairpin RNA (shRNA) sequences targeting the *REV3* messenger RNA (shREV3). Additional details can be found in Supplemental Materials and Methods.

Colony Formation Assay

Crystal violet staining was performed after colonies were visible by eye and, the number of colonies was determined by eye, applying the same threshold for colony size to all transduced cell lines. The number of colonies obtained by mock treatment was set to 100%.

Quantitative Real-time Polymerase Chain Reaction

RNA from samples was isolated using RNeasy Mini kit (Qiagen, Germantown, MD), and reverse transcription was performed on 300 ng of RNA (QuantiTect Reverse Transcription Protocol; Qiagen). The quantitative expression of *REV3* mRNA was measured by SYBR Green polymerase chain reaction (PCR) assay (PE Applied Biosystems, Foster City, CA) on a Prism 5700 detection system (SDS; PE Applied Biosystems). Additional details can be found in Supplemental Materials and Methods.

Immunofluorescence Microscopy

Immunofluorescence microscopy was essentially performed as described [28]. Details can be found in Supplemental Materials and Methods.

Flow Cytometry

Detection of bromodeoxyuridine (BrdU) incorporation in DNA-synthesizing cells was carried out using the anti-BrdU antibody (no. 555627; BD Biosciences, San Jose, CA) according to the manufacturer's instructions. Additional details can be found in Supplemental Materials and Methods.

Senescence-Associated β-Galactosidase Assay

The expression of senescence-associated (SA) β-galactosidase was determined by SA-β-galactosidase staining as described [29].

Western Analysis

Protein extracts (30 μg) were separated by 4% to 20% SDS-PAGE and transferred onto polyvinylidene fluoride membranes. Immunoblot analysis was performed as described [30]. Details can be found in Supplemental Materials and Methods.

Enzyme-Linked Immunosorbent Assay

Cells were washed three times with phosphate-buffered saline (PBS) and serum-free DMEM was added for 24 hours. Conditioned medium was filtered, and cell number was determined in every experiment by

hemocytometer. Enzyme-linked immunosorbent assay (ELISA) was performed using human interleukin 6 (IL-6) Quantikine ELISA Kit (no. D6050; R&D Systems, Minneapolis, MN). Data were normalized to the cell number and reported as fold difference compared with mock-treated control.

Statistical Analysis

P values were calculated using the two-tailed Student's *t* test; $*P < .05$ and $**P < .01$.

Results

Depletion of REV3 Per Se *Suppresses Colony Formation of Cancer Cells*

To study the effect of *REV3* depletion on cisplatin-induced mutagenesis, we established a lentiviral-based system, which allowed us to significantly inhibit *REV3* expression in all cell lines and the primary culture used in this study (Figure W1, *A* and *B*). Inhibition of *REV3* expression did not significantly reduce colony formation of the control cell line AD293 (99% remaining colonies compared with mock-treated control), the primary mesothelial culture SDM104 (81%), and the hTERT-immortalized derivative of the mesothelial primary culture LP9 (LP9-hTERT, 98%; Figures 1*A* and W2*A*). Surprisingly, *REV3* depletion *per se* significantly suppressed colony formation of the p53-proficient adenocarcinoma cell line A549 (30%), the p53-deficient adenocarcinoma cell line Calu-3 (57%), the p53-deficient breast cancer cell line MDA-MB-231 (47%), the p53-proficient breast cancer cell line MCF-7 (32%), the human mesothelioma cell line ZL55 (27%), and the rat mesothelioma cell line IL45 (4%) compared with the mock-treated control (Figures 1*A* and W2*A*).

In the isogenic p53-proficient and -deficient HCT116 colorectal carcinoma cell lines, there was no significant difference in the reduction of *REV3* expression levels after transduction with a multiplicity of infection (MOI) of 170, as used for the cell lines described previously, or an MOI of 800 (Figure W1*B*). However, only the high-titer transduction significantly suppressed colony formation of p53-proficient (49%) and -deficient HCT116 (54%) compared with the mock control (Figures 1*B* and W2*B*). *REV3* depletion by high-titer transduction did not significantly reduce colony formation of the control cell line AD293 (74%) compared with the mock control (Figures 1*B* and W2*B*).

Inhibition of *REV3* expression by transduction with three plasmids, one encoding the same small interfering RNA (siRNA) as the lentiviral-based particles plus two plasmids encoding siRNA targeting alternative sites of the *REV3* mRNA (named REV3-5 and REV3-6), significantly reduced colony formation in the mesothelioma cell line IL45, whereas the control cell line AD293 was not affected (Figure W3). Therefore, we conclude that the observed reduction in colony formation is due to the inhibition of *REV3* expression and not due to an unspecific off-target effect of the REV3-4 siRNA. Thus, *REV3* depletion *per se* significantly suppresses colony formation in cancer cell lines, whereas colony formation of control cell lines and a primary mesothelial culture is less affected.

Cancer Cells Accumulate Persistent DNA DSBs after REV3 *Depletion*

53BP1 and γH2AX foci formation is regarded as a maker for DSBs [28], and a recent study showed that their numbers were increased after persistent DNA damage induction [31]. Seven days after transduction, *REV3* depletion in A549 cells increased the

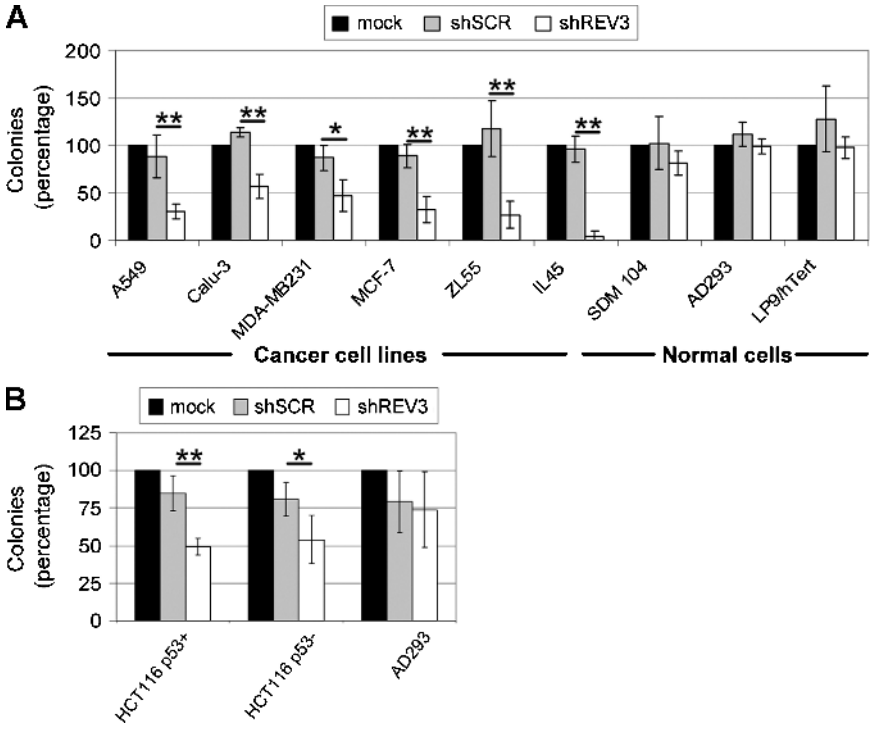

Figure 1. Inhibition of *REV3* expression specifically reduces colony formation of cancer cell lines. Cells were mock treated or transduced with lentiviral-based particles containing either shSCR or shREV3. (A and B) Cells were stained by crystal violet, and total colonies were counted after 2 to 4 weeks. Colonies were counted from at least three independent experiments for all cell lines. Colony numbers of mock-treated cells were set as 100%. $*P < .05$. $**P < .01$. Shown are means ± standard deviation (SD).

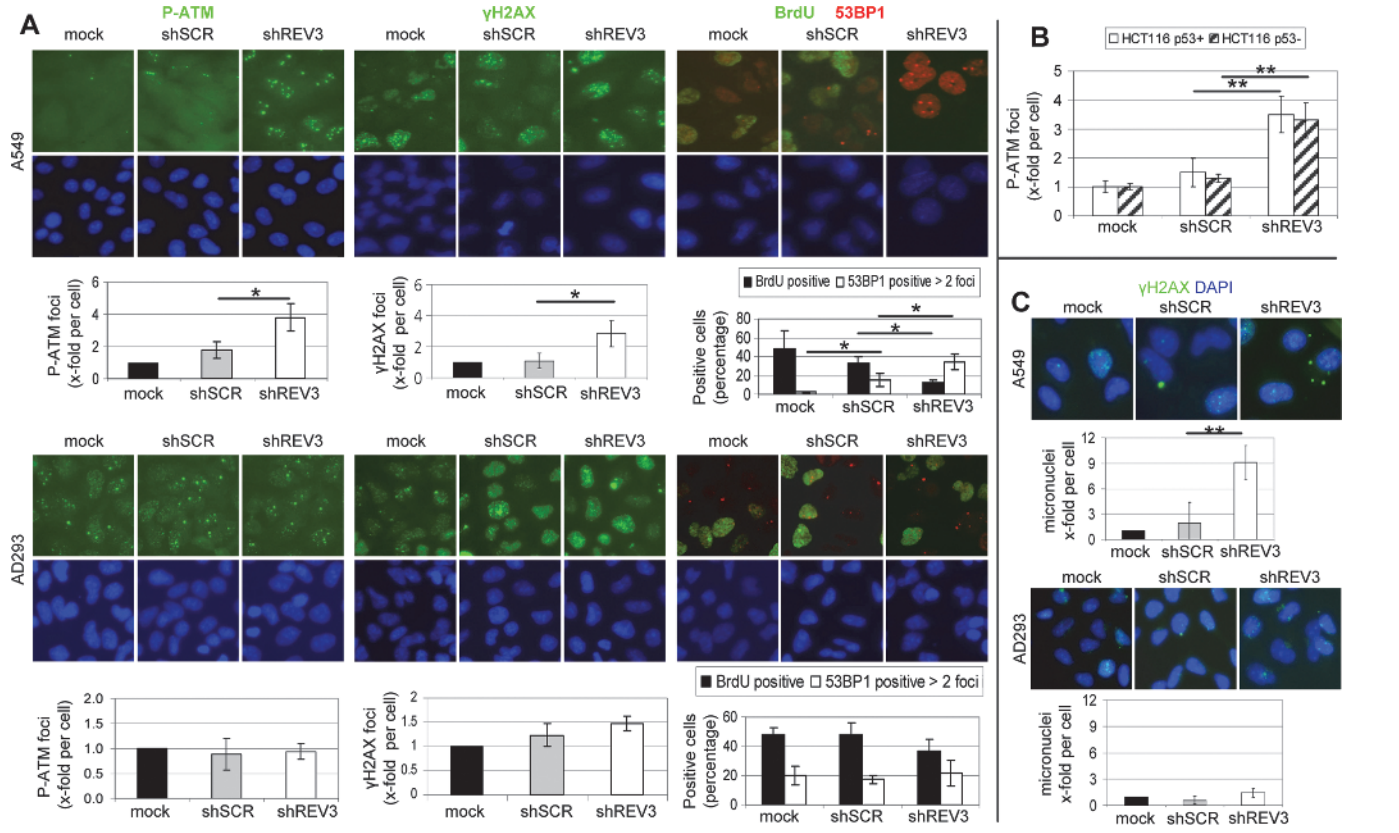

Figure 2. *REV3* depletion induces persistent DNA damage and genomic instability specifically in cancer cells. Cells were mock treated or transduced with lentiviral-based particles containing either shSCR or shREV3 and analyzed after 1 week. (A) Cells were stained for P-ATM, γH2AX, or BrdU (all green) and 53BP1 (red) and quantified by immunofluorescence microscopy. Cells containing more than two 53BP1 foci per cell were considered as 53BP1 positive. (B) Cells were stained for P-ATM, and foci per cell were quantified by immunofluorescence microscopy. (C) Cells were stained for γH2AX (green) and nuclear DNA was labeled with DAPI (blue). Micronuclei formation was identified by immunofluorescence microscopy–based analysis of DAPI staining. At least three independent experiments were analyzed. *$P < .05$. **$P < .01$. Shown are means ± SD.

average number of P-ATM and γH2AX foci per cell by a factor of 3.8 and 2.3, respectively, compared with the mock control (Figure 2*A*). Inhibition of *REV3* expression increased the fraction of A549 cells containing more than two 53BP1 foci to 34% compared with mock (2%) and scrambled (16%) control (Figure 2*A*). Similarly, *REV3* depletion in MCF-7 breast cancer cells increased the average number of γH2AX and 53BP1 foci per cell by a factor of 3.2 and 2.5, respectively, compared with the mock control (Figure W4). P-ATM foci formation was also elevated in both p53-proficient and -deficient HCT116 cells after *REV3* depletion by a factor of 2.3 and 2.5, respectively, compared with the scrambled control (Figure 2*B*). In contrast, inhibition of *REV3* expression in the control cell line AD293 did not significantly increase P-ATM, 53BP1, or γH2AX foci formation compared with the scrambled control (Figure 2*A*).

DSBs, which are not repaired either due to complex DNA modifications or to deficiencies in molecular mechanisms result in the formation of persistent DSBs (reviewed in d'Adda di Fagagna [24]). P-ATM foci at persistent DSBs are significantly larger than the initial foci detectable immediately after damage initiation [32]. Microscopic analysis revealed that the DDR foci induced in *REV3*-depleted cells 7 days after transduction were larger compared with the background DDR foci present in the mock controls (Figure 2*A*).

Gross chromosomal instability indicated by an elevated number of micronuclei were observed in MEFs with *REV3* deletion [21]. Similarly, the number of micronuclei increased in A549 cells by a factor of 9 after inhibition of *REV3* expression compared with the mock control (Figure 2*C*). Micronuclei formation was not significantly elevated after inhibition of *REV3* expression in AD293 cells (Figure 2*C*). Thus, inhibition of *REV3* expression induces the formation of persistent DSBs and accumulation of gross chromosomal instability in cancer cell lines, whereas the control cell line AD293 is significantly less affected ($P < .05$ for γH2AX, P-ATM, and 53BP1 foci and micronuclei per cell for both A549 and MCF-7 *vs* AD293; numbers of P-ATM foci per cell were not determined in MCF-7 cells). In addition, our results indicate that persistent DDR foci formation after *REV3* depletion is not dependent on the p53 status.

Inhibition of REV3 *Expression Suppresses Proliferation of Cancer Cells*

Because persistent DNA adducts block DNA replication and activate the DDR pathway, we investigated whether inhibition of *REV3* expression results in reduced cellular proliferation. Labeling of newly synthesized DNA with BrdU is an established method for the assessment of cellular proliferation (reviewed in Quinn and Wright [33]).

Quantitative analysis of BrdU incorporation revealed that cellular proliferation of A549 cells was reduced by *REV3* depletion to 21% compared with 37% and 38% in mock and scrambled controls, respectively (Figure 3, see also Figure 2*A*). Inhibition of *REV3* expression reduced the proliferation of p53-proficient HCT116 cells to 25% and that of p53-deficient HCT116 cells, to a lesser extent, to 33% compared with 41% and 45% in their corresponding scrambled controls, respectively (Figure 3). Similarly, *REV3* depletion also reduced the proliferation of MCF-7 breast cancer cells to 9.2% compared with 17% and 19% in mock and scrambled controls, respectively (Figure W4). In contrast, the percentage of replicating cells in the control cell line AD293 and the primary cell culture SDM104 was not diminished by the inhibition of *REV3* expression (Figure 3). Thus, *REV3* depletion suppresses cellular proliferation of the analyzed cancer cells, whereas proliferation of control cells is not affected.

REV3 *Depletion Activates the DNA Damage Response Pathway in Cancer Cells*

We investigated whether the observed accumulation of persistent DSBs in cancer cells results in the activation of the canonical ATM-kinase–mediated DDR pathway, which is induced by DSBs (reviewed in d'Adda di Fagagna [24]). As described here, the number of phospho-ATM foci per cell increased after the inhibition of *REV3* expression compared with mock and scrambled controls in A549 and p53-proficient and -deficient HCT116 cells, whereas no significant increase occurred in AD293 control cells (Figure 2, *A* and *B*). In A549 cells, *REV3* depletion resulted in increased phosphorylation of the checkpoint kinase Chk2 (P-Chk2) and the accumulation of p53 and the senescence mediator p21 (Figure 4*A*), which was also observed in MCF-7 breast cancer cells but not in the normal mesothelial primary culture SDM104 (Figure W5). In p53-proficient HCT116 cancer cells, inhibition of *REV3* expression also resulted in an accumulation of p21, which was absent in the p53-deficient isogenic cell line (Figure 4*A*). Thus, in the analyzed p53-proficient cancer cells, inhibition of *REV3* expression results in the activation of the canonical ATM-dependent DDR pathway.

REV3 *Depletion Induces a G_1 Arrest in p53-Proficient Cancer Cells*

We tested whether the activation of the DDR pathway and the reduction in BrdU incorporation due to *REV3* depletion change the cell cycle distribution of cancer cells. Depletion of the S phase after *REV3* depletion, as mentioned here, was accompanied by a significant increase in the fraction of A549 cells in the G_1 phase of the

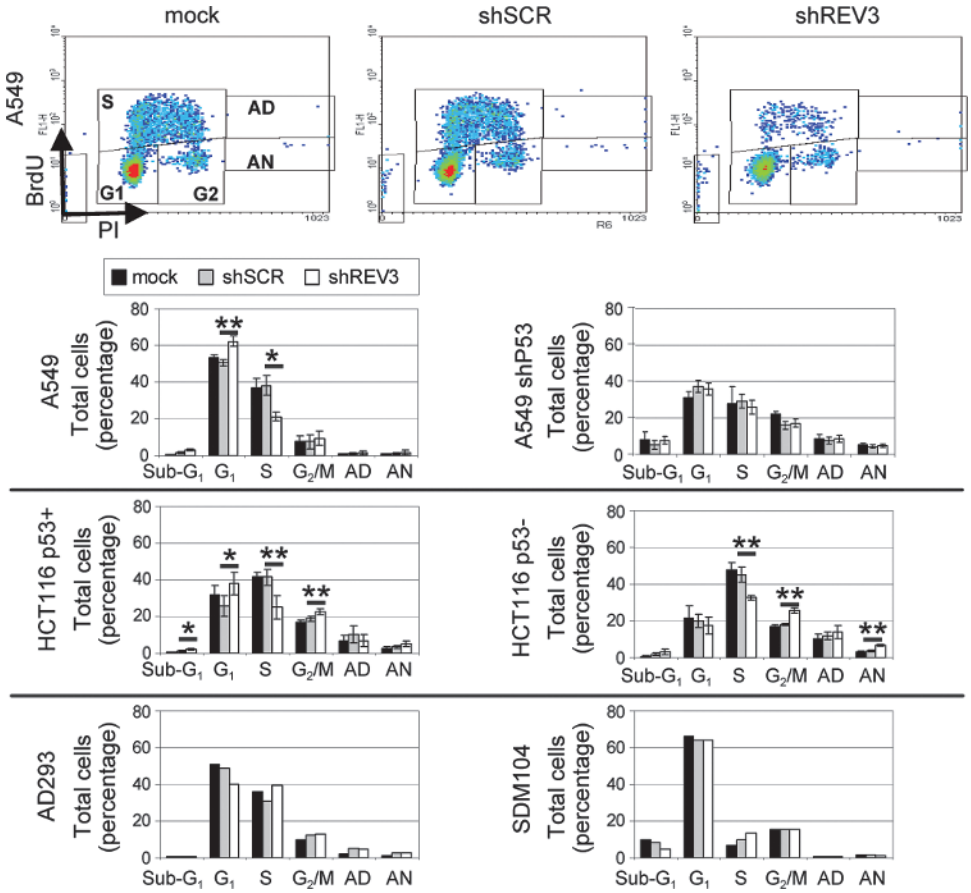

Figure 3. *REV3* depletion changes cell cycle distribution of cancer cell lines. Cells were mock treated or transduced with lentiviral-based particles containing either shSCR or shREV3 and/or lentiviral-based particles containing shP53. After 1 week, cell cycle distribution was measured by BrdU/propidium iodide staining and subsequent FACS analysis. The averages of three independent experiments are given for A549, A549 shP53, p53-proficient HCT116, and p53-deficient HCT116 cells, whereas representative experiments are shown for SDM104 and AD293 cells. *$P < .05$. **$P < .01$. Shown are means ± SD.

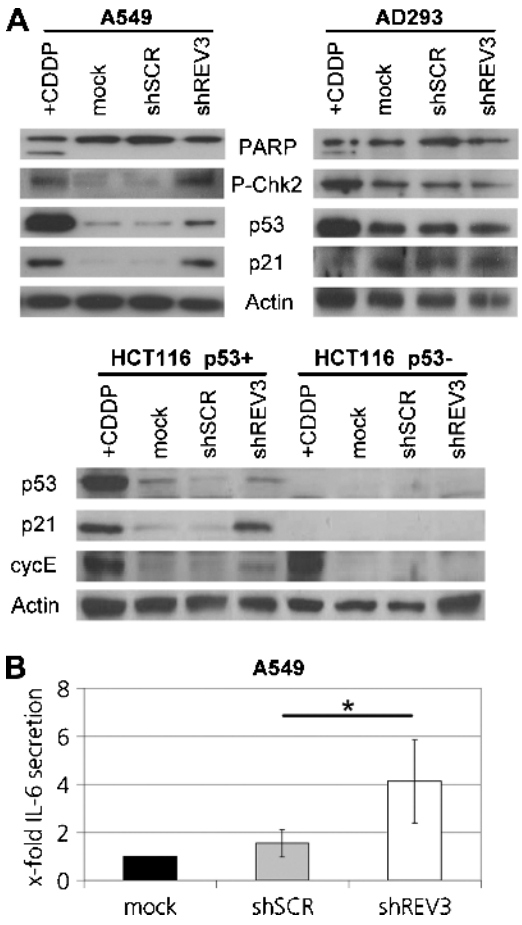

Figure 4. *REV3* depletion induces DDR pathway in cancer cells. Cells were cisplatin or mock treated or transduced with lentiviral-based particles containing either shSCR or shREV3. (A) After 1 week, whole-cell lysates were analyzed by Western analysis. (B) After 24 hours, IL-6 secretion in serum-free DMEM was assessed by ELISA, normalized to the cell number and reported as fold increase compared with mock-treated control. The averages of at least three independent experiments are given. Shown are means ± SD.

cell cycle to 62% compared with 53% and 51% in the mock and scrambled controls, respectively (Figure 3). Similarly, the fraction of p53-proficient HCT116 cells in the G_1 phase increased to 38% after inhibition of *REV3* expression compared with 26% in scrambled control, respectively (Figure 3). In the control cell line AD293 and the primary cell culture SDM104, neither the fraction of cells in the S phase was decreased nor was the fraction of cells in the G_1 phase increased after inhibition of *REV3* expression compared with mock and scrambled controls (Figure 3). A small but significant increase in the fraction of cells in the G_2 phase was observed in p53-proficient HCT116 cells after *REV3* depletion (23%) compared with mock (17%) and scrambled controls (19%). In addition, protein levels of cyclin E, which accumulate during the G_1 phase and are required for the transition from the G_1 phase to the S phase, increased after inhibition of *REV3* expression in p53-proficient but not in p53-deficient HCT116 cancer cells (Figure 4*A*). Thus, inhibition of *REV3* expression in the investigated p53-proficient cancer cell lines induces a G_1 arrest, respectively, S-phase depletion, whereas the cell cycle distribution of the investigated control cell line and the primary mesothelial culture was not affected.

Inhibition of REV3 *Expression Induces Senescence in p53-Proficient Cancer Cells*

Although inhibition of *REV3* expression slightly increased the fraction of sub-G_1 cells in p53-proficient A549 and HCT116 cells, no significant induction of apoptosis as indicated by an increased fraction of sub-G_1 cells (Figure 3) or poly(ADP-ribose) polymerase (PARP) cleavage (Figure 4*A*) was observed in the remaining control and cancer cell lines tested in this study.

Because senescence can be induced by persistent DNA damage [31], we investigated whether cells are senescent after *REV3* depletion. Induction of senescence cannot be identified by a single marker but is associated with a variety of distinct cellular and molecular changes (reviewed in Collado and Serrano [34]). Microscopic analysis after crystal violet staining revealed that the morphology of control AD293 cells was not changed 7 days after inhibition of *REV3* expression compared with mock and scrambled controls (Figure W6). In the p53-proficient cancer cell lines included in this study, most colonies were smaller after *REV3* depletion, and the cells of these colonies displayed morphologic changes that are associated with senescence, namely, increased cell size and flattened shape, whereas cell morphology was not affected in mock and scrambled controls (Figure W6). SA-β-galactosidase staining revealed increased SA-β-galactosidase activity in IL45, A549, and HCT116 p53-proficient cells after inhibition of *REV3* expression (Figure W6 and Table 1). No increase in SA-β-galactosidase staining after inhibition of *REV3* expression was detectable in the control cells AD293 or in the p53-deficient MDA-MB-231 and HCT116 cancer cell lines. As mentioned previously, G_1 arrest, respectively, S-phase depletion and p21 accumulation were observed in A549 and p53-proficient HCT116 cells after *REV3* depletion (Figures 3 and 4*A*).

An increase in persistent DNA damage indicated by residual 53BP1/γH2AX foci is associated in human foreskin fibroblasts with a senescence-associated secretory phenotype including cytokine secretion such as IL-6 [31]. Twelve days after transduction, IL-6 secretion was increased in A549 cell after inhibition of *REV3* expression compared with mock and scrambled controls (Figure 4*B*). In contrast, *REV3* depletion in p53-deficient HCT116 cells did not result in a G_1 accumulation nor did it increase p21 levels or increase SA-β-galactosidase staining (Figures 3, 4*A*, and W6 and Table 1). Similarly, G_1 accumulation and SA-β-galactosidase staining were abolished in A549 by p53 inhibition (Figure 3 and Table 1). Thus, among the analyzed cancer cell lines, *REV3* depletion *per se* induces senescence in p53-proficient cancer cells only.

REV3 *Depletion Induces a G_2/M Arrest and Aneuploidy in p53-Deficient Cancer Cells*

No G_1 arrest was detectable in p53-deficient HCT116 cell after inhibition of *REV3* expression (Figure 3). Instead, *REV3* depletion

Table 1. Induction of Senescence after REV3 Inhibition Is Dependent on p53 Level.

p53	Cell Line	Mock	shSCR	shREV3	*t* test shSCR/shREV3
+	IL45	2.3 ± 0.7	2.8 ± 1.0	44.2 ± 4.0	*
+	A549	5.8 ± 0.7	6.0 ± 1.4	16.1 ± 2.3	*
−	A549 shP53	1.0 ± 0.3	0.9 ± 0.3	0.9 ± 0.3	NS
−	MDA-MB-231	0	0	0	N/A
+	AD293 (normal)	0	0	0	N/A

Three independent experiments were analyzed for all cell lines. Shown are means (%) of senescent cells ± SEM.
N/A indicates not applicable; NS, not significant.
*$P < .01$%.

in the p53-deficient HCT116 cell line significantly increased the fraction of cells in the G_2/M phase to 26% compared with 17% and 18% in the mock and scrambled controls, respectively (Figure 3). In addition, inhibition of *REV3* expression also increased the fraction of aneuploid cells, which did not incorporate BrdU (AN, aneuploid nondividing) to 7% compared with 3% and 4% in the mock and scrambled controls (Figure 3). The fraction of aneuploid cells, which were still incorporating BrdU (AD, aneuploid dividing), was not increased after *REV3* depletion in p53-deficient HCT116 cells compared with mock and scrambled controls (Figure 3). Thus, inhibition of *REV3* expression in the investigated p53-deficient cancer cells results in the accumulation of G_2/M arrested and AN cells.

In an effort to provide proof-of-principle, we inhibited p53 expression in p53-proficient A549 cancer cells (Figure W1*C*). Inhibition of p53 expression in A549 cells resulted in a significant increase of the cells in the G_2 phase (22%) and in aneuploidy (total 14%) compared with p53-proficient A549 cells (7.5% and 1.8%, respectively; Figure 3), which is in agreement with the dominant role of p53 in the induction of the G_1 arrest [35]. The dominant role of p53 in protection from aneuploidy is highlighted by the finding that additional inhibition of *REV3* expression in combination with p53 inhibition did not further increase aneuploidy in A549 cancer cells.

Discussion

During our study on the involvement of REV3 in chemotherapy response, we found that lentiviral-based inhibition of *REV3* expression was as efficient in the analyzed cancer cell lines as in the primary mesothelial culture and the control cell lines, but surprisingly, colony formation was reduced in the cancer cell lines only. Therefore, we conclude that reduction in colony formation does not simply mirror the degree of *REV3* expression inhibition relative to the scrambled control.

We found that colony formation was not significantly reduced in the control cell lines AD293 and LP9-hTERT and the primary mesothelial culture SDM104 and after inhibition of REV3 expression. This is consistent with previous studies where no deficiency in cell growth/survival was mentioned after antisense-based inhibition of *REV3* expression in human nontumor cell lines [17,36]. In contrast, it was shown by different groups that *REV3* knockout reduced cell growth of MEFs [21,37]. Thus, additional studies will be necessary to clarify how normal cells adapt their DDR to tolerate the loss of REV3 function. At this point, it is worth mentioning that investigations of cancer-specific pathways are usually performed using so-called normal cells as control. However, normal cells have a limited life span [38], which also applies to the primary mesothelial culture SDM104. In contrast, the control cell lines AD293 and LP9-hTERT are virally transformed or immortalized by transfection with human telomerase, respectively, to achieve unlimited proliferation in cell culture. Thus, AD293 and LP9-hTERT might not fully represent normal cells, although they have been widely used as normal controls [39,40] and their response to REV3 depletion was consistent with the reaction of the primary mesothelial cell culture SDM104.

Studies have shown controversial results on the effect of *REV3* depletion on cancer cell growth. On one hand, no deficiency in cell growth/survival was mentioned after si/shRNA–based inhibition of *REV3* expression in HCT116, U2OS, and HeLa cancer cells [10,14,41]. Conversely, it was shown that knockout of *REV3* resulted in a pronounced growth retardation in Burkitt lymphoma cells [42]. We found that inhibition of *REV3* expression *per se* reduced colony formation in lung, breast, mesothelioma, and colon tumor cell lines. There are two possible explanations for these apparently controversial observations on the effects of *REV3* depletion in cancer cells. First, the absence of cell growth inhibition in stable cancer cell lines depleted of *REV3* might be due to the genetic modifications acquired during clonal selection, namely, rewiring of cell cycle checkpoint pathways [43]. Thus, it would be interesting to identify if the clones isolated in the studies mentioned acquired genetic modifications compared with their parental cell lines. Second, when investigated, it was found that inhibition of *REV3* expression *per se* increased DNA damage levels in cancer cells even when no effect on cell growth/survival was mentioned [10,14,42]. Thus, it is possible that the DNA damage level necessary for DDR activation is different in the tested cell lines, explaining the presence or absence of growth arrest (reviewed in Al-Ejeh et al. [44]).

The second possibility is illustrated by the fact that only inhibition of *REV3* expression by high-titer transduction resulted in a reduction of colony formation in MMR-deficient HCT116 cells, although *REV3* expression was not further reduced. It was shown before that activation of the DDR is impaired in MMR-deficient HCT116 cells [45]. Thus, a higher level of cellular stress in form of additional DSBs due to more viral integration events after high-titer transduction might be required in HCT116 cells for the induction of a DDR resulting in the reduced colony formation after inhibition of *REV3* expression.

In addition, the p53 status influences cell fate after *REV3* depletion. The p53 status did not affect the accumulation of persistent DSBs indicated by P-ATM foci after inhibition of *REV3* expression in HCT116 cells. Similarly, a recent study showed that DNA damage accumulation after prolonged activation of the mitotic checkpoint is also independent of the p53 status [46]. Thus, p53 does not protect cancer cells from damage accumulation due to *REV3* depletion, although the subsequent cellular outcome, as discussed below, is dependent on the p53 status.

Previously, accumulation of H2AX phosphorylation in U2OS human osteosarcoma cells was observed after REV3 depletion [10]. Microscopic analysis revealed that inhibition of REV3 expression in cancer cells resulted in the accumulation of persistent DNA damage foci, which was also observed after exposure to high-dose ionizing radiation [31], suggesting the accumulation of irreparable DSBs. Similarly, the accumulation of large 53BP1 foci was also observed after the induction of mild replication stress or the genetic ablation of the BLM helicase [47]. Interestingly, a very recent publication showed that large 53BP1 foci mark sites of replication stress, which is passed onto daughter cells [48], giving rise to the possibility that the large 53BP1 foci detected after REV3 depletion mark sites of incomplete DNA synthesis rather than DSBs due to replication fork breakdown.

Cellular senescence limits the proliferation of damaged cells that are at risk for neoplastic transformation (reviewed in Collado and Serrano [34]). Our data indicate that, at least in p53-proficient cancer cells, senescence induction after *REV3* depletion might prevent further transformation of cancer cells by establishing an essentially irreversible growth arrest. It is also proposed that the senescence-associated secretory phenotype, which we observed after inhibition of *REV3* expression indicated by increased IL-6 secretion, might stimulate the immune system to clear senescent cells (reviewed in Collado and Serrano [34]). However, if senescent cells are not cleared by the immune system, they remain in a "dormant" state representing a dangerous potential for tumor relapse.

A recent study showed that nocodazole (a microtubule polymerization inhibitor) treatment of p53-deficient HCT116 cells leads to prolonged mitosis and subsequent return of the mitotically arrested cells to interphase without cell division resulted in aneuploidy [46], a process known as mitotic slippage. We observed that *REV3* depletion in the p53-deficient HCT116 cell line and in combination with p53 inhibition in the A549 cell line leads to an accumulation of G_2/M arrested cells and an increase in the frequency of aneuploid cells, which was also described in p53-deficient *REV3*-null MEFs [37].

On the basis of these results, we propose a model (Figure 5) in which inhibition of *REV3* expression can be tolerated in normal cells but results in the accumulation of persistent DNA damage in cancer cells harboring cancer-specific alterations. Accumulation of persistent DNA damage leads in p53-proficient cancer cells to senescence, whereas *REV3* depletion in *p53*-deficient cells results in growth inhibition and a G_2/M arrest. A small fraction of the p53-deficient cancer cells can overcome the G_2/M arrest, which results in mitotic slippage and aneuploidy.

The concept of "synthetic lethality," where defects in two pathways alone can be tolerated but become lethal when combined, has been originally described in *Drosophila* and yeast genetic studies [49,50]. This concept has been extended by the idea of "synthetic sickness," whereas the combined loss/mutation of function of two genes does not kill cells but significantly impairs cellular fitness [51].

A recent study showed that inhibiting specific DNA repair polymerases induces synthetic sickness/lethality specifically in MMR-deficient cells [52]. In analogy, we found that *REV3* depletion induces synthetic sickness/lethality in the investigated cancer cells. It will be interesting to identify the underlying cancer-specific alteration(s), which render the investigated cancer cell lines prone to growth inhibition due to REV3 depletion. In this context it was shown that DNA repair and/or cell cycle checkpoint mechanisms are frequently abrogated in cancer cells [53], and the concentration of endogenous DNA damage is higher in human tumoral tissue compared with the corresponding adjacent normal tissue (reviewed in Croteau and Bohr [54]). Therefore, differences in repair capacity or DNA damage levels between normal and cancer cells might be the underlying cause for the observed increased sensitivity of cancer cells to *REV3* depletion. Alternatively, replication stress due to the activation of oncogenes might sensitize cancer cells to the inhibition of *REV3* expression. A recent study showed that overexpression of Sch9, the *S. cerevisiae* homolog of the mammalian proto-oncogenes *Akt* and *S6*, increases superoxide-dependent DNA damage, which subsequently leads to the REV3-dependent formation of point mutations to avoid gross chromosomal rearrangements [55]. However, we cannot exclude that the specific genetic or epigenetic alterations underlying the observed synthetic sickness/lethality after *REV3* depletion might differ between the tested cancer cell lines. Indeed, a recent study showed that REV3 deletion in a *S. cerevisiae* strain containing a particular additional chromosome resulted in decreased colony formation [56].

Cancer cells can be addicted not only to oncogenes but also to nononcogenes (reviewed in Luo et al. [57]). "Nononcogene addiction" genes are also required for maintenance of the tumorigenic state but are in contrast to oncogenes not functionally altered or mutated. The most prominent example of a "nononcogene addiction" gene is PARP, which is essential in BRCA-deficient breast cancer cells. Thus, based on the results of our study, we propose that *REV3* functions as a "nononcogene addiction" gene, whose depletion induces synthetic sickness/lethality specifically in the investigated cancer cell lines. Along those lines, we are performing a genome-wide screen to identify essential molecular pathways in cancer cells whose inhibition will further enhance cell killing in combination with REV3 inhibition.

It will be interesting to determine whether 1) DNA damage tolerance by REV3-dependent TLS, 2) REV3-dependent DNA repair, or 3) a yet-to-be-identified function of REV3 is essential for cancer

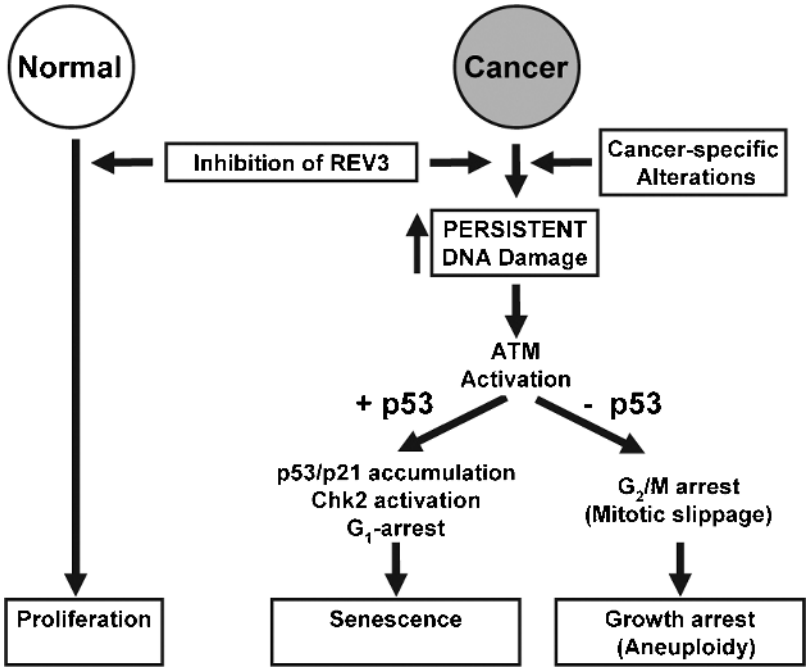

Figure 5. Model: REV3 depletion induces persistent DNA damage specifically in cancer cells, which subsequently results in the induction of senescence in p53-proficient cancer cells and G_2/M arrest in p53-deficient cancer cells. See text for details.

cell growth. Indeed, the size of mammalian REV3 is approximately double the size of the yeast homolog, giving rise to the possibility that the nonconserved region of REV3 harbors a yet-to-be-identified functional domain, necessary only in higher organisms.

Acknowledgments

The authors thank Alexandra Graf for her help in the initial experiments and Bert Vogelstein for HCT116 (p53+/+) and HCT116 (p53−/−) cell lines.

References

[1] Lemontt JF (1971). Mutants of yeast defective in mutation induced by ultraviolet light. *Genetics* **68**, 21–33.

[2] Morrison A, Christensen RB, Alley J, Beck AK, Bernstine EG, Lemontt JF, and Lawrence CW (1989). REV3, a Saccharomyces cerevisiae gene whose function is required for induced mutagenesis, is predicted to encode a nonessential DNA polymerase. *J Bacteriol* **171**, 5659–5667.

[3] Lawrence CW, Das G, and Christensen RB (1985). *REV7*, a new gene concerned with UV mutagenesis in yeast. *Mol Gen Genet* **200**, 80–85.

[4] Waters LS, Minesinger BK, Wiltrout ME, D'Souza S, Woodruff RV, and Walker GC (2009). Eukaryotic translesion polymerases and their roles and regulation in DNA damage tolerance. *Microbiol Mol Biol Rev* **73**, 134–154.

[5] Bemark M, Khamlichi AA, Davies SL, and Neuberger MS (2000). Disruption of mouse polymerase ζ (Rev3) leads to embryonic lethality and impairs blastocyst development *in vitro*. *Curr Biol* **10**, 1213–1216.

[6] Esposito G, Godindagger I, Klein U, Yaspo ML, Cumano A, and Rajewsky K (2000). Disruption of the Rev3l-encoded catalytic subunit of polymerase ζ in mice results in early embryonic lethality. *Curr Biol* **10**, 1221–1224.

[7] Wittschieben J, Shivji MK, Lalani E, Jacobs MA, Marini F, Gearhart PJ, Rosewell I, Stamp G, and Wood RD (2000). Disruption of the developmentally regulated *Rev3l* gene causes embryonic lethality. *Curr Biol* **10**, 1217–1220.

[8] O-Wang J, Kajiwara K, Kawamura K, Kimura M, Miyagishima H, Koseki H, and Tagawa M (2002). An essential role for *REV3* in mammalian cell survival: absence of *REV3* induces p53-independent embryonic death. *Biochem Biophys Res Commun* **293**, 1132–1137.

[9] Rajpal DK, Wu X, and Wang Z (2000). Alteration of ultraviolet-induced mutagenesis in yeast through molecular modulation of the *REV3* and *REV7* gene expression. *Mutat Res* **461**, 133–143.

[10] Brondello JM, Pillaire MJ, Rodriguez C, Gourraud PA, Selves J, Cazaux C, and Piette J (2008). Novel evidences for a tumor suppressor role of *Rev3*, the catalytic subunit of Pol ζ. *Oncogene* **27**, 6093–6101.

[11] Wang H, Zhang SY, Wang S, Lu J, Wu W, Weng L, Chen D, Zhang Y, Lu Z, Yang J, et al. (2009). REV3L confers chemoresistance to cisplatin in human gliomas: the potential of its RNAi for synergistic therapy. *Neuro Oncol* **11**, 790–802.

[12] Nojima K, Hochegger H, Saberi A, Fukushima T, Kikuchi K, Yoshimura M, Orelli BJ, Bishop DK, Hirano S, Ohzeki M, et al. (2005). Multiple repair pathways mediate tolerance to chemotherapeutic cross-linking agents in vertebrate cells. *Cancer Res* **65**, 11704–11711.

[13] Raschle M, Knipscheer P, Enoiu M, Angelov T, Sun J, Griffith JD, Ellenberger TE, Scharer OD, and Walter JC (2008). Mechanism of replication-coupled DNA interstrand crosslink repair. *Cell* **134**, 969–980.

[14] Hicks JK, Chute CL, Paulsen MT, Ragland RL, Howlett NG, Gueranger Q, Glover TW, and Canman CE (2010). Differential roles for DNA polymerases ε, ζ, and REV1 in lesion bypass of intrastrand *versus* interstrand DNA cross-links. *Mol Cell Biol* **30**, 1217–1230.

[15] Wu F, Lin X, Okuda T, and Howell SB (2004). DNA polymerase ζ regulates cisplatin cytotoxicity, mutagenicity, and the rate of development of cisplatin resistance. *Cancer Res* **64**, 8029–8035.

[16] Schenten D, Kracker S, Esposito G, Franco S, Klein U, Murphy M, Alt FW, and Rajewsky K (2009). Pol ζ ablation in B cells impairs the germinal center reaction, class switch recombination, DNA break repair, and genome stability. *J Exp Med* **206**, 477–490.

[17] Gibbs PE, McGregor WG, Maher VM, Nisson P, and Lawrence CW (1998). A human homolog of the *Saccharomyces cerevisiae REV3* gene, which encodes the catalytic subunit of DNA polymerase ζ. *Proc Natl Acad Sci USA* **95**, 6876–6880.

[18] Diaz M, Watson NB, Turkington G, Verkoczy LK, Klinman NR, and McGregor WG (2003). Decreased frequency and highly aberrant spectrum of ultraviolet-induced mutations in the *hprt* gene of mouse fibroblasts expressing antisense RNA to DNA polymerase ζ. *Mol Cancer Res* **1**, 836–847.

[19] Xie K, Doles J, Hemann MT, and Walker GC (2010). Error-prone translesion synthesis mediates acquired chemoresistance. *Proc Natl Acad Sci USA* **107**, 20792–20797.

[20] Doles J, Oliver TG, Cameron ER, Hsu G, Jacks T, Walker GC, and Hemann MT (2010). Suppression of Rev3, the catalytic subunit of Pol{ζ}, sensitizes drug-resistant lung tumors to chemotherapy. *Proc Natl Acad Sci USA* **107**, 20786–20791.

[21] Wittschieben JP, Reshmi SC, Gollin SM, and Wood RD (2006). Loss of DNA polymerase ζ causes chromosomal instability in mammalian cells. *Cancer Res* **66**, 134–142.

[22] Van Sloun PP, Varlet I, Sonneveld E, Boei JJ, Romeijn RJ, Eeken JC, and De Wind N (2002). Involvement of mouse *Rev3* in tolerance of endogenous and exogenous DNA damage. *Mol Cell Biol* **22**, 2159–2169.

[23] Sonoda E, Okada T, Zhao GY, Tateishi S, Araki K, Yamaizumi M, Yagi T, Verkaik NS, van Gent DC, Takata M, et al. (2003). Multiple roles of Rev3, the catalytic subunit of pol ζ in maintaining genome stability in vertebrates. *EMBO J* **22**, 3188–3197.

[24] d'Adda di Fagagna F (2008). Living on a break: cellular senescence as a DNA-damage response. *Nat Rev Cancer* **8**, 512–522.

[25] Thurneysen C, Opitz I, Kurtz S, Weder W, Stahel RA, and Felley-Bosco E (2009). Functional inactivation of NF2/merlin in human mesothelioma. *Lung Cancer* **64**, 140–147.

[26] Reed SE, Staley EM, Mayginnes JP, Pintel DJ, and Tullis GE (2006). Transfection of mammalian cells using linear polyethylenimine is a simple and effective means of producing recombinant adeno-associated virus vectors. *J Virol Methods* **138**, 85–98.

[27] Salmon P and Trono D (2007). Production and titration of lentiviral vectors. *Curr Protoc Hum Genet* **Chapter 12**, Unit 12 10.

[28] Marti TM, Hefner E, Feeney L, Natale V, and Cleaver JE (2006). H2AX phosphorylation within the G_1 phase after UV irradiation depends on nucleotide excision repair and not DNA double-strand breaks. *Proc Natl Acad Sci USA* **103**, 9891–9896.

[29] Dimri GP, Lee X, Basile G, Acosta M, Scott G, Roskelley C, Medrano EE, Linskens M, Rubelj I, Pereira-Smith O, et al. (1995). A biomarker that identifies senescent human cells in culture and in aging skin *in vivo*. *Proc Natl Acad Sci USA* **92**, 9363–9367.

[30] Hopkins-Donaldson S, Ziegler A, Kurtz S, Bigosch C, Kandioler D, Ludwig C, Zangemeister-Wittke U, and Stahel R (2003). Silencing of death receptor and caspase-8 expression in small cell lung carcinoma cell lines and tumors by DNA methylation. *Cell Death Differ* **10**, 356–364.

[31] Rodier F, Coppe JP, Patil CK, Hoeijmakers WA, Munoz DP, Raza SR, Freund A, Campeau E, Davalos AR, and Campisi J (2009). Persistent DNA damage signalling triggers senescence-associated inflammatory cytokine secretion. *Nat Cell Biol* **11**, 973–979.

[32] Yamauchi M, Oka Y, Yamamoto M, Niimura K, Uchida M, Kodama S, Watanabe M, Sekine I, Yamashita S, and Suzuki K (2008). Growth of persistent foci of DNA damage checkpoint factors is essential for amplification of G_1 checkpoint signaling. *DNA Repair* **7**, 405–417.

[33] Quinn CM and Wright NA (1990). The clinical-assessment of proliferation and growth in human tumors—evaluation of methods and applications as prognostic variables. *J Pathol* **160**, 93–102.

[34] Collado M and Serrano M (2010). Senescence in tumours: evidence from mice and humans. *Nat Rev Cancer* **10**, 51–57.

[35] Di Leonardo A, Linke SP, Clarkin K, and Wahl GM (1994). DNA damage triggers a prolonged p53-dependent G_1 arrest and long-term induction of Cip1 in normal human fibroblasts. *Genes Dev* **8**, 2540–2551.

[36] Li Z, Zhang H, McManus TP, McCormick JJ, Lawrence CW, and Maher VM (2002). *hREV3* is essential for error-prone translesion synthesis past UV or benzo[*a*]pyrene diol epoxide–induced DNA lesions in human fibroblasts. *Mutat Res* **510**, 71–80.

[37] Zander L and Bemark M (2004). Immortalized mouse cell lines that lack a functional *Rev3* gene are hypersensitive to UV irradiation and cisplatin treatment. *DNA Repair* **3**, 743–752.

[38] Hayflick L (1965). The limited *in vitro* lifetime of human diploid cell strains. *Exp Cell Res* **37**, 614–636.

[39] Tu Y and Kim JS (2010). Selective gene transfer to hepatocellular carcinoma using homing peptide-grafted cationic liposomes. *J Microbiol Biotechnol* **20**, 821–827.

[40] Hillegass JM, Shukla A, MacPherson MB, Bond JP, Steele C, and Mossman BT (2010). Utilization of gene profiling and proteomics to determine mineral pathogenicity in a human mesothelial cell line (LP9/TERT-1). *J Toxicol Environ Health A* **73**, 423–436.

[41] Lin X and Howell SB (2006). DNA mismatch repair and p53 function are major determinants of the rate of development of cisplatin resistance. *Mol Cancer Ther* **5**, 1239–1247.

[42] Gueranger Q, Stary A, Aoufouchi S, Faili A, Sarasin A, Reynaud CA, and Weill JC (2008). Role of DNA polymerases ε, ι and ζ in UV resistance and UV-induced mutagenesis in a human cell line. *DNA Repair* **7**, 1551–1562.

[43] Reinhardt HC, Aslanian AS, Lees JA, and Yaffe MB (2007). p53-deficient cells rely on ATM- and ATR-mediated checkpoint signaling through the p38MAPK/MK2 pathway for survival after DNA damage. *Cancer Cell* **11**, 175–189.

[44] Al-Ejeh F, Kumar R, Wiegmans A, Lakhani SR, Brown MP, and Khanna KK (2010). Harnessing the complexity of DNA-damage response pathways to improve cancer treatment outcomes. *Oncogene* **29**, 6085–6098.

[45] Brown KD, Rathi A, Kamath R, Beardsley DI, Zhan Q, Mannino JL, and Baskaran R (2003). The mismatch repair system is required for S-phase checkpoint activation. *Nat Genet* **33**, 80–84.

[46] Dalton WB, Yu B, and Yang VW (2010). p53 suppresses structural chromosome instability after mitotic arrest in human cells. *Oncogene* **29**, 1929–1940.

[47] Lukas C, Savic V, Bekker-Jensen S, Doil C, Neumann B, Pedersen RS, Grofte M, Chan KL, Hickson ID, Bartek J, et al. (2011). 53BP1 nuclear bodies form around DNA lesions generated by mitotic transmission of chromosomes under replication stress. *Nat Cell Biol* **13**, 243–253.

[48] Harrigan JA, Belotserkovskaya R, Coates J, Dimitrova DS, Polo SE, Bradshaw CR, Fraser P, and Jackson SP (2011). Replication stress induces 53BP1-containing OPT domains in G_1 cells. *J Cell Biol* **193**, 97–108.

[49] Dobzhansky T (1946). Genetics of natural populations. XIII. Recombination and variability in populations of *Drosophila pseudoobscura*. *Genetics* **31**, 269–290.

[50] Hartman JLT, Garvik B, and Hartwell L (2001). Principles for the buffering of genetic variation. *Science* **291**, 1001–1004.

[51] Kaelin WG Jr (2005). The concept of synthetic lethality in the context of anticancer therapy. *Nat Rev Cancer* **5**, 689–698.

[52] Martin SA, McCabe N, Mullarkey M, Cummins R, Burgess DJ, Nakabeppu Y, Oka S, Kay E, Lord CJ, and Ashworth A (2010). DNA polymerases as potential therapeutic targets for cancers deficient in the DNA mismatch repair proteins MSH2 or MLH1. *Cancer Cell* **17**, 235–248.

[53] Bartkova J, Horejsi Z, Koed K, Kramer A, Tort F, Zieger K, Guldberg P, Sehested M, Nesland JM, Lukas C, et al. (2005). DNA damage response as a candidate anti-cancer barrier in early human tumorigenesis. *Nature* **434**, 864–870.

[54] Croteau DL and Bohr VA (1997). Repair of oxidative damage to nuclear and mitochondrial DNA in mammalian cells. *J Biol Chem* **272**, 25409–25412.

[55] Madia F, Wei M, Yuan V, Hu J, Gattazzo C, Pham P, Goodman MF, and Longo VD (2009). Oncogene homologue *Sch9* promotes age-dependent mutations by a superoxide and Rev1/Pol ζ–dependent mechanism. *J Cell Biol* **186**, 509–523.

[56] Sheltzer JM, Blank HM, Pfau SJ, Tange Y, George BM, Humpton TJ, Brito IL, Hiraoka Y, Niwa O, and Amon A (2011). Aneuploidy drives genomic instability in yeast. *Science* **333**, 1026–1030.

[57] Luo J, Solimini NL, and Elledge SJ (2009). Principles of cancer therapy: oncogene and non-oncogene addiction. *Cell* **136**, 823–837.

Supplemental Materials and Methods

Cell Lines

The human MPM cell line ZL55 and the primary cell culture SDM104 were generated in our laboratory [25,30]. The rat MPM cell line IL45 was generated elsewhere (Craighead et al., *Am J Pathol.* 1987;129:448–462). The breast cancer cell lines MDA-MB-231 and MCF-7, the adenocarcinoma Calu-3, the squamous non–small cell lung cancer cell line A549 and the HEK 293T were purchased from American Type Culture Corporation (Manassas, VA). The AD293 cell line, a HEK 293 derivative with improved cell adherence, was purchased from Stratagene (La Jolla, CA). The colorectal carcinoma cell lines HCT116 40.16 (p53+/+) and HCT116 379.2 (p53–/–) were kindly provided by Dr Bert Vogelstein (Johns Hopkins University, Baltimore, MD).

Reagents

When indicated, 20 μM cisplatin (Ebewe Pharma, Cham, Switzerland) was added for 24 hours.

To clone the short hairpin constructs into the plasmid pSuperior.puro, the following DNA oligonucleotides were ordered from Microsynth:

shREV3-4:
5′-GATCCCCCAAAGATGCTGCTACATTATTCAAGAGATAATGTAGCAGCATCTTTGTTTTTA-3′
5′-AGCTTAAAAACAAAGATGCTGCTACATTATCTCTTGAATAATGTAGCAGCATCTTTGGGG-3′

shREV3-5:
5′-GATCCCCGATATTCCATCTGTTACAATTCAAGAGATTGTAACAGATGGAATATCTTTTTA-3′
5′-AGCTTAAAAAGATATTCCATCTGTTACAATCTCTTGAATTGTAACAGATGGAATATCGGG-3′

shREV3-6:
5′-GATCCCCTAGTCAGACTTTTCAGCCTTTCAAGAGAAGGCTGAAAAGTCTGACTATTTTTA-3′
5′-AGCTTAAAAATAGTCAGACTTTTCAGCCTTCTCTTGAAAGGCTGAAAAGTCTGACTAGGG-3′

shSCR:
5′-GATCCCCATTCTAGGTGAAAGCTAATTTCAAGAGATAAGATCCACTTTCGATTATTTTTA-3′
5′-AGCTTAAAAATAATCGAAAGTGGATCTTATCTCTTGAAATTAGCTTTCACCTAGAATGGG-3′

shP53:
5′-GATCCCCGACTCCAGTGGTAATCTACTTCAAGAGAGTAGATTACCACTGGAGTCTTTTTA-3′
5′-AGCTTAAAAAGACTCCAGTGGTAATCTACTCTCTTGAAGTAGATTACCACTGGAGTCGGG-3′

To quantitatively measure the expression of *REV3* mRNA by real-time PCR, the following DNA oligonucleotides were ordered from Microsynth:

REV3:
Forward 5′-TGAGTTCAAATTTGGCTGTACCT-3′
REV3:
Reverse 5′-TCTAGTCTTCAAAATTTCTTCAAGCA-3′

Histone H3:
Forward 5′-TAAAGCACCCAGGAAACAACTGGC-3′
Reverse 5′-ACCAGGCCTGTAACGATGAGGTTT-3′

P53:
Forward 5′-GCTTTGAGGTTCGTGTTTGTGCCT-3′
Reverse 5′-GCCCACGGATCTTAAGGGTGAAAT-3′

For Western analysis, the following primary antibodies were diluted at 1:1000: PARP (no. 9542; Cell Signaling, Beverly, MA), P-Chk2 (no. AF1626; R&D Systems), p53 (no. 9282; Cell Signaling), p21 (no. sc-756; Santa Cruz, Santa Cruz, CA), cyclin E (no. sc-247; Santa Cruz), and MAD2B/Rev7 (no. 612266; BD Biosciences). The primary antibody β-actin (no. 691001; MP Biomedicals, Solon, OH) was incubated 1:10,000 for 1 hour at room temperature. The secondary polyclonal antibodies coupled to horseradish peroxidase were diluted at 1:10,000.

For immunofluorescence microscopy, the following primary antibodies were used: P-ATM 1:1000 (no. sc-4526; Cell Signaling), γH2AX 1:1000 (no. 05-636; Upstate Biotechnology, Lake Placid, NY), 53BP1 1:500 (no. 4937; Cell Signaling), and BrdU 1:1000 (no. 555627; BD Biosciences).

Vector Production and Transduction

Short hairpin REV3-4 and scrambled (shSCR) oligos were ligated into pSuperior.puro as described by the manufacturer (OligoEngine, Seattle, WA). The shRNA and H1 promoter fragments were subsequently ligated into the constitutive expressing lentiviral vector pLVTHM (Addgene, Cambridge, MA). Replication-deficient lentiviral particles were produced and titrated as described previously [26,27].

Cells were seeded in six-well plates (colony formation, immunofluorescence, and SA-β-galactosidase assay: 500 cells/well [SDM104: 1000 cells/well]; FACS and Western analysis: 2500 cells/well [SDM104: 5000 cells/well]; real-time PCR and ELISA: 5000 cells/well) in 2 ml of medium. After 6 hours, the medium was removed, and lentivirus suspension was added for 30 minutes in 300 μl (immunofluorescence, FACS, and real-time PCR: MOI = 100; Western analysis and colony formation: MOI = 170). All transductions of HCT116 and the corresponding control AD293 cells were performed with an MOI of 800 and were incubated for 1 hour. Subsequently, medium was added to final volume of 1.5 ml. For mock treatment, 0.5-μm filtered conditioned medium from a HEK 293T culture was added. After 7 days, cells were further processed for distinct experiment as described below except for colony formation, which were incubated longer as described below.

Quantitative Real-time PCR

Real-time PCR cycle conditions were as follows: one cycle of 95°C for 10 minutes, 40 cycles of 95°C for 15 seconds and 60°C for 1 minute, and one cycle of 95°C for 15 seconds and from 60°C slowly elevating to 95°C for several minutes for dissociation curve analysis. *Histone H3* expression was used to standardize the total amount of complementary DNA, and the specificity of the PCR was confirmed by analysis of the melting curve.

Immunofluorescence Microscopy

Immunofluorescence microscopy was performed essentially as described before [28]. In detail, for BrdU staining, cells were incubated with 10 μM BrdU for 1 hour. Fixation and permeabilization were done with 100% methanol at −20°C and acetone-methanol (50:50) at −20°C for 20 minutes at room temperature, respectively. Cells were washed 2 × 5 minutes with PBS. For BrdU staining, cells were denatured with 2 M HCl for 30 minutes at room temperature and subsequently washed 3 × 5 minutes with PBS. PBS containing 1% fetal bovine serum and 10% bovine serum albumin was used as blocking solution for 1 hour at room temperature. First, antibodies were diluted in blocking solution and incubated at 4°C overnight. The following antibodies were used: P-ATM 1:1000 (no. sc-4526; Cell Signaling), γH2AX 1:1000 (no. 05-636; Upstate), 53BP1 1:500 (no. 4937; Cell Signaling), and BrdU 1:1000 (no. 555627; BD Biosciences). Cells were washed 2 × 5 minutes in PBS. Secondary antibodies were diluted at 1:10,000 in blocking solution and incubated at 37°C for 1 hour. Cells were washed 2 × 5 minutes with PBS and mounted with ProLong Gold Antifade reagent with 4′,6-diamidino-2-phenylindole (no. P36931; Invitrogen). Images were acquired with an inverse wide-field fluorescence microscope (DM IRBE; Leica, Bensheim, Germany) equipped with a black and white camera (ORKA-ER; Hamamatsu, Hamamatsu, Japan). Image processing with Photoshop (Adobe Systems) was applied to whole images only. Images used for comparison between different transductions were acquired with the same instrument settings and exposure time and were processed equally.

Flow Cytometry

Cell cycle distribution was assessed by using a FACSCalibur (FACScan, 488-nm excitation laser; BD Biosciences) and WinMDI software.

Western Analysis

Cells were lysed for 30 minutes on ice in 1× RIPA buffer (Upstate) containing 2 × HALT protease and phosphatase inhibitor cocktail (Thermo Scientific, Rockford, IL). Cell extracts were denatured at 95°C for 5 minutes and homogenized by successive passing through a 30-gauge syringe needle, and protein concentrations were determined using bicinchoninic acid protein assay (Pierce, Rockford, IL).

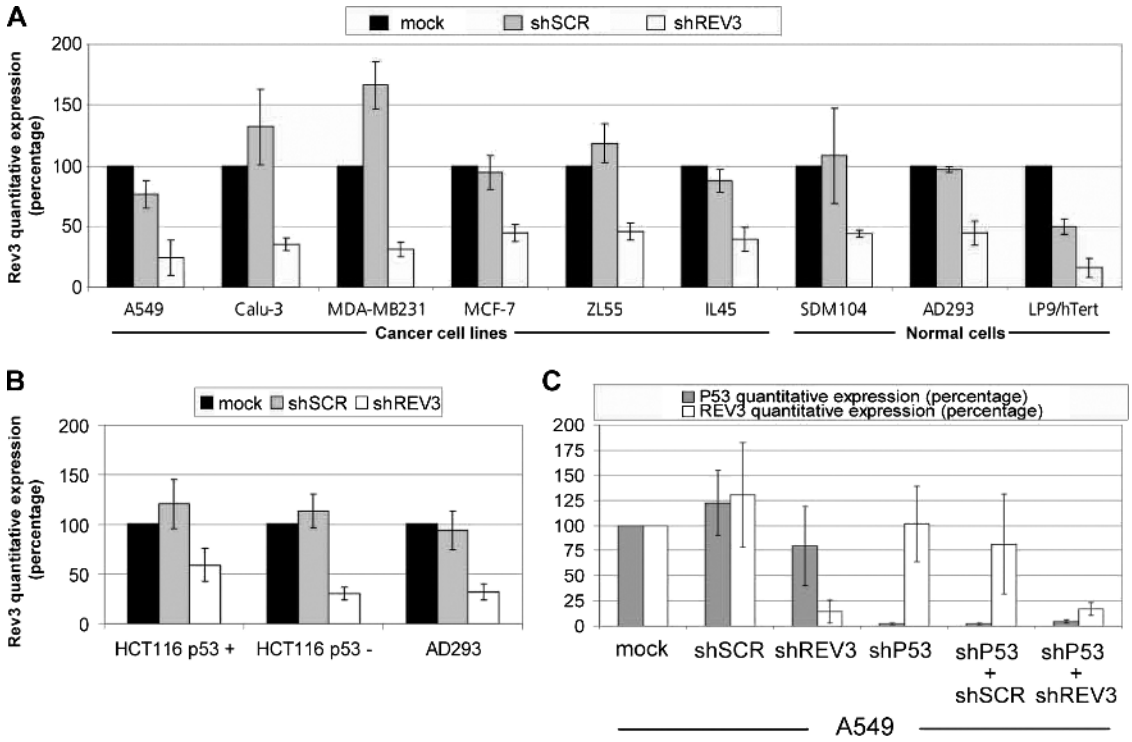

Figure W1. Efficient inhibition of *REV3* expression after transduction with lentiviral-based particles. Cells were mock treated or transduced with lentiviral-based particles containing either shSCR or shREV3 and/or lentiviral-based particles containing shP53. REV3 (A and B) and P53 (C) expression were analyzed by quantitative real-time PCR 7 days after transduction. The averages of at least three independent experiments are given for A549, IL45, p53-proficient HCT116, p53-deficient HCT116, SDM104, and AD293 cells, whereas representative experiments are shown for Calu-3, MDA-MB-231, MCF-7, ZL55, and LP9-hTERT cells. Rev3 expression levels were normalized to histone H3 expression levels. All Rev3 and p53 expression levels are reported as percentage compared with mock-treated A549 (A and C) or p53-proficient HCT116 (B) cells, which was set as 100%. Shown are means ± SD.

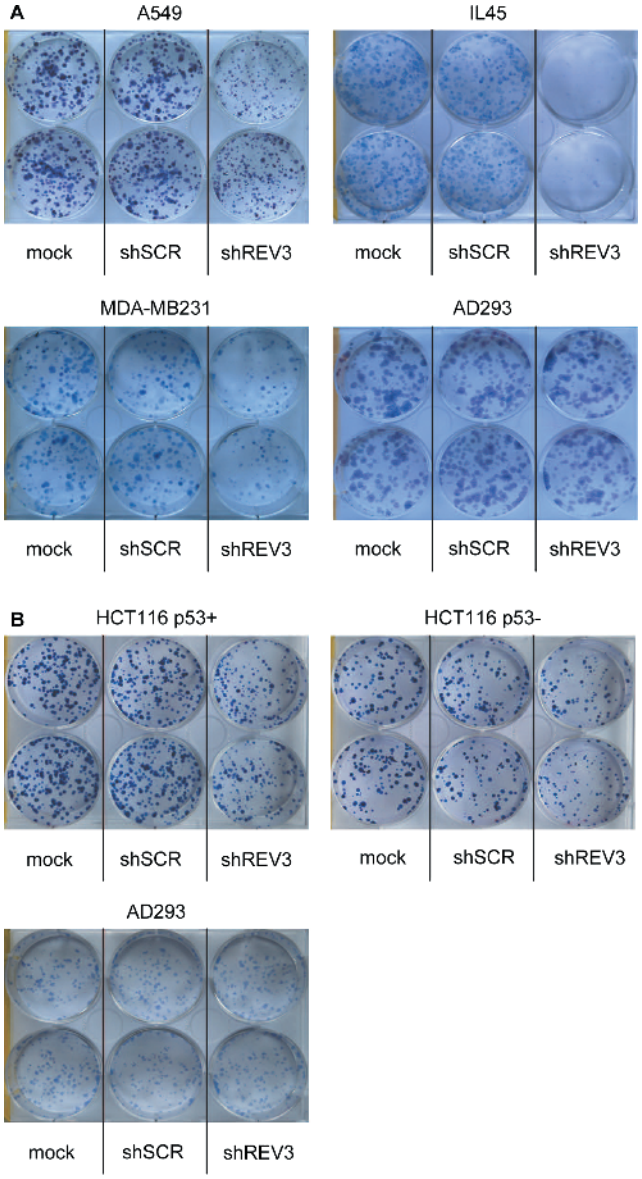

Figure W2. *REV3* silencing specifically reduces colony formation of cancer cells. Cancer cells A549, IL45, MDA-MB-231, p53-proficient HCT116, p53-deficient HCT116, and normal cells AD293 were either mock treated or transduced with lentiviral-based particles containing shSCR or shREV3. Crystal violet staining was performed once colonies were visible by eye. (A) MOI = 170. (B) MOI = 800. Experiments were made in duplicate wells. See also related Figure 1.

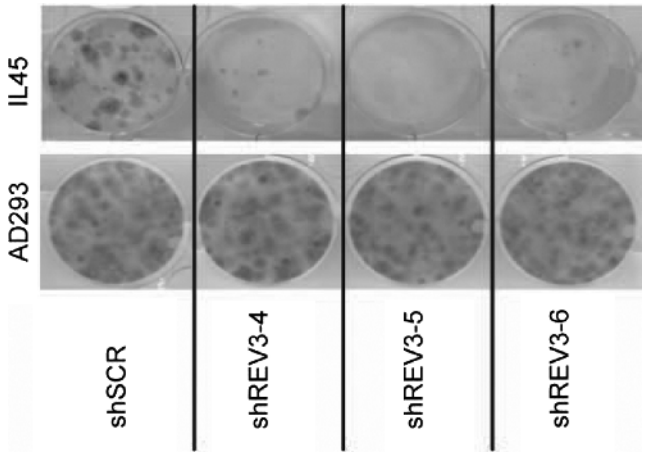

Figure W3. Reduced colony formation after *REV3* silencing is not due to an siRNA off-target effect. IL45 mesothelioma cancer cells and AD293 normal cells were either mock treated or transfected with three different plasmids containing shRNA constructs targeting Rev3. Colonies were stained with crystal violet and counted after 2 weeks. Experiment was made in duplicate wells.

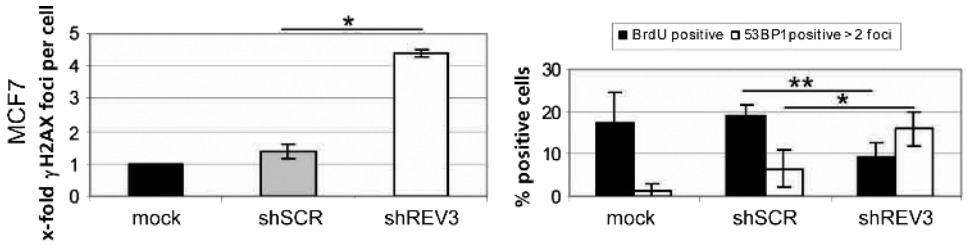

Figure W4. *REV3* depletion induces persistent DNA damage in MCF-7 breast cancer cells. Cells were mock treated or transduced with lentiviral-based particles containing either shSCR or shREV3 and analyzed after 1 week. Cells were stained for γH2AX or BrdU and 53BP1 and quantified by immunofluorescence microscopy. Cells containing more than two 53BP1 foci per cell were considered as positive for 53BP1. At least two independent experiments were analyzed. *$P < .05$. **$P < .01$. Shown are means ± SD.

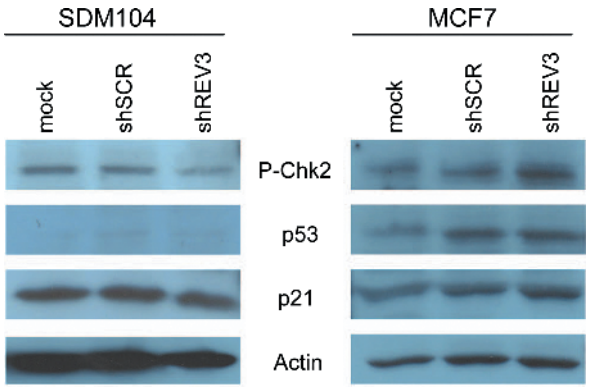

Figure W5. *REV3* depletion induces DDR pathway specifically in cancer cells. Cells were mock treated or transduced with lentiviral-based particles containing either shSCR or shREV3. After 1 week, whole-cell lysates were analyzed by Western analysis.

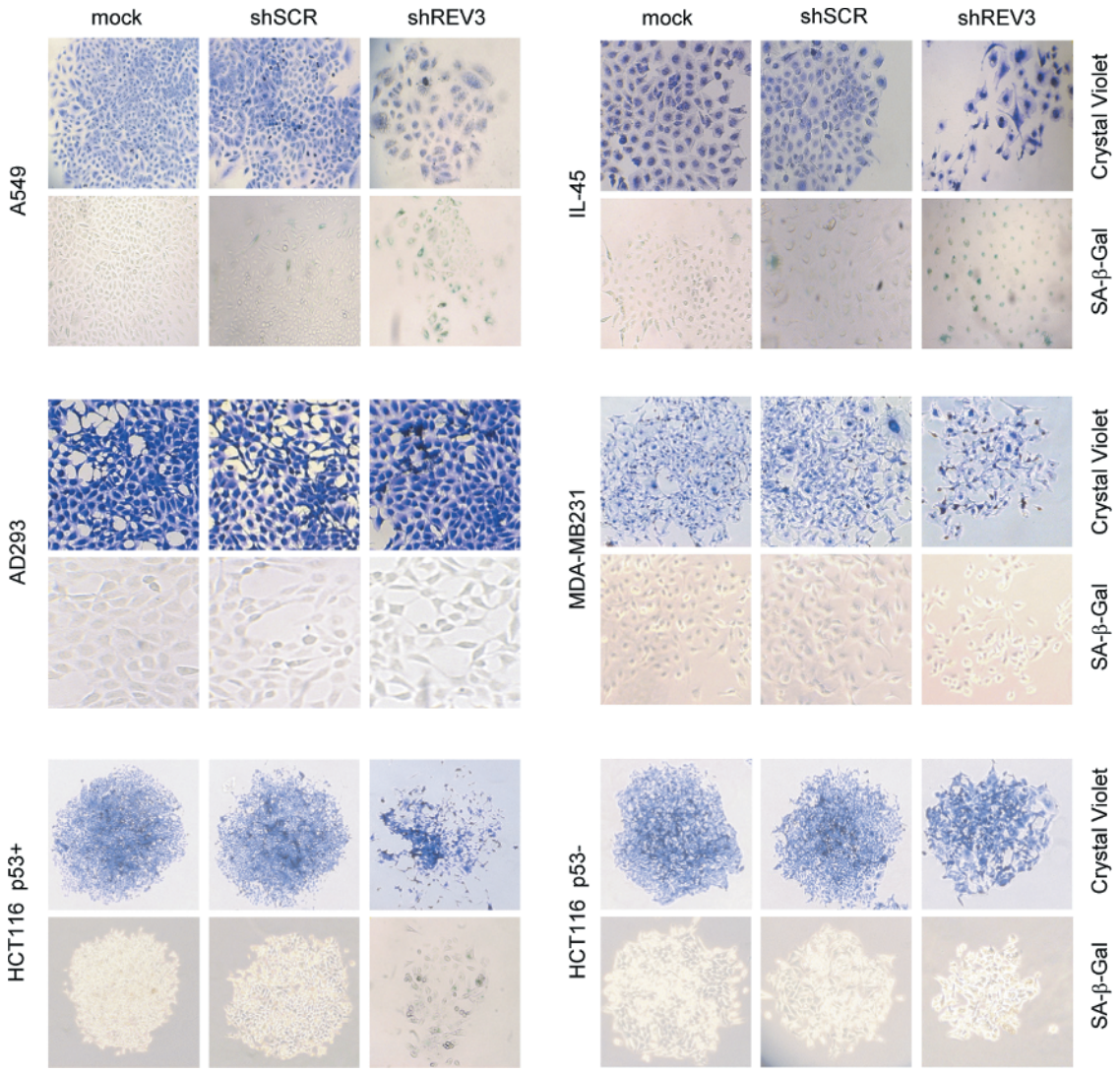

Figure W6. *REV3* silencing induces senescence in p53-proficient cancer cells. Cancer cells A549, IL45, MDA-MB-231, p53-proficient HCT116, and p53-deficient HCT116 and normal cells AD293 were mock treated or transduced with either lentiviral-based particles containing shSCR or shREV3. Crystal violet assay (upper lines) or SA-β-galactosidase assay (bottom lines) was performed after 7 days.

4. Whole genome silencing screens reveal a critical role of REV3 in tolerance of replication stress

Ilya N. Kotov[1], Philip A. Knobel[1]*, Ellen Siebring - van Olst[2], Emanuela Felley-Bosco[1], Victor W. van Beusechem[3], Egbert F. Smit[2], Rolf A. Stahel[1] and Thomas M. Marti[1]**

[1]Clinic of Oncology, University Hospital Zurich, Zurich, Switzerland [2]Department of Pulmonary Diseases and [3]Department of Medical Oncology, VU University Medical Center, Amsterdam, the Netherlands

* Present address: Institute for Research in Biomedicine, Barcelona, Spain

**Present address: Clinic of Thoracic Surgery, University Hospital Bern, Bern, Switzerland

Correspondence should be addressed to Thomas M. Marti thomas.marti@insel.ch

4.1. Abstract

REV3, the catalytic subunit of translesion polymerase zeta (polζ), is commonly associated with DNA damage bypass and repair. Despite sharing accessory subunits with replicative polymerase δ, very little is known about the role of polζ in DNA replication. We previously demonstrated that inhibition of REV3 expression induces persistent DNA damage and growth arrest in cancer cells. To reveal determinants of this sensitivity and obtain insights into the cellular function of REV3, we performed whole-genome silencing screens aimed at identification of synthetic lethal interactions with REV3 in A549 lung cancer cells. The top confirmed hit was RRM1, the large subunit of ribonucleotide reductase (RNR), a critical enzyme of *de novo* nucleotide synthesis. Treatment with the RNR-inhibitor hydroxyurea (HU) synergistically increased the fraction of REV3-deficient cells containing single stranded DNA (ssDNA) as indicated by an increase in replication protein A (RPA). However, this increase was not accompanied by accumulation of the DNA damage marker γH2AX suggesting a role of REV3 in tolerance of replication stress (RS). Consistent with a role of REV3 in DNA replication, increased RPA staining was confined to S-phase cells. Additionally, we found genes related to RS to be significantly enriched among the top hits of the synthetic lethality screen further corroborating the importance of REV3 for replication under conditions of RS.

4.2. Introduction

Integrity and fidelity of the genomic material is constantly compromised in various ways but cells possess multiple mechanisms to cope with it [1]. If DNA damage cannot be removed completely it can be tolerated in order to continue replication without formation of lethal intermediates. Translesion synthesis (TLS) is a key DNA damage tolerance pathway that allows bypass of different types of lesions. Dependent on the nature of the lesion and recruited enzymes, this process can result in faithful or error-prone, thus mutagenic, DNA replication (reviewed in [2]).

Polymerase zeta (polζ), with its catalytic subunit REV3L (hereafter REV3), plays a unique role in TLS. Even though it can bypass various DNA lesions by itself [3], it is thought to be mainly involved in the extension from a nucleotide inserted opposite the lesion by other TLS polymerases (TLS pols). REV3 is therefore able to contribute to mutagenesis in two ways: by introducing mismatches or by extending from a mismatch introduced by another polymerase. Besides, in contrast to other TLS pols, REV3 belongs to B-family and its knockout is embryonic lethal in mice [4, 5]. Despite the development of conditional knockout mice models, [6, 7] the molecular basis for this developmental significance still remains elusive.

Apart from its function in TLS, polζ is known to play a role in homologous recombination [8], non-homologous end-joining [9] and inter- and intrastrand crosslink repair [10, 11]. Additionally, yeast polζ is able to replicate undamaged DNA [12] and shares accessory subunits with polymerase δ [13, 14] emphasizing its tight relationship with normal DNA replication.

Inhibition of REV3 expression in human cells leads to accumulation of DNA double strand breaks (DSB), activation of DNA damage response (DDR) and reduced fraction of S-phase cells [15], which results in increased formation of anaphase bridges and chromosomal breaks/gaps, expression of common fragile sites (CFS), genomic instability [16] and ultimately cell cycle arrest or senescence [15].

Cancer cells harbor multiple mutations in their genome, many of which affect DDR and lead to genomic instability but can be tolerated because of the redundant function of some of the DNA repair pathways [1]. Targeting the genes that carry out the function of the gene disturbed by a mutation is an attractive approach to cancer therapy [17]. In a more general sense there are pathways, disruption of which by itself can be tolerated but become lethal when combined with cancer-specific mutations. This so-called principle of synthetic lethality demonstrated its applicability for targeted cancer therapy of BRCA2-deficient breast cancer by PARP-inhibitors not only at the bench [18, 19] but also at the bedside [20]. Recent publications follow this example by discovering synthetic lethality between MSH2 and DNA polymerase β (POLB), MLH1 and polymerase γ (POLG)[21] as well as Chk1 and polymerase λ (POLL)[22], confirming that synthetic lethality between DDR genes is a common phenomenon.

Loss-of-function genetic screening is a powerful approach for novel target gene discovery that can be employed for detection of synthetic lethal gene interactions in cancer cells (reviewed in [23, 24]). RNA interference technology was successfully used to identify vulnerabilities of cancers driven by certain oncogenes [25]. We took advantage of the whole-genome siRNA library to explore in an unbiased manner synthetic lethality in REV3-deficient cancer cells in order to gain an insight into cellular function of REV3.

4.3. Materials and Methods

Cell culture, plasmid transfections, gene expression analysis

The non-small cell lung cancer (NSCLC) cell line A549 was authenticated by DNA fingerprinting of short tandem repeat loci (Microsynth, Switzerland). All cell lines were cultured in Dulbecco's Modified Eagle's Medium (DMEM) high glucose (Sigma) supplemented with 2mM L-glutamine, 10% fetal calf serum (FCS) and 1% (w/v) penicillin/streptomycin. Cells were grown at 37°C in humidified atmosphere containing 5% CO_2.

Stable cell lines used for the siRNA screening were generated by transfection of A549 cells with either shSCR or shREV3-4 plasmids. Plasmid transfections were performed using Lipofectamine^{TM} 2000 (Invitrogen) according to the manufacturer's instructions. Subsequent selection of resistant clones was performed with 1ug/ml puromycin.

Gene expression was assessed by quantitative real-time PCR (rtPCR) as described previously [15].

Reagents

For siRNA transfections we used DharmaFECT 1 (DF) transfection reagent and siRNA duplexes acquired from Dharmacon (Thermo Fisher Scientific, USA). In the screen and the follow-up experiments siGENOME non-targeting control pool#2 and the PLK1 SMARTpool siRNA were used as negative and positive control, respectively. For flow cytometry and colony formation experiments, REV3 expression was silenced with ON-TARGETplus SMART pool REV3L (siREV3) while ON-TARGETplus non-targeting pool (siNT) was used as a negative control.

Hydroxyurea (HU) was acquired from Applichem, Germany.

CellTiter-Blue® Cell Viability Assay reagent was purchased from Promega, USA.

Oligonucleotides used for cloning and primers for rtPCR were ordered from Microsynth, Switzerland.

Sequences of shREV3-4 and shSCR were disclosed previously [15].

shRRM1 oligo sequence:

5’-GATCCCCGCACAGAAATAGTGGAGTATTCAAGAGA-
TACTCCACTATTTCTGTGCTTTTTA-3’

5’-AGCTTAAAAAGCACAGAAATAGTGGAGTATCTCTTG-
AATACTCCACTATTTCTGTGCGGG-3’

The following primers were used for detection of RRM1 mRNA levels by qPCR:

Forward 5’- CCTGGGAACCATCAAATGCAGCAA-3’

Reverse 5’- GGGCCAGGGAAGCCAAATTACAAA-3’

Vector cloning and transfection

The short hairpin RRM1 oligo was annealed and ligated into pSuperior.puro as described by the manufacturer (OligoEngine,Seattle, WA). The shRNA and H1 promoter fragments were subsequently transferred into the constitutive expressing lentiviral vector pLVTHM (Addgene, Cambridge, MA).
Replication-deficient lentiviral particles were produced and titrated as described previously [15]

Lentiviral transduction and colony forming assay

Lentiviral transduction and subsequent colony forming assay were performed as described previously [15].

For siRNA transfection, lentiviral transduction and subsequent colony formation, the procedure was as follows. 25000 cells per well were seeded in 6 well plates and were transfected 24 hours later with 50nM siRNA (targeting REV3 or non-targeting control) using 2.5µl of DF per well. 24 hours after transfection the medium was exchanged. Another 24 hours later, cells were trypsinized, counted and 500 cells per well were seeded in 6 well plates for the subsequent shRRM1 lentiviral transduction and colony formation assay, which was performed as described previously [15].

Genome-wide siRNA screening and follow –up experiments

The equipment used for the screening was described previously [26]. One day before the transfection, either S1C6 or R1B6 cells (750 cells per well) was seeded in 272 transparent flat-bottom 96 well plates (TPP, Switzerland) in 80µl of medium. Next day 10µl of DF diluted 1:250 in DMEM was added to the siRNA library plates prepared in advance by dilution of the siGENOME stock library and addition of the negative and positive control siRNA. The resulting 20µl transfection mixes were transferred to the cell culture plates, resulting in a final siRNA concentration of 25nM. After transfection, cells were grown for 5 days before 20µl per well of CellTiter-Blue Reagent was added. The plates were subsequently incubated for 4 hours at 37°C and 50µl of 3% SDS solution was added to stop the reaction. Fluorescence of each well was determined with excitation/emission of 540/590nm.

For the deconvolution of the siRNA pools, the experimental conditions were identical, i.e. 25nM of siRNA and 0.04µl of DF per well in 96 well plates. For double transfections 25nM of each siRNA and 0.08µl of DF were used.

Data and statistical analysis

For reading, pre-processing and normalization of the raw fluorescence data the *cellHTS2* Bioconductor package was employed [27]. The data were per plate normalized to the negative control and log-transformed. To generate the differential viability list, genes were sorted by the absolute difference of the viability scores for two screened cell lines and Bayesian statistics for linear models in *limma* package *[28]* was used to calculate the P-value for each gene. For gene set enrichment analysis we employed ROMER from *limma* [29].

To assess statistical significance of treatment (siREV3, shREV3, shRRM1 and HU) effect interactions Analysis of Variance (ANOVA) was performed.

For pairwise comparisons two-tailed Student’s t test was employed.

Flow cytometry

For flow cytometry after 24 hours of HU treatment, 25000 cells per well were seeded in 6 well plates and transfected as described above (50nM siRNA + 2.5µl DF). For flow cytometry after 72 hours of HU treatment, 5000 cells per well were seeded in 6 well plates and transfected with 20nM siRNA and 1µl of DF. 24 hours after transfection the medium was exchanged and another 24 hours later, cells were treated with 0.25µM of HU. After 24 or 72 hours, respectively, cells were labeled with 10 µM EdU for 60 min (according to the manufacturer's instructions (C35002; Invitrogen)) harvested by trypsinization, and fixed for 20 min with ice-cold 70% Ethanol at room temperature. Cells were washed with 1% BSA/PBS, pH 7.4, permeabilized with 0.5% saponin/1% BSA/PBS for 10minutes , and stained in the fixation buffer with anti–γ-H2AX antibody (05-636, EMD Millipore) or anti-RPA32/RPA2 antibody (ab2175, Abcam) overnight at 4°C, followed by incubation with a secondary antibody (a31553, Invitrogen) for 30 min at room temperature. Subsequently, cells were treated with 20ug/ml RNase A and DNA was stained with 0.5 µg/ml propidium iodide (Sigma-Aldrich). Cell fluorescence was measured on an Attune flow cytometer (Applied Biosystems) and analyzed with the Attune cytometric software v1.2.5 (Applied Biosystems).

4.4. Results

Characterization of cell lines used for the screening

In order to define synthetic lethal gene interactions with REV3, we generated cell lines containing short hairpin targeting REV3 as well as control cell lines containing the vector with the scrambled short hairpin sequence. Translesion synthesis is a major pathway involved in bypass and repair of DNA crosslinks and it is known that reduction of REV3 levels is associated with the increased sensitivity to DNA crosslinking agents [10, 11].Thus we based selection of the cell lines used for the screening on their REV3 expression levels and their cisplatin sensitivity as a functional readout.

Compared to the parental cell line A549, the REV3 mRNA expression level in the control cell line S1C6 was identical whereas REV3 expression in the cell line R1B6 was decreased to 49% (Fig.1). The cisplatin sensitivity assessed by quantitation of cell viability 5 days after continuous drug treatment differed significantly for the two cell lines. The REV3 deficient cell line R1B6 was up to three times more sensitive than its proficient counterpart S1C6 (Fig.1) indicating that the decrease of REV3 mRNA expression is of functional relevance.

Genome wide siRNA screening reveals a role of REV3 in tolerance of nucleotide deprivation

First we optimized the general screening setup, i.e. number of seeded cells per well and incubation time after transfection, and established positive and negative controls. To find the most suitable conditions for the automated forward transfection of the selected cell lines we optimized siRNA and transfection reagent concentration to minimize toxicity of transfection and to maximize target gene knockdown assessed by rtPCR, reduction of enzymatic activity in a functional GAPDH knockdown assay and performance of positive control (data not shown). The optimized transfection conditions resulted in efficient gene knockdown and were also used for further experiments (Suppl.Fig.1).

Whole genome silencing siRNA screens were carried out with cell viability as readout (Fig.2). In detail, R1B6 or S1C6 cells were seeded in 96 well plates and transfected with

the library containing pooled siRNA (4 siRNA per gene) targeting more than 20000 human transcripts. Cell viability was assessed using CellTiter-Blue Cell Viability Assay and resulting values were normalized to non-targeting siRNA (siNT) control, log-transformed and scored. The screens showed high correlation between replicates, i.e. Pearson correlation coefficient between replicates was 0.87 for S1C6 and 0.84 for R1B6 (Suppl. Table 1). The positive (PLK1) and negative (non-targeting) controls performed well as evidenced by Z' factors [30] generally exceeding 0.5.

To identify genes whose silencing induced synthetic lethality specifically in REV3–deficient cells, the gene list with the corresponding values of viability was sorted by the robust score of absolute difference in viability between S1C6 and R1B6 (Suppl. Table 2). To exclude low-confidence genes we applied a filter of $P<0.05$ (Suppl. Table 3).

Validation of the screening results was performed using S1C6, R1B6 and the original lung cancer cells A549. For validation, we selected genes with the highest confidence scores (i.e. lowest p-values) and highest absolute value of the differential viability effect. First, we performed silencing of the selected genes by manual transfection with the pools from the library used for the screens (Suppl.Fig.2A). Positive control PLK1 had similar killing effect on the three cell lines with the residual viability in the range of 10-15% indicating that the transfection efficiency was the same for the three cell lines. The REV3-deficient cell line R1B6 was in general more sensitive to gene silencing than the two control cell lines confirming the validity of the results obtained by the high throughput screen.

We further deconvolved 15 selected genes by separately transfecting with the four individual siRNAs composing the pools. In total, 11 genes out of 15 had 2 or more siRNA with preferential killing of R1B6 when compared to S1C6 and A549 (Suppl. Fig.3). Silencing of RRM1, the large subunit of ribonucleotide reductase, showed the second strongest differential effect in the screen and a very robust profile in deconvolution process, i.e. all siRNA had more pronounced effect on REV3-deficient cells (Suppl. Fig.2B). Silencing of the small subunit of ribonucleotide reductase (RNR), RRM2, also scored in the top 2% (rank 292), suggesting that the inhibition of the

catalytic function of RNR is involved in the observed reduction of viability in a REV3-deficient background rather than a subunit-specific effect.

To assess whether alterations in nucleotide synthesis pathways in general are synergistic with REV3 silencing, we employed gene set enrichment analysis for linear models using rotation tests (ROMER) [29], which is particularly suitable for the analysis of experiments with a small number of replicates [31]. We tested a set of KEGG pathways related to nucleotide metabolism and found both purine and pyrimidine metabolisms as significantly enriched (Table 2).

Since inhibition of RNR reduces concentration of deoxynucleotides and leads to induction of replication stress [32] we tested whether the reduction in viability upon silencing of REV3 in combination with RNR inhibition can be extended to the genes associated with the replication stress. To guarantee an unbiased analysis, we generated a gene set by search of the NCBI human gene database with the term “replication+stress” (Suppl. Table 4). The “replication+stress” gene set was significantly enriched among the genes that had high differential score in the screen (Table 2).

REV3 is essential to tolerate the inhibition of ribonucleotide reductase in cancer cells

To exclude a clonal effect, we investigated whether we could reproduce in the parental cell line A549 the reduction in colony formation observed in REV3-depleted cells after RRM1 silencing . For RRM1 silencing, we produced lentiviral particles carrying short hairpin targeting RRM1 mRNA (LV-shRRM1). Down-regulation of REV3 expression in combination with subsequent RRM1 silencing synergistically reduced cell growth of parental A549 cells (Fig.3A).

We hypothesized that the reduction of cancer cell growth in a REV3-deficient background is dependent on the catalytic function of RNR. In this case a drug targeting the enzymatic activity of RNR should mimic the reduction of colony formation after RRM1 silencing in a REV3-deficient background. Hydroxyurea (HU) is a drug used in the treatment of myeloproliferative disorders that inhibits RNR by scavenging tyrosyl free radicals of the small subunit required for reduction of ribonucleotides to deoxyribonucleotides. We performed colony formation assays after siRNA transfection

(with siNT or siREV3) followed by continuous HU treatment (Fig.3 B,C). While the colony formation was reduced by REV3 silencing alone, its combination with the HU treatment caused more pronounced decrease in cell viability than expected by mere superposition of the individual effects, the interaction effect (HU:iREV3) being statistically significant.

Down-regulation of REV3 expression enhances replication stress induced by inhibition of ribonucleotide reductase

The synergy of REV3-depletion and inhibition the catalytic function of RNR taken together with the enrichment of other genes associated with replication stress in the screen results led us to a hypothesis that REV3 might be involved in the tolerance of nucleotide deprivation-induced replication stress in cancer cells. To test this hypothesis we performed a series of flow cytometry experiments to investigate changes of EdU incorporation,and determine the fraction of γH2AX and RPA positive cells as well as the cell cycle distribution after REV3 silencing for 48 hours and HU treatment for 24 hours.

HU treatment and REV3 depletion both significantly reduced the median EdU incorporation (Fig.4). EdU incorporation was significantly decreased after siREV3 transfection and subsequent HU treatment compared to HU-treated cells previously transfected with the non-targeting control siRNA (siNT).

Replication protein A (RPA) is a protein that binds single-stranded DNA (ssDNA), detection of chromatin-bound RPA2 can be used to track the increase in cellular ssDNA [33], a characteristic feature of replication stress [34]. Down-regulation of REV3 expression did not change significantly the fraction of RPA-positive cells, compared to control transfection. HU treatment significantly increased the number of RPA-positive cells, which was further increased by the control transfection and even more after REV3 silencing. We found the synergy between HU treatment and REV3 silencing to be significant evidenced by the low p-value for the interaction effect HU:iREV3.

An increased RPA signal can not only be due to enhanced replication stress but also due to increased end-resection during the process of DSB repair. To differentiate between these two causes we investigated whether observed increase in RPA staining is accompanied by changes in DNA damage induction. H2AX phosphorylation is a widely associated with various types of DNA damage including DSBs [35]. We took

advantage of that to rule out the induction of DSBs as the cause for RPA induction in our system. HU treatment was associated with a moderate but significant increase of the fraction of γH2AX positive cells. Unexpectedly, preceding siNT transfection increased γH2AX induction by HU treatment, while siREV3 transfection did not lead to a significant change compared to HU treated cells. Interestingly, comparison of siNT+HU and siREV3+HU revealed a significant decrease of H2AX phosphorylation by REV3 silencing upon HU treatment.

In summary, the synergistic accumulation of ssDNA as indicated by the increased fraction of RPA-positive cells when combining siREV3 transfection with HU treatment without increase in γH2AX (or even with a decrease when compared to siNT+HU) leads us to the conclusion that REV3 depletion leads to aggravated replication stress induced by HU treatment.

To further investigate in more details the role of REV3 in the tolerance of replication stress we analyzed the cell cycle distribution after inhibition of REV3 expression and HU treatment (Fig.5). We showed previously that siRNA-mediated REV3 silencing significantly decreased the fraction of cancer cells in S-phase whereas the fraction of cells in the G_2-phase of the cell cycle was significantly increased [15]. This observation is in agreement with a suggested function of REV3 outside of S-phase [36]. As expected, HU treatment induced a pronounced S-phase accumulation. This accumulation was not further enhanced by additional REV3 silencing, but the HU:iREV3 interaction was significant in all cell cycle phases reflecting that the cell cycle distribution of REV3-deficient cells was more perturbed by HU treatment than that of the controls. We also compared the fractions of RPA positive cells in different cell cycle phases (Fig.6). In S-phase, the fraction of RPA positive siREV3+HU treated cells was significantly higher than that of siNT+HU and HU treated cells, whereas the corresponding difference was not significant in G_1- and G_2-phases. This indicates that the synergistic RPA increase for the combination of siREV3 transfection and HU treatment (Fig.4) occurs mainly in the S-phase of the cell cycle.

In summary, in REV3-deficient cells upon HU-treatment, a significant increase in the fraction of cells with positive RPA staining is confined to S-phase consistent with the role of polζ in DNA replication upon RS.

4.5. Discussion

This study aimed to identify synthetic lethal gene interactions with REV3 in lung cancer cells. For screening, we used stable cell lines obtained from A549 by transfection with the vector carrying short hairpin against REV3 or the control vector. The 50% decrease in REV3 expression in the cell line R1B6 is of physiological relevance since it conferred cisplatin sensitivity

Screening of a whole genome library allowed us to determine synthetic lethal interactions with REV3 in an unbiased way. Therefore a top position of a gene in the screen indicates that the viability of the tested REV3-deficient NSCLC cells is heavily dependent on this gene. Our analysis revealed that silencing of RRM1, the large subunit of RNR, had the second most pronounced effect in reduction of cell viability specifically in a REV3-deficient background. Additionally, RRM2, the small subunit of RNR, also ranked under the top genes in our screen (#292) further corroborating that inhibition of RNR is synthetic lethal with REV3 depletion. RRM2 is overexpressed in many tumor types. For example, it was shown that RRM2 is highly (~15x) overexpressed in NSCLC [37]. Moreover, RRM2 was suggested to act in cooperation with a variety of oncogenes to increase their transformation and tumorigenic potential [38]. It is well known that inhibition of RNR function affects proliferation of cancer cells to a greater extent than the normal cells which allows successful application of small molecule inhibitors targeting RNR in the clinics for cancer treatment (reviewed in [39]). All these data suggest that cancer cells are frequently addicted to RNR overexpression. Therefore, we further focused our analysis on the synthetic lethal interaction of REV3 with RNR.

Downregulation of RRM1 expression and treatment with HU, a drug inhibiting small subunit RRM2 of RNR, in combination with transient siRNA based depletion of REV3 resulted in the synergistic inhibition of cell proliferation. This indicates that the observed effects are not RNR-subunit specific and rather related to RNR catalytic function and nucleotide deprivation as a result of its inhibition. Inhibition of RNR catalytic activity leads to deprivation of deoxyribonucleotides, reduced replication rate and stalling of replication forks [40]. Higher concentrations of HU (~2mM) can induce complete cell cycle arrest which is often exploited for synchronization of cultured cells. The concentrations that we use (0.2-0.3mM) create nucleotide shortage thereby generating

conditions of mild replication stress but still allowing replication. Therefore we tested whether RS-related genes were overrepresented among the genes whose inhibition induced synthetic lethality in the REV3-deficient background and found this enrichment to be significant. We proceeded with detection of chromatin-bound RPA, an indication for replication associated ssDNA formation, and controlling levels of DNA damage measured by H2AX phosphorylation. Compared to individual treatments, combination of HU treatment with REV3 silencing synergistically increased the fraction of RPA positive cells, which was not accompanied by increased levels of **γ**H2AX, suggesting that it was caused not by increase in DNA damage repair, but by induction of RS. Thus, under conditions of RS, silencing of REV3 impairs DNA replication but does not lead to increased DNA damage accumulation indicating that polζ is directly involved in DNA replication. This is further corroborated by our finding that the fraction of S-phase cells after siREV3+HU treatment is significantly higher than could be expected from a simple additive effect of HU treatment and REV3 silencing, which corroborates a significant role of REV3 in S-phase of HU-treated cells. Moreover, the significant increase in RPA positive cells was found only in S phase and not in G_1 and G_2 phases of the cell cycle.

The role of REV3 in the tolerance of nucleotide depletion can be associated either with its function in DNA damage repair/tolerance or its direct involvement in DNA replication [12]. Even though Polζ is thought to be mainly involved in the first, recently it was shown that Polζ takes part in the replication of fragile sites [16]. We did not expect that the concentrations of HU that we used would strongly increase amount of DNA DSB since treatment of cells with 8 times higher HU concentration for the same time (24 hours) resulted only in a moderate induction of DSB as shown by pulse-field gel electrophoresis [40]. Also single stranded breaks were not detected by alkaline unwinding technique [41] after treatment with comparably low concentration of HU (0.1mM). Nevertheless, due to the high sensitivity of the flow cytometry method, we detected increased H2AX phosphorylation upon HU treatment that was further increased by preceding transfection with control siRNA. Lipid-mediated siRNA transfection is known to affect permeability of the cell membrane. For example, recommendation to use an antibiotic-free medium for transfection is given to avoid increased antibiotic uptake and associated cell toxicity (http://www.thermoscientificbio.com/uploadedFiles/Resources/basic-dharmafect-

protocol.pdf). In analogy, we speculate that the increased H2AX phosphorylation detectable after control transfection and subsequent HU treatment is due to increased drug penetration and therefore the higher effective intracellular HU concentration even when cells were treated after removal of the transfection reagent.

It was shown previously that mild RS can cause formation of 53BP1 nuclear bodies and increased H2AX phosphorylation specifically at common fragile sites when the cells carry unreplicated regions through mitosis [42]. HU treatment significantly reduced the replication rates of REV3-deficient cells compared to REV3-proficient cells therefore we assume that the fraction of cells undergoing mitosis was also reduced in REV3-deficient cells. Thus, we speculate that the decreased level of γH2AX in siREV3+HU treated cells compared to siNT+HU control can be attributed to the decreased replication rate, demonstrated by decreased EdU incorporation, upon REV3 silencing and thereby reduced level of HU-induced replication associated DNA damage. Consistently, it was previously reported that DNA damage induced H2AX phosphorylation is replication dependent and can be reduced by contact inhibition [35].

Nucleotide biosynthesis is commonly up-regulated to cope with increased metabolic requirements of cancer cells [43]. Therefore many oncogenes not only induce replication stress [44] [45, 46], but also activate nucleotide synthesis [47]. Thus, concentrations of the 4 dNTPs in tumor cells are on average 6-11 fold over normal cells [48]. But if the cell fails to adjust its metabolism, nucleotide deficiency promotes genomic instability [47] and also can lead to oncogene-induced senescence [49]. Interestingly, cells lacking REV3 undergo senescence and accumulate persistent DNA DSBs at later time points [7, 15] possibly reflecting their inability to cope with RS [32]. Based on our present findings it is tempting to hypothesize that oncogene-induced RS could be the unifying feature responsible for the observed cancer cell specific growth arrest upon REV3 silencing described earlier by our group [15].

The function of Polζ in the replication under conditions of nucleotide deficiency associated replication stress might also help in understanding its role in embryogenesis. Rev3 knockout is embryonic lethal in mice causing depletion of hematopoietic compartment and embryonic stem cells [4]. A recent study showed that hematopoietic

tissue is highly prone to RS associated with nucleotide pool imbalance [50]. During hematopoiesis, a state similar to thymidine block occurs making this process strongly dependent on the activity of *de novo* nucleotide synthesis pathway. Besides, human embryonic stem cells are very sensitive to RS [51] and high levels of RS are observed upon stem cell induction [52]. Apparently, hematopoietic and embryonic stem cells overexpress REV3 in order to cope with excessive RS and suffer the most upon REV3 depletion.

In summary, our study identifies a novel function of human polζ in the tolerance of replication stress thereby broadening our understanding of its role in cell biology.

4.6. References

1. Jackson, S.P. and J. Bartek, *The DNA-damage response in human biology and disease.* Nature, 2009. **461**(7267): p. 1071-8.
2. Knobel, P.A. and T.M. Marti, *Translesion DNA synthesis in the context of cancer research.* Cancer Cell Int, 2011. **11**: p. 39.
3. Stone, J.E., et al., *Lesion bypass by S. cerevisiae Pol zeta alone.* DNA Repair (Amst), 2011. **10**(8): p. 826-34.
4. Esposito, G., et al., *Disruption of the Rev3l-encoded catalytic subunit of polymerase zeta in mice results in early embryonic lethality.* Curr Biol, 2000. **10**(19): p. 1221-4.
5. Wittschieben, J., et al., *Disruption of the developmentally regulated Rev3l gene causes embryonic lethality.* Curr Biol, 2000. **10**(19): p. 1217-20.
6. Wittschieben, J.P., et al., *Loss of DNA Polymerase {zeta} Enhances Spontaneous Tumorigenesis.* Cancer Res.
7. Lange, S.S., et al., *Dual role for mammalian DNA polymerase zeta in maintaining genome stability and proliferative responses.* Proc Natl Acad Sci U S A, 2013.
8. Sharma, S., et al., *REV1 and polymerase zeta facilitate homologous recombination repair.* Nucleic Acids Res, 2012. **40**(2): p. 682-91.
9. Covo, S., et al., *Translesion DNA synthesis-assisted non-homologous end-joining of complex double-strand breaks prevents loss of DNA sequences in mammalian cells.* Nucleic Acids Res, 2009.
10. Hicks, J.K., et al., *Differential roles for DNA polymerases eta, zeta, and REV1 in lesion bypass of intrastrand versus interstrand DNA cross-links.* Mol Cell Biol, 2010. **30**(5): p. 1217-30.
11. Enoiu, M., J. Jiricny, and O.D. Scharer, *Repair of cisplatin-induced DNA interstrand crosslinks by a replication-independent pathway involving transcription-coupled repair and translesion synthesis.* Nucleic Acids Res, 2012. **40**(18): p. 8953-64.
12. Northam, M.R., et al., *Participation of DNA polymerase zeta in replication of undamaged DNA in Saccharomyces cerevisiae.* Genetics, 2010. **184**(1): p. 27-42.

13. Johnson, R.E., L. Prakash, and S. Prakash, *Pol31 and Pol32 subunits of yeast DNA polymerase delta are also essential subunits of DNA polymerase zeta.* Proc Natl Acad Sci U S A, 2012. **109**(31): p. 12455-60.
14. Makarova, A.V., J.L. Stodola, and P.M. Burgers, *A four-subunit DNA polymerase zeta complex containing Pol delta accessory subunits is essential for PCNA-mediated mutagenesis.* Nucleic Acids Res, 2012. **40**(22): p. 11618-26.
15. Knobel, P.A., et al., *Inhibition of REV3 expression induces persistent DNA damage and growth arrest in cancer cells.* Neoplasia, 2011. **13**(10): p. 961-70.
16. Bhat, A., et al., *Rev3, the catalytic subunit of Polzeta, is required for maintaining fragile site stability in human cells.* Nucleic Acids Res, 2013.
17. Kaelin, W.G., Jr., *The concept of synthetic lethality in the context of anticancer therapy.* Nat Rev Cancer, 2005. **5**(9): p. 689-98.
18. Bryant, H.E., et al., *Specific killing of BRCA2-deficient tumours with inhibitors of poly(ADP-ribose) polymerase.* Nature, 2005. **434**(7035): p. 913-7.
19. Farmer, H., et al., *Targeting the DNA repair defect in BRCA mutant cells as a therapeutic strategy.* Nature, 2005. **434**(7035): p. 917-21.
20. Fong, P.C., et al., *Inhibition of poly(ADP-ribose) polymerase in tumors from BRCA mutation carriers.* N Engl J Med, 2009. **361**(2): p. 123-34.
21. Martin, S.A., et al., *DNA polymerases as potential therapeutic targets for cancers deficient in the DNA mismatch repair proteins MSH2 or MLH1.* Cancer Cell, 2010. **17**(3): p. 235-48.
22. Zucca, E., et al., *Silencing of human DNA polymerase lambda causes replication stress and is synthetically lethal with an impaired S phase checkpoint.* Nucleic Acids Res, 2013. **41**(1): p. 229-41.
23. Mullenders, J. and R. Bernards, *Loss-of-function genetic screens as a tool to improve the diagnosis and treatment of cancer.* Oncogene, 2009. **28**(50): p. 4409-20.
24. Nijman, S.M., *Synthetic lethality: general principles, utility and detection using genetic screens in human cells.* FEBS Lett, 2011. **585**(1): p. 1-6.
25. Luo, J., et al., *A genome-wide RNAi screen identifies multiple synthetic lethal interactions with the Ras oncogene.* Cell, 2009. **137**(5): p. 835-48.

26. Siebring-van Olst, E., et al., *Affordable luciferase reporter assay for cell-based high-throughput screening.* J Biomol Screen, 2013. **18**(4): p. 453-61.
27. Boutros, M., L.P. Bras, and W. Huber, *Analysis of cell-based RNAi screens.* Genome Biol, 2006. **7**(7): p. R66.
28. Smyth, G.K., *Linear models and empirical bayes methods for assessing differential expression in microarray experiments.* Stat Appl Genet Mol Biol, 2004. **3**: p. Article3.
29. Majewski, I.J., et al., *Opposing roles of polycomb repressive complexes in hematopoietic stem and progenitor cells.* Blood, 2010. **116**(5): p. 731-9.
30. Zhang, J.H., T.D. Chung, and K.R. Oldenburg, *A Simple Statistical Parameter for Use in Evaluation and Validation of High Throughput Screening Assays.* J Biomol Screen, 1999. **4**(2): p. 67-73.
31. Dorum, G., et al., *Rotation testing in gene set enrichment analysis for small direct comparison experiments.* Stat Appl Genet Mol Biol, 2009. **8**: p. Article34.
32. Feng, W., et al., *Replication stress-induced chromosome breakage is correlated with replication fork progression and is preceded by single-stranded DNA formation.* G3 (Bethesda), 2011. **1**(5): p. 327-35.
33. Forment, J.V., R.V. Walker, and S.P. Jackson, *A high-throughput, flow cytometry-based method to quantify DNA-end resection in mammalian cells.* Cytometry A, 2012. **81**(10): p. 922-8.
34. Vassin, V.M., et al., *Human RPA phosphorylation by ATR stimulates DNA synthesis and prevents ssDNA accumulation during DNA-replication stress.* J Cell Sci, 2009. **122**(Pt 22): p. 4070-80.
35. Marti, T.M., et al., *H2AX phosphorylation within the G1 phase after UV irradiation depends on nucleotide excision repair and not DNA double-strand breaks.* Proc Natl Acad Sci U S A, 2006. **103**(26): p. 9891-6.
36. Brondello, J.M., et al., *Novel evidences for a tumor suppressor role of Rev3, the catalytic subunit of Pol zeta.* Oncogene, 2008. **27**(47): p. 6093-101.
37. Hou, J., et al., *Gene expression-based classification of non-small cell lung carcinomas and survival prediction.* PLoS One, 2010. **5**(4): p. e10312.

38. Fan, H., et al., *The mammalian ribonucleotide reductase R2 component cooperates with a variety of oncogenes in mechanisms of cellular transformation.* Cancer Res, 1998. **58**(8): p. 1650-3.
39. Cerqueira, N.M., et al., *Overview of ribonucleotide reductase inhibitors: an appealing target in anti-tumour therapy.* Curr Med Chem, 2005. **12**(11): p. 1283-94.
40. Petermann, E., et al., *Hydroxyurea-stalled replication forks become progressively inactivated and require two different RAD51-mediated pathways for restart and repair.* Mol Cell, 2010. **37**(4): p. 492-502.
41. Skog, S., et al., *Hydroxyurea-induced cell death in human T lymphoma cells as related to imbalance in DNA/protein cycle and deoxyribonucleotide pools and DNA strand breaks.* Anticancer Drugs, 1992. **3**(4): p. 379-86.
42. Lukas, C., et al., *53BP1 nuclear bodies form around DNA lesions generated by mitotic transmission of chromosomes under replication stress.* Nat Cell Biol, 2011. **13**(3): p. 243-53.
43. Tong, X., F. Zhao, and C.B. Thompson, *The molecular determinants of de novo nucleotide biosynthesis in cancer cells.* Curr Opin Genet Dev, 2009. **19**(1): p. 32-7.
44. Gorgoulis, V.G., et al., *Activation of the DNA damage checkpoint and genomic instability in human precancerous lesions.* Nature, 2005. **434**(7035): p. 907-13.
45. Halazonetis, T.D., V.G. Gorgoulis, and J. Bartek, *An oncogene-induced DNA damage model for cancer development.* Science, 2008. **319**(5868): p. 1352-5.
46. Neelsen, K.J., et al., *Oncogenes induce genotoxic stress by mitotic processing of unusual replication intermediates.* J Cell Biol, 2013. **200**(6): p. 699-708.
47. Bester, A.C., et al., *Nucleotide deficiency promotes genomic instability in early stages of cancer development.* Cell, 2011. **145**(3): p. 435-46.
48. Traut, T.W., *Physiological concentrations of purines and pyrimidines.* Mol Cell Biochem, 1994. **140**(1): p. 1-22.
49. Aird, K.M., et al., *Suppression of nucleotide metabolism underlies the establishment and maintenance of oncogene-induced senescence.* Cell Rep, 2013. **3**(4): p. 1252-65.

50. Austin, W.R., et al., *Nucleoside salvage pathway kinases regulate hematopoiesis by linking nucleotide metabolism with replication stress.* J Exp Med, 2012. **209**(12): p. 2215-28.
51. Desmarais, J.A., et al., *Human embryonic stem cells fail to activate CHK1 and commit to apoptosis in response to DNA replication stress.* Stem Cells, 2012. **30**(7): p. 1385-93.
52. Pasi, C.E., et al., *Genomic instability in induced stem cells.* Cell Death Differ, 2011. **18**(5): p. 745-53.

4.7. Figures and tables

Rank	Gene	P-value	Viability difference score*	Gene name
1	GPR27	1.7E-03	2.67	G protein-coupled receptor 27
2	RRM1	1.6E-02	2.49	ribonucleotide reductase M1
3	CFLAR	4.9E-05	2.24	CASP8 and FADD-like apoptosis regulator
4	LMTK3	1.2E-02	2.19	lemur tyrosine kinase 3
5	CCR6	4.6E-04	2.13	chemokine (C-C motif) receptor 6
7	CACNA1A	2.3E-03	2.10	calcium channel, voltage-dependent, P/Q type, alpha 1A subunit
8	COPZ1	9.4E-03	2.09	coatomer protein complex, subunit zeta 1
9	CDY1	2.4E-02	2.09	chromodomain protein, Y-linked, 1
10	CSAD	2.2E-02	2.08	cysteine sulfinic acid decarboxylase
11	RASGRP2	8.6E-03	2.00	RAS guanyl releasing protein 2, CDC25L
12	SERPINH1	1.9E-02	1.93	serpin peptidase inhibitor, clade H (heat shock protein 47), member 1, (collagen binding protein 1)
…	…	…	…	…
30	UBE2N	8.4E-04	1.63	ubiquitin-conjugating enzyme E2N (UBC13 homolog)
292	RRM2	4.9E-03	0.85	ribonucleotide reductase M2

Table 1. Highest ranking genes with a stronger effect on viability of REV3-deficient cells compared to control cells.

*All the genes in the screen were scored based on the normalized viability of the cells after its silencing. In the final list genes are sorted according to the difference of scores for control and REV3-deficient cell lines. Filter of $P<0.05$ is applied to exclude low-confidence genes. Results are from four whole-genome silencing screens summarized as described in the material and methods section

Gene set	P-value
Purine metabolism KEGG: hsa00230	0.0041
Pyrimidine metabolism KEGG: hsa00240	<1E-5
Replication stress [Homo sapiens]*	0.00034

Table 2. Selected gene sets whose silencing had stronger effect on the viability of REV3-deficient cells

We tested whether nucleotide synthesis pathways and genes associated with replication stress are enriched among the genes whose silencing had stronger effect on the viability of REV3-deficient cells. The testing was performed by ROMER. *Replication stress gene list was generated by searching NCBI gene database with the term “replication+stress” (Table S4).

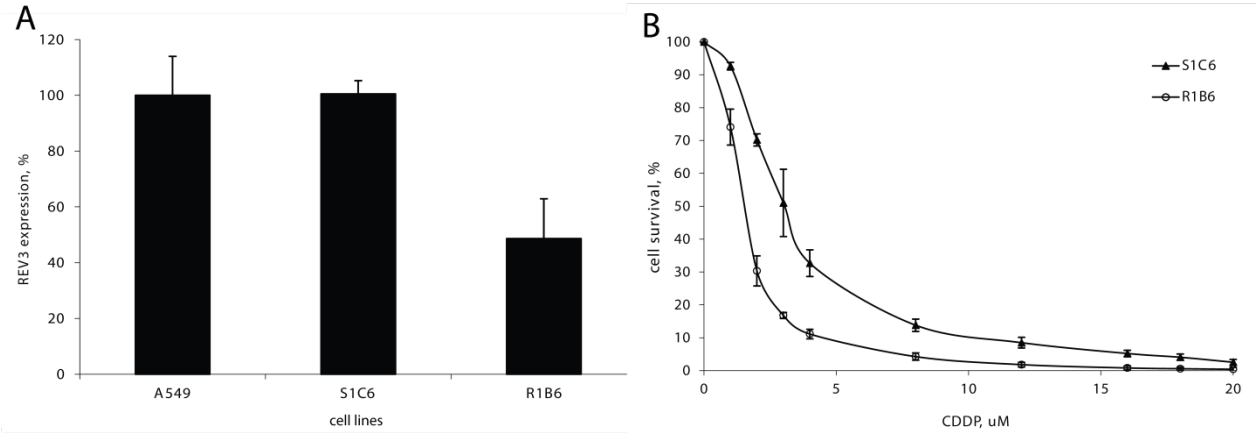

Figure 1. Characterization of the cell lines used for the screening

(A) REV3 mRNA level determined by rtPCR in the parental cell line A549, clone R1B6 carrying short-hairpin targeting REV3 mRNA and the control cell line S1C6 carrying the scrambled control construct. (B) Sensitivity of the generated cell lines to continuous cisplatin treatment. Cell viability was determined after 5 days of cisplatin (CDDP) treatment.

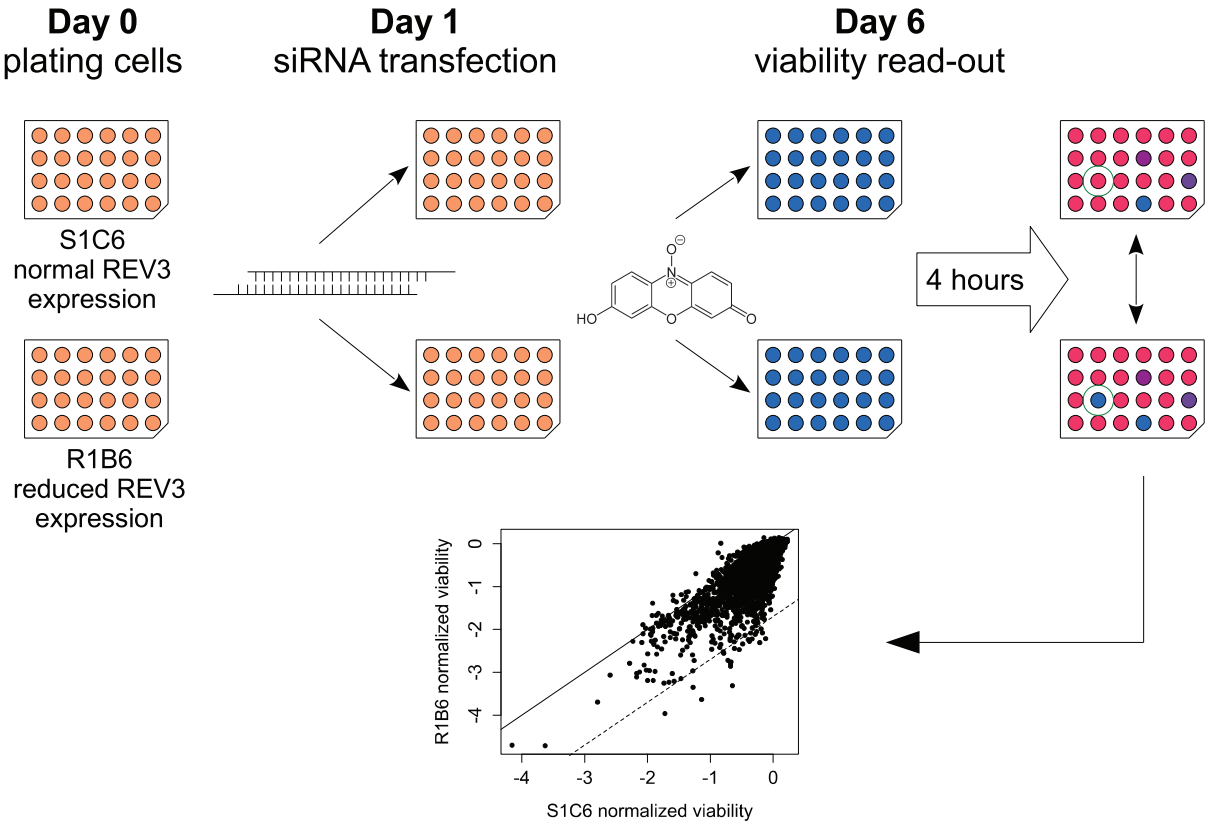

Figure 2. Schematic representation of the screening procedure. 24 hours after plating, cells are transfected with the siRNA from the Dharmacon library targeting >20 000 transcripts. Cells are incubated for 5 days and CellTiter Blue viability assay is used to assess amount of cells in every well. Fluorescent signal is normalized and compared between two cell lines – S1C6 with normal and R1B6 with reduced REV3 expression – to find the genes whose silencing predominantly affects viability of REV3-deficient cells.

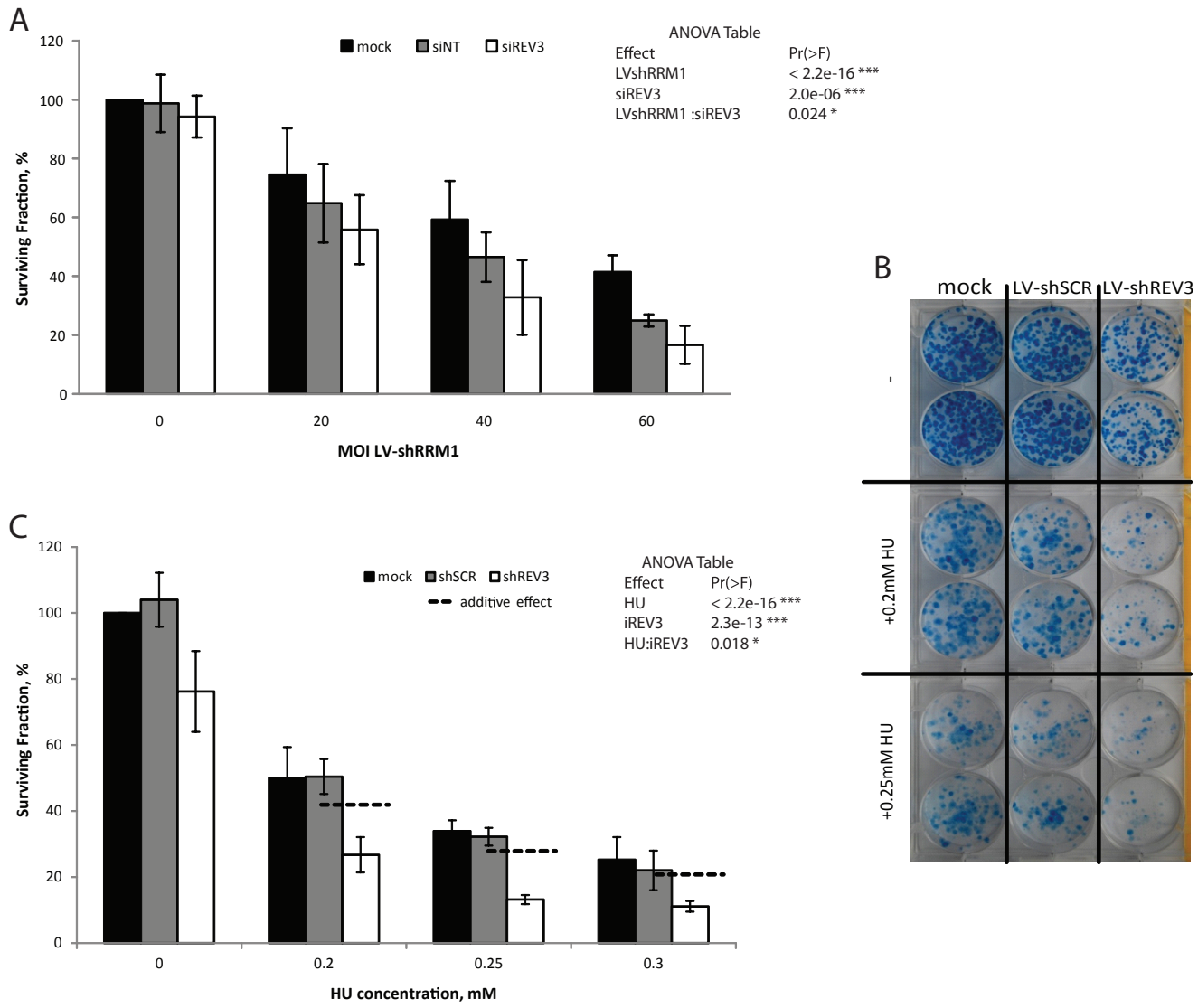

Figure 3. Inhibition of ribonucleotide reductase (RNR) function and REV3 silencing have synergistic effect on viability of cancer cells.

(A) Quantitation of the colony formation after REV3 silencing by siRNA and transduction of lentivirus carrying short hairpin targeting RRM1 mRNA.

(B) Image of a representative plate from a colony formation assay after REV3 silencing by LV-shREV3 and subsequent HU treatment.

(C) Quantitation of the colony formation after REV3 silencing by LV-shREV3 and subsequent HU treatment.

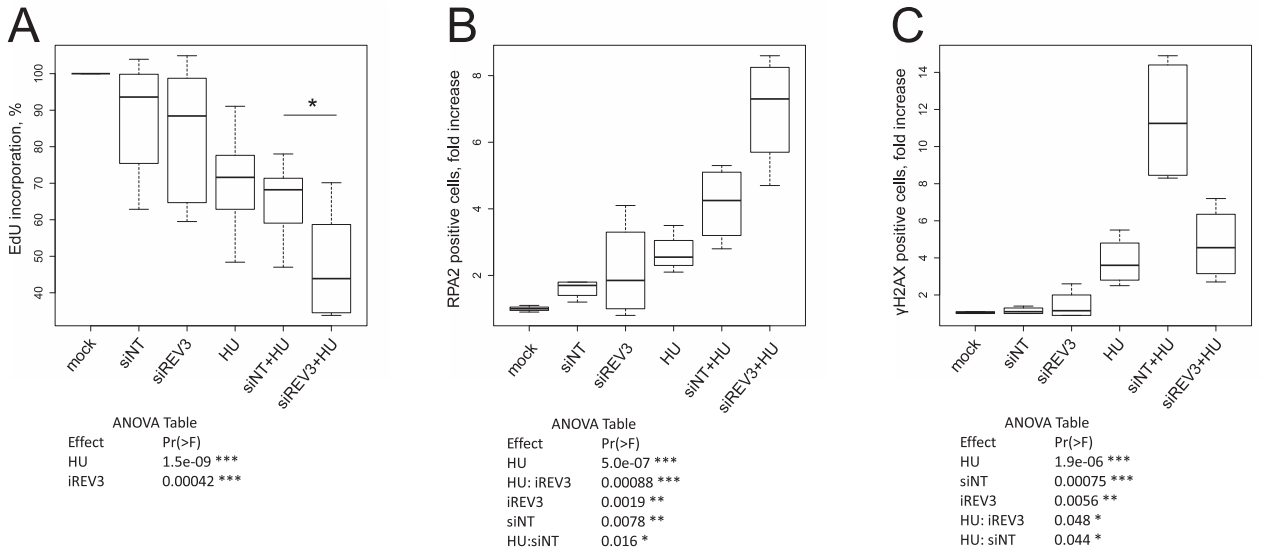

Figure 4. Effects of REV3 silencing and HU treatment on (A) EdU incorporation, (B) RPA2 and (C) γH2AX levels determined by flow cytometry . The cells were seeded and transfected after 24 hours. 24 hours later the medium was exchanged and after 24 hours cells were treated with HU. After 24 hours of treatment, EdU was applied for 1 hour after which cells were harvested, fixed and stained. *P<0.05

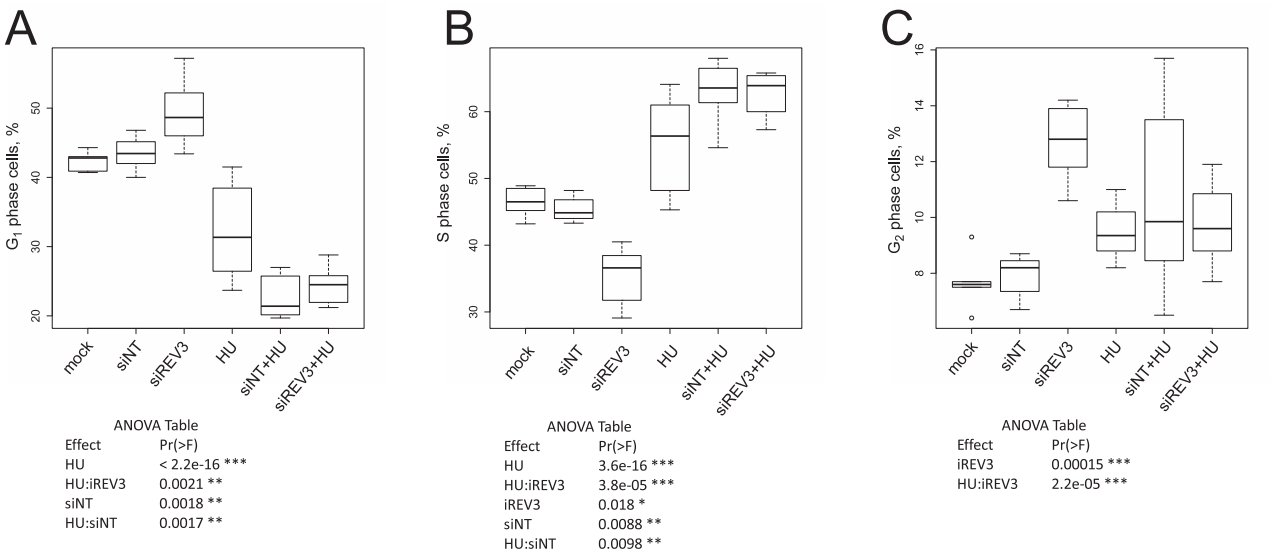

Figure 5. Effects of REV3 silencing and HU treatment on cell cycle distribution: percentages of (A) G1, (B) S and (C) G2 phase cells.

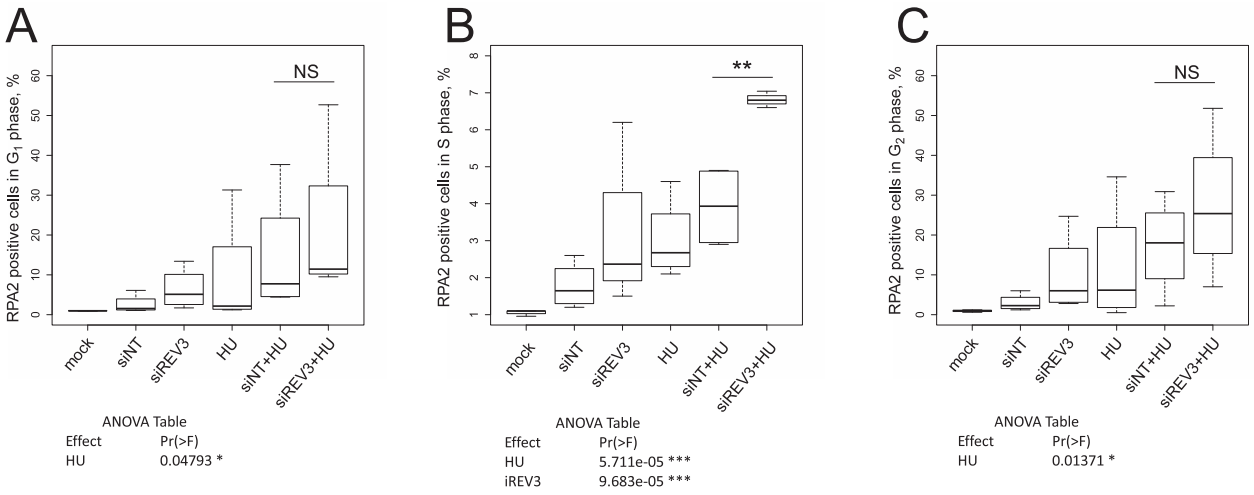

Figure 6. Effects of REV3 silencing and HU treatment on RPA levels in different cell cycle phases determined by flow cytometry: in (A) G1, in (B) S and (C) G2 -phases.

4.8. Supplementary materials

	S1C6-1	S1C6-2	R1B6-1	R1B6-2
S1C6-1	1.00	0.87	0.81	0.76
S1C6-2	0.87	1.00	0.77	0.75
R1B6-1	0.81	0.77	1.00	0.84
R1B6-2	0.76	0.75	0.84	1.00

Supplementary Table 1. Pearson's correlation values between the whole-genome silencing screens of the control (S1C6) and REV3-deficient (R1B6) cell lines.

Supplementary Table 2 (available electronically only). Complete results of the silencing screens sorted by absolute difference of normalized viability scores between the control (S1C6) and REV3-deficient (R1B6) cell lines.

Supplementary Table 3 (short version is included in the supplementary of the thesis). Results of the silencing screens (Suppl.Table 2.), filtered with the $P<0.05$ to exclude low-confidence genes.

Supplementary Table 4. Replication stress gene list, obtained by search of NCBI human gene database with the term “replication+stress”.

ID	Symbol	Name
7157	TP53	tumor protein p53
1029	CDKN2A	cyclin-dependent kinase inhibitor 2A
4609	MYC	v-myc myelocytomatosis viral oncogene homolog (avian)
472	ATM	ataxia telangiectasia mutated
324	APC	adenomatous polyposis coli
3320	HSP90AA1	heat shock protein 90kDa alpha (cytosolic), class A member 1
1111	CHEK1	checkpoint kinase 1
545	ATR	ataxia telangiectasia and Rad3 related
983	CDK1	cyclin-dependent kinase 1
2272	FHIT	fragile histidine triad
5591	PRKDC	protein kinase, DNA-activated, catalytic polypeptide
7486	WRN	Werner syndrome, RecQ helicase-like
898	CCNE1	cyclin E1
641	BLM	Bloom syndrome, RecQ helicase-like
3014	H2AFX	H2A histone family, member X
1025	CDK9	cyclin-dependent kinase 9
6117	RPA1	replication protein A1, 70kDa
7158	TP53BP1	tumor protein p53 binding protein 1
55294	FBXW7	F-box and WD repeat domain containing 7, E3 ubiquitin protein ligase
2177	FANCD2	Fanconi anemia, complementation group D2
83990	BRIP1	BRCA1 interacting protein C-terminal helicase 1
7465	WEE1	WEE1 homolog (S. pombe)
6118	RPA2	replication protein A2, 32kDa
5976	UPF1	UPF1 regulator of nonsense transcripts homolog (yeast)
11073	TOPBP1	topoisomerase (DNA) II binding protein 1
64421	DCLRE1C	DNA cross-link repair 1C
5424	POLD1	polymerase (DNA directed), delta 1, catalytic subunit
8317	CDC7	cell division cycle 7
9025	RNF8	ring finger protein 8, E3 ubiquitin protein ligase
571	BACH1	BTB and CNC homology 1, basic leucine zipper transcription factor 1
79840	NHEJ1	nonhomologous end-joining factor 1
5884	RAD17	RAD17 homolog (S. pombe)
10769	PLK2	polo-like kinase 2
64919	BCL11B	B-cell CLL/lymphoma 11B (zinc finger protein)
80198	MUS81	MUS81 endonuclease homolog (S. cerevisiae)
25842	ASF1A	ASF1 anti-silencing function 1 homolog A (S. cerevisiae)
55723	ASF1B	ASF1 anti-silencing function 1 homolog B (S. cerevisiae)
10116	FEM1B	fem-1 homolog b (C. elegans)
8812	CCNK	cyclin K
79915	ATAD5	ATPase family, AAA domain containing 5
80169	CTC1	CTS telomere maintenance complex component 1
4796	TONSL	tonsoku-like, DNA repair protein
84893	FBXO18	F-box protein, helicase, 18
79991	OBFC1	oligonucleotide/oligosaccharide-binding fold containing 1
84083	ZRANB3	zinc finger, RAN-binding domain containing 3
51550	CINP	cyclin-dependent kinase 2 interacting protein
92797	HELB	helicase (DNA) B
253714	MMS22L	MMS22-like, DNA repair protein

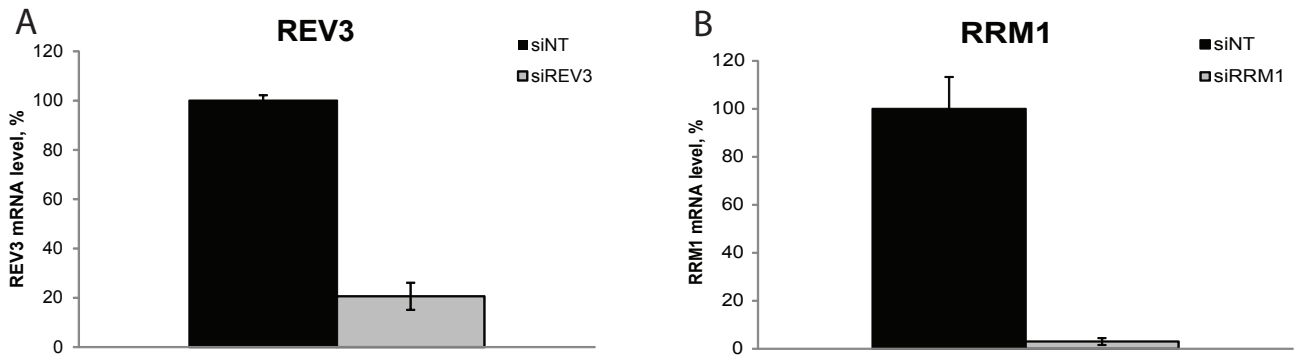

Supplementary Figure 1. siRNA silencing results in a strong decrease of mRNA levels of (A) REV3 and (B) RRM1 48 hours after transfection assessed by rtPCR

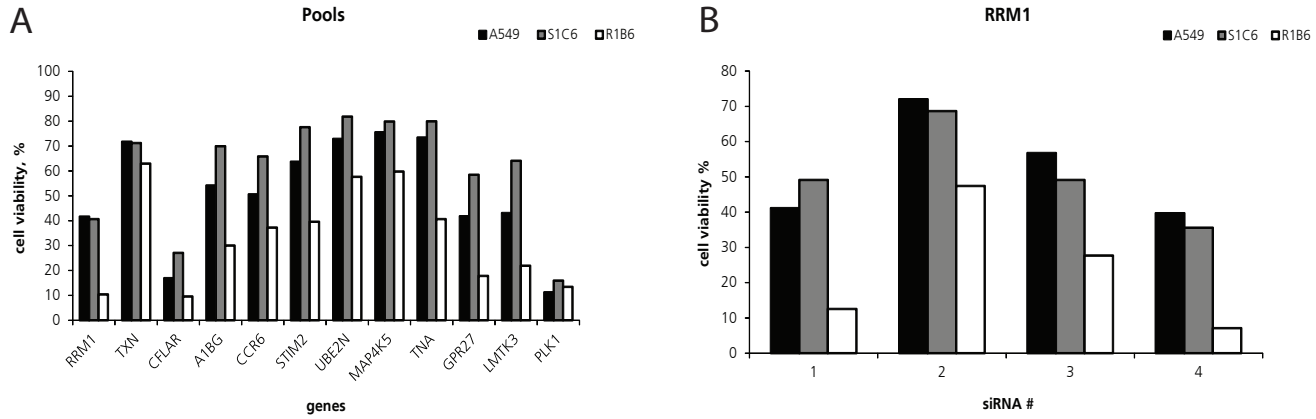

Supplementary Figure 2. Effect of manual transfection of (A) siRNA pools targeting the genes with the highest specificity for killing of REV3 deficient cells and (B) individual siRNA from RRM1 pool on viability of A549, S1C6 and R1B6.

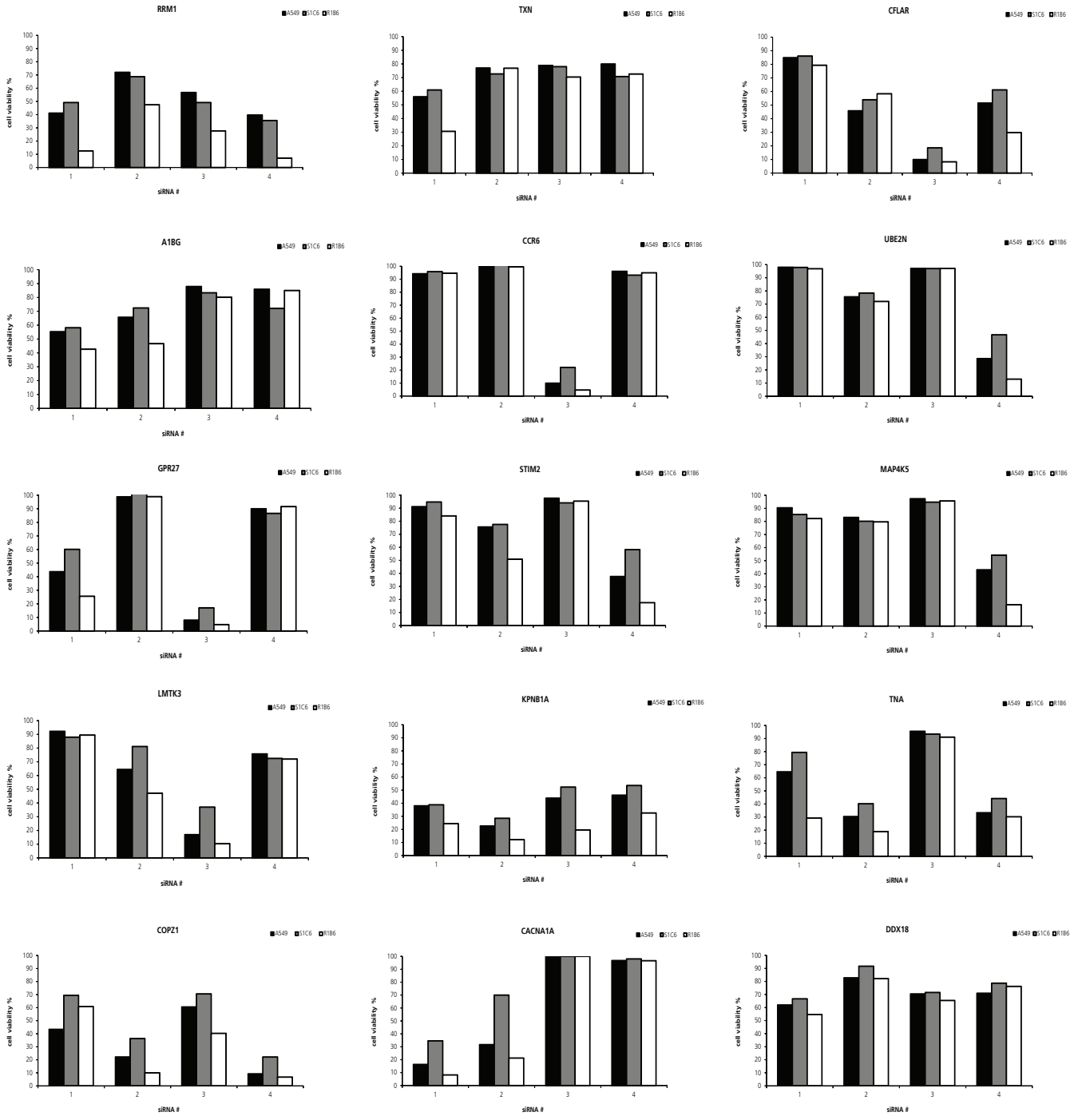

Supplementary Figure 3. Deconvolution of the pools with the highest differential viability scores in the screens. The graphs show the cell survival after transfection of individual siRNA composing the pools.

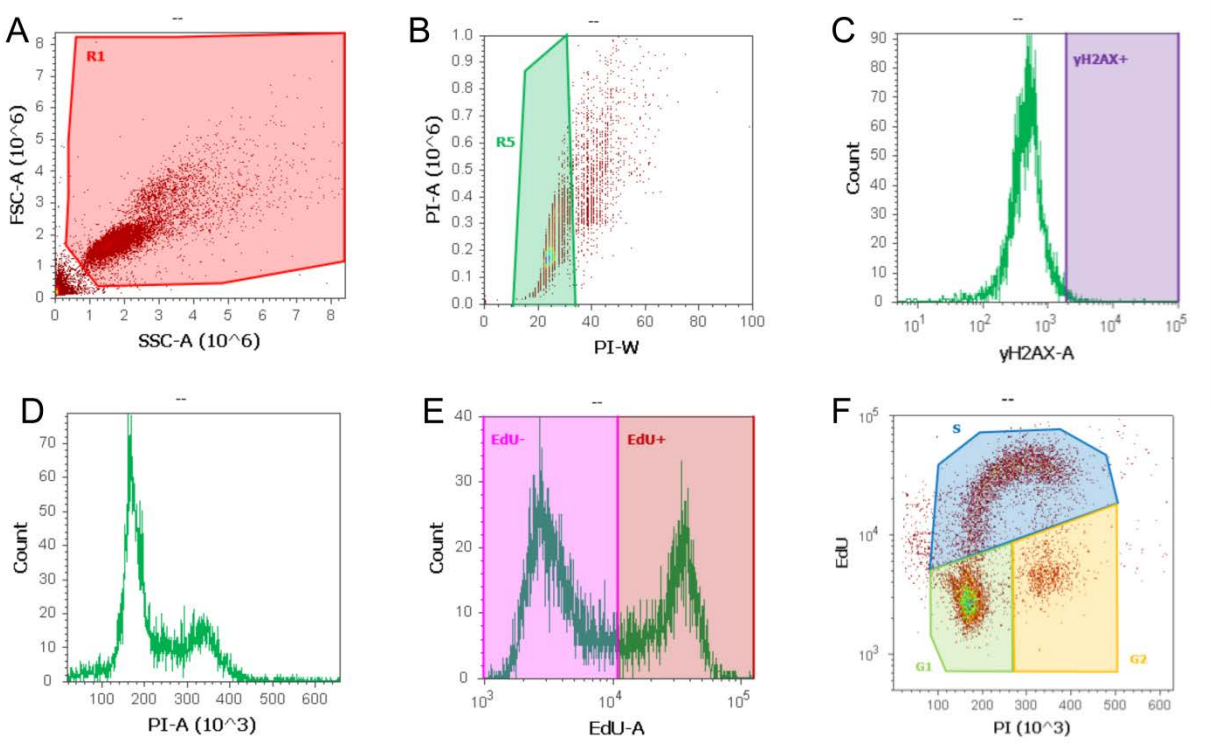

Supplementary Figure 4. Gating strategy for the flow cytometry experiments: (A) exclusion of debris, (B) exclusion of cell douplets, (C) γH2AX staining, (D) PI staining, (E) EdU staining, (F) cell cycle analysis.

5. Conclusions and perspective

Sustained proliferative signaling is acknowledged to be one of the hallmarks of cancer which might be exploited for preferential targeting of cancer cells [1, 2]. In agreement with this, we show in the first part of this work that cancer cells whose proliferation is frequently stimulated by oncogenic signaling are more sensitive to downregulation of REV3 expression than untransformed cells [3]. In the second manuscript included in the thesis, we investigate synthetic lethal gene interactions with REV3 in cancer cells and demonstrated that REV3 is essential for tolerance of replication stress induced by hydroxyurea treatment. In addition to its conventional role in DNA damage repair and tolerance, recently it was suggested that REV3 is essential for overcoming cellular senescence in response to a potent proliferation stimulus [4], but the nature of this stimulus wasn't clarified. Our finding suggests that replication stress can be a type of proliferation stimulus that sensitizes cells to REV3 silencing.

For our work we used the artificially created cell lines: one with normal REV3 expression and another one with REV3 mRNA level reduced by 50%. We speculate that this level of downregulation is physiologically relevant since mutations leading to the complete inactivation of REV3 are not common in tumors. In detail, in the Catalogue of Somatic Mutations in Cancer (COSMIC) [5] only 1.7% of unique 7241 tumor samples have mutations in the Rev3l gene, 23.6% of which are synonymous substitutions not changing the protein sequence and other 65.9% are missense substitutions which should not affect catalytic function because of their positioning outside of N- and C-terminal domains.

In a series of siRNA screens we found some of the genes that are known to be involved in parallel or complimentary to TLS pathways. For example, TLS and HR-mediated post-replication repair (HR-PRR) are synthetic lethal in yeast in the presence of DNA damaging agents [6]. Yeast UBC13 is a ubiquitin ligase that is known to promote the switch from TLS to HR-PRR by PCNA polyubiquitination. We found in lung cancer cells that silencing of UBE2N, a human homologue of yeast UBC13, was synthetic lethal with

REV3 deficiency even in the absence of the exogenous DNA damage. Thus, our screen indeed identified synthetic lethal interactions of functional relevance.

In our study we used only one agent inducing RS – hydroxyurea. Another RS inducing agent topoisomerase I inhibitor camptothecin was previously shown to have stronger effect on REV3 deficient cells [7] that doesn't seem to be due to HR repair, because low concentrations of CPT used in the study don't cause formation of DNA DSB [8]. As opposed to other RS inducing drugs, camptothecin not only doesn't induce expression of fragile sites, but even stabilizes them [9]. This can be explained by a different mechanism involving blockage of DNA unwinding and thereby reducing amount of ssDNA and not increasing it like in case of other RS inducing drugs. Camptothecin treatment unlike other replication poisons induces G_2 and not S-phase arrest [10] and upregulates RRM1 and RRM2 expression [11] likely causing the delay of late replication state onset.

Nucleotide concentrations are tightly regulated throughout the cell cycle and perturbation of this regulation leads to increased mutation rates [12]. One of the key components of this regulation is the regulation of RNR activity. In yeast, upregulation of RNR activity increases replication fork speed, indicating that nucleotide pools are limiting for normal replication [13]. Both in yeast and mammalian cells the nucleotide pools are expanded upon entry in the S-phase. In mammalian cells, exit from S phase is associated with decrease of dN pools, most notably of deoxycytidine changing 3-fold [14, 15]. Because nucleotide concentrations in the nucleus are higher than in the cytoplasm, the absolute changes of nuclear nucleotide pools during the cell cycle are more pronounced [16] perhaps making them limiting for late replication. Thus, in addition to the role of Polζ in replication after HU generated nucleotide deprivation, we speculate that Polζ might also be involved in the late replication.

In this context, the recently discovered role of Polζ in the stability of fragile sites can be viewed as a particular case of late replication since fragile sites are known to be replicated late during the cell cycle and their stability is compromised by RS inducing agents (aphidicolin, hydroxyurea, low folate medium). In detail, common fragile sites (CFS) are replicated in late S phase and their replication is even further delayed by

aphidicolin, causing the replication of CFS to persist in G_2 phase [17]. In our study, upon REV3 silencing in the absence of HU treatment, an increase in the fraction of cells in the G_2-phase was the most prominent effect (1.5 fold) suggesting that REV3 plays the most important role in this cell cycle phase, which is in agreement with the recently reported enrichment of REV3 on the chromatin in G_2/M and its role in fragile site maintenance [18]. However, HU treatment increased S-phase fraction of REV3 depleted cells more than that of the cells without REV3 silencing, which suggests its increased role in S-phase upon nucleotide deprivation. Thus, we speculate that under our experimental conditions, the HU treatment induces in A549 cells the early onset of the "late replication" in S-phase by creating conditions of nucleotide shortage more typical for G_2-phase.

Polymerase	K_m values, μM			
	dCTP-G	dTTP-A	dATP-T	dGTP-C
Yeast polζ	0.14 [30]	-	0.39 [31]	0.11[30]
Yeast polδ	1.4 [32]	6.6 [32]	2.1 [32]	2.5 [32]
Yeast polη	0.43 [33]	1.3 [33]	1.7 [33]	5.0 [33]

Table 5.1. Steady-state kinetic parameters K_m of yeast polymerases ζ, δ and η.

Late replicating regions were shown to be particularly prone to mutagenesis in both yeast [19] and humans [20], indicating a likely conservation of the mechanism underlying this phenomenon. In yeast, comparison of available catalytic parameters K_m of polymerases ζ, δ and η (Table 5.1) suggests that in the conditions of nucleotide shortage ($dN<<K_m$) Polζ can bind nucleotides with the highest affinity because its K_m values for incorporation of 3 nucleotides are 5-20 times lower than those of Polδ. This is due to Polζ lysine residue K1061 that binds triphosphate group of nucleotides, increasing the binding affinity, but decreasing replication fidelity [21, 22]. This error-

prone nature of Polζ suggests that it can contribute to the late replication mutagenesis by participating in this process as suggested above.

Our data suggest that reduction of the nucleotide pools represents a mechanism that could control the replicative polymerase switch in the late S and G_2 phases and/or RS induction. Possible mediators in this non-TLS polymerase switch include REV1 and Spartan. In yeast, REV1 dependent recruitment of Polζ to DNA was shown to be independent from Rad6-Rad18-mediated PCNA ubiquitination [23] that is required for initiation of TLS. This recruitment is controlled by phosphorylation of ATR-homolog Mec1, which is one of the main players in RS response [24]. Besides, Rev1 is highly expressed during G_2/M phase rather than S phase and its association with Polζ is highest in G_2 phase [25]. Another possible player in RS-induced Polζ recruitment is Spartan (DVC1, C1orf124), a ubiquitin-binding p97 adaptor protein that accumulates at sites of RS independently from RAD18-mediated PCNA monoubiquitylation [26]. Spartan is a substrate of cycle-regulated anaphase-promoting complex (APC), it prevents the binding of Polζ and REV1 to POLD2, an accessory subunit of Polδ, thereby suppressing TLS [27]. Additionally, it was shown that exchange of Polδ and Polζ is redox-dependent since both of the polymerases have iron-sulfur clusters sensitive to oxidation [28]. This might represent an additional level of control for the choice of the replicative polymerase because redox state of the cell and the nucleus is known to be cell cycle dependent [29]. Which of these or other mechanisms control the REV3 function in replication is unclear and could represent an interesting topic for the future investigation.

Like it is often the case in scientific research, our study raises even more questions than gives the answers and I will try to address some of them and give my view of possible directions for the future research on the topic. Even though our flow cytometry data indicate the participation of REV3 in replication under conditions of replication stress, the direct evidence of that is still missing. There are several experiments that could further clarify this issue. The most suitable for that is the method of DNA fiber spreading analysis that is used to assess progression of individual replication forks. Reduction of the average speed of replication fork caused by depletion of REV3 upon replication stress could prove its direct involvement in the DNA replication.

Unfortunately the direct biochemical detection of human REV3 is complicated by the large size and very low abundance of this protein as well as inferior quality of commercially available antibodies. Therefore immunofluorescent detection would require prior development of a working antibody. Once available, antibodies could be used in a wide range of experiments such as protein coimmunoprecipitation (IP) followed by either targeted detection of protein of interest using Western blotting or unbiased mass-spectrometry. These experiments would allow finding the direct interaction partners of REV3 in different conditions, e.g. normal versus replication stress.

Another interesting question is how REV3 is recruited to the replication fork and what is inducing the polymerase switch in the conditions of replication stress. The switch can be carried out in a PCNA monoubiquitination-dependent manner similar to how it is made in translesion synthesis. Alternatively, PCNA-ubiquitination might not be strictly required for it and REV3 recruitment can be mediated by other proteins like REV1 and Spartan as discussed above. Determination of PCNA ubiquitination status under conditions of replication stress would be helpful for finding an answer to this question.

To investigate whether REV3 is involved in the tolerance of oncogene-induced replication stress, isogenic cell lines that differ in oncogene expression could be used. Especially interesting would be to investigate how the nature of the oncogene influences extent of involvement of REV3 in DNA replication. Thus, both c-myc and Cyclin E are strong inducers of replication stress, but c-myc activation additionally upregulates the rate of nucleotide synthesis likely alleviating nucleotide deficiency caused by oncogenic stress. Comparison of oncogenes of these two types (like c-myc and Cyclin E) and role of REV3 upon their activation could provide a clue about whether nucleotide shortage is essential for the recruitment of REV3 upon oncogene-induced replication stress. This is another possible direction of the future research and an important issue for understanding the function of REV3 in replication stress tolerance.

5.1. References

1. Hanahan, D. and R.A. Weinberg, *The hallmarks of cancer.* Cell, 2000. **100**(1): p. 57-70.
2. Hanahan, D. and R.A. Weinberg, *Hallmarks of cancer: the next generation.* Cell, 2011. **144**(5): p. 646-74.
3. Knobel, P.A., et al., *Inhibition of REV3 expression induces persistent DNA damage and growth arrest in cancer cells.* Neoplasia, 2011. **13**(10): p. 961-70.
4. Lange, S.S., et al., *Dual role for mammalian DNA polymerase zeta in maintaining genome stability and proliferative responses.* Proc Natl Acad Sci U S A, 2013.
5. Forbes, S.A., et al., *COSMIC (the Catalogue of Somatic Mutations in Cancer): a resource to investigate acquired mutations in human cancer.* Nucleic Acids Res, 2010. **38**(Database issue): p. D652-7.
6. Ball, L.G., et al., *The yeast Shu complex couples error-free post-replication repair to homologous recombination.* Mol Microbiol, 2009. **73**(1): p. 89-102.
7. Sharma, S., et al., *REV1 and polymerase zeta facilitate homologous recombination repair.* Nucleic Acids Res, 2012. **40**(2): p. 682-91.
8. Ray Chaudhuri, A., et al., *Topoisomerase I poisoning results in PARP-mediated replication fork reversal.* Nat Struct Mol Biol, 2012. **19**(4): p. 417-23.
9. Arlt, M.F. and T.W. Glover, *Inhibition of topoisomerase I prevents chromosome breakage at common fragile sites.* DNA Repair (Amst), 2010. **9**(6): p. 678-89.
10. Tsao, Y.P., P. D'Arpa, and L.F. Liu, *The involvement of active DNA synthesis in camptothecin-induced G2 arrest: altered regulation of p34cdc2/cyclin B.* Cancer Res, 1992. **52**(7): p. 1823-9.
11. Zhang, Y.W., et al., *Implication of checkpoint kinase-dependent up-regulation of ribonucleotide reductase R2 in DNA damage response.* J Biol Chem, 2009. **284**(27): p. 18085-95.
12. Kumar, D., et al., *Mechanisms of mutagenesis in vivo due to imbalanced dNTP pools.* Nucleic Acids Res, 2011. **39**(4): p. 1360-71.
13. Poli, J., et al., *dNTP pools determine fork progression and origin usage under replication stress.* EMBO J, 2012. **31**(4): p. 883-94.
14. Leeds, J.M., M.B. Slabaugh, and C.K. Mathews, *DNA precursor pools and ribonucleotide reductase activity: distribution between the nucleus and cytoplasm of mammalian cells.* Mol Cell Biol, 1985. **5**(12): p. 3443-50.
15. Skoog, K.L., B.A. Nordenskjold, and K.G. Bjursell, *Deoxyribonucleoside-triphosphate pools and DNA synthesis in synchronized hamster cells.* Eur J Biochem, 1973. **33**(3): p. 428-32.
16. Bjursell, G. and L. Skoog, *Control of nucleotide pools in mammalian cells.* Antibiot Chemother, 1980. **28**: p. 78-85.
17. Le Beau, M.M., et al., *Replication of a common fragile site, FRA3B, occurs late in S phase and is delayed further upon induction: implications for the mechanism of fragile site induction.* Hum Mol Genet, 1998. **7**(4): p. 755-61.
18. Bhat, A., et al., *Rev3, the catalytic subunit of Polzeta, is required for maintaining fragile site stability in human cells.* Nucleic Acids Res, 2013.
19. Agier, N. and G. Fischer, *The mutational profile of the yeast genome is shaped by replication.* Mol Biol Evol, 2012. **29**(3): p. 905-13.
20. Stamatoyannopoulos, J.A., et al., *Human mutation rate associated with DNA replication timing.* Nat Genet, 2009. **41**(4): p. 393-5.

21. Howell, C.A., C.M. Kondratick, and M.T. Washington, *Substitution of a residue contacting the triphosphate moiety of the incoming nucleotide increases the fidelity of yeast DNA polymerase zeta.* Nucleic Acids Res, 2008. **36**(5): p. 1731-40.
22. Zhong, X., et al., *The fidelity of DNA synthesis by yeast DNA polymerase zeta alone and with accessory proteins.* Nucleic Acids Res, 2006. **34**(17): p. 4731-42.
23. Hirano, Y. and K. Sugimoto, *ATR homolog Mec1 controls association of DNA polymerase zeta-Rev1 complex with regions near a double-strand break.* Curr Biol, 2006. **16**(6): p. 586-90.
24. Flynn, R.L. and L. Zou, *ATR: a master conductor of cellular responses to DNA replication stress.* Trends Biochem Sci, 2011. **36**(3): p. 133-40.
25. Waters, L.S. and G.C. Walker, *The critical mutagenic translesion DNA polymerase Rev1 is highly expressed during G(2)/M phase rather than S phase.* Proc Natl Acad Sci U S A, 2006. **103**(24): p. 8971-6.
26. Mosbech, A., et al., *DVC1 (C1orf124) is a DNA damage-targeting p97 adaptor that promotes ubiquitin-dependent responses to replication blocks.* Nat Struct Mol Biol, 2012. **19**(11): p. 1084-92.
27. Kim, M.S., et al., *Regulation of error-prone translesion synthesis by Spartan/C1orf124.* Nucleic Acids Res, 2013. **41**(3): p. 1661-8.
28. Baranovskiy, A.G., et al., *DNA polymerase delta and zeta switch by sharing accessory subunits of DNA polymerase delta.* J Biol Chem, 2012. **287**(21): p. 17281-7.
29. Markovic, J., et al., *Glutathione is recruited into the nucleus in early phases of cell proliferation.* J Biol Chem, 2007. **282**(28): p. 20416-24.
30. Haracska, L., et al., *Roles of yeast DNA polymerases delta and zeta and of Rev1 in the bypass of abasic sites.* Genes Dev, 2001. **15**(8): p. 945-54.
31. Johnson, R.E., et al., *Yeast DNA polymerase zeta (zeta) is essential for error-free replication past thymine glycol.* Genes Dev, 2003. **17**(1): p. 77-87.
32. Dieckman, L.M., et al., *Pre-steady state kinetic studies of the fidelity of nucleotide incorporation by yeast DNA polymerase delta.* Biochemistry, 2010. **49**(34): p. 7344-50.
33. Washington, M.T., et al., *Fidelity and processivity of Saccharomyces cerevisiae DNA polymerase eta.* J Biol Chem, 1999. **274**(52): p. 36835-8.

6. Acknowledgements

There are many people that made this PhD thesis possible and helped me on the way.

First of all, I would like to thank Prof. Rolf Stahel for giving me the opportunity to be a part of his lab and his support of my thesis.

I am especially grateful to Dr. Thomas Marti for his great guidance and for teaching me so many things.

I would like to express my gratitude to Prof. Massimo Lopes for agreeing to be my faculty supervisor, for his important input to my thesis and work in general.

A special thank goes to Dr. Emanuela Felley-Bosco for her critical advice and friendly support.

I would like to thank Prof. Jonathan Hall for being a member of my thesis committee and his useful suggestions for my project.

I thank all members of the Molecular Oncology Lab that I had a chance to work with for great time in- and outside of the lab.

I am very grateful to Dr. Victor van Beusechem for his collaboration and assistance in setting up the screen.

I very much appreciate the help and hospitality of Ellen Siebring-van Olst and all other members of RIFOL Lab of VUMC in Amsterdam where I performed the RNAi screens. My work there would not be possible without assistance of many people, especially Ida van der Meulen, who worked with me a lot during the screening.

I thank Dr. Renee Menezes for her help with statistical analysis of the screens.

My warm thanks go to Dr. Philip Knobel for his contribution to my work and his friendship.

Finally, I would like to sincerely thank my family and Stefano for their support during the time of the thesis.

7. Curriculum Vitae

Name: Ilya Kotov

Date of birth: 19.01.1987

Nationality: Russia

E-mail: inkotov@gmail.com

EDUCATION

2009 – present	PhD thesis “Identification of Synthetic Lethal Gene Interactions with REV3 in Lung Cancer Cells”. University of Zurich, Cancer Biology PhD Program
2003 – 2008	Honours Diploma (chemical enzymology). Chemistry Department; Lomonosov Moscow State University, Russia (GPA 5.00 out of 5.00)
2005 – 2008	M.A. Teaching. Department of Education, Lomonosov Moscow State University, Russia (GPA 5.00 out of 5.00)

RESEARCH EXPERIENCE

2009 – present	Laboratory of Molecular Oncology, Clinic of Oncology, University Hospital Zurich. Prof. Dr. med. Rolf A. Stahel, supervisor Dr. Thomas Marti, PhD
2004 – 2008	Laboratory of Medical Enzymology, Chemical Enzymology Division, Chemistry Department, Lomonosov Moscow State University. Supervisor: Olga A. Kost, PhD; Petr V. Binevsky, PhD. Research project: “Functioning of angiotensin-converting enzyme (ACE) upon binding substrates and inhibitors with tetrapeptide structure”.
2007 – 2008	Laboratory of Chemistry Education, Chemistry Department, Lomonosov Moscow State University. Supervisor: Prof. Vyacheslav V. Zagorskii, Dr. Educ. Sc., PhD. Research project: “Computer animations in chemistry teaching”.
2003 – 2004	Laboratory of Inorganic Crystal Chemistry, Inorganic Chemistry Division, Chemistry Department, Lomonosov Moscow State University. Supervisor: Associate Prof. Oleg G. Dyachenko, PhD. Research project: “Pyrogenic synthesis and investigation of niobium sulfides with variable composition $NbS_{2\pm x}$”.

8. Supplemetary Table. Screening results: genes with P value less than 0.05 sorted by the difference of normalized viability (delta). Included are only 500 genes with the strongest synthetic lethal effect (highest delta) and all significant synthetic rescue genes (lowest delta).

S1 and S2 are the results of 1st and 2nd screens of S1C6, R1 and R2 - of R1B6

A. Synthetic lethal genes

Rank	Input Nr	Accession	LocusID	Gene	t statistic	p value	delta	plate	well	S1.raw	S1.norm	S2.raw	S2.norm	R1.raw	R1.norm	R2.raw	R2.norm
1	1408	NM_018971	2850	GPR27	-9.4013	0.00174	2.67	15	F04	18055	-0.9856	26132	-0.3078	3372	-3.4391	3924	-3.1877
2	4143	NM_001033	6240	RRM1	-4.58496	0.01594	2.49	44	B03	10484	-1.831	25593	-0.4491	2814	-3.7186	3079	-3.5495
3	5142	NM_003879	8837	CFLAR	-28.2725	4.88E-05	2.24	54	E06	11638	-1.6846	10160	-1.7597	2587	-3.8758	2084	-4.0475
4	431	XM_055866	114783	LMTK3	-5.08851	0.01172	2.19	5	D11	19894	-0.8741	23885	-0.4822	7427	-2.351	3505	-3.3772
5	1220	NM_004367	1235	CCR6	-14.2674	0.00045	2.13	13	F08	18640	-0.8636	24076	-0.4927	4903	-2.8337	5143	-2.7815
7	7307	NM_000068	773	CACNA1A	-8.62504	0.00229	2.09	77	A11	30993	-0.3725	34891	-0.056	9119	-2.0424	6452	-2.5722
8	12209	NM_016057	22818	COPZ1	-5.47059	0.00943	2.09	128	B05	22777	-0.8757	27083	-0.465	7943	-2.3169	4108	-3.2021
9	2051	NM_004680	9085	CDY1	-3.95557	0.02436	2.08	22	C11	11663	-1.649	18687	-0.8976	2396	-3.908	5163	-2.7935
10	3700	NM_015989	51380	CSAD	-4.08081	0.0223	2	39	E04	21244	-0.7535	21102	-0.6866	3498	-3.3495	8282	-2.0957
11	2812	NM_005825	10235	RASGRP2	-5.64644	0.00857	1.93	30	C04	20380	-0.7945	27249	-0.2855	5162	-2.8237	8227	-2.1151
12	2829	NM_001235	871	SERPINH1	-4.2818	0.01944	1.91	30	D09	28533	-0.3091	32506	-0.031	5882	-2.6353	12360	-1.5279
13	4191	NM_003898	8871	SYNJ2	-5.40838	0.00976	1.9	44	F03	23787	-0.649	32498	-0.1045	9769	-1.923	5790	-2.6384
14	23123	XM_114621	0	LOC203076	-5.68053	0.00841	1.88	241	G11	32641	-0.3724	30254	-0.3009	11445	-1.7993	5952	-2.6432
15	6669	NM_004831	9441	CRSP7	-4.13362	0.0215	1.85	70	D09	28089	-0.4957	26617	-0.4748	11322	-1.7641	4741	-2.9095
17	20922	NM_198822	267020	ATP5L2	-3.45301	0.03546	1.83	218	H06	28103	-0.5477	22407	-0.6846	11363	-1.7692	4111	-3.1159
18	9219	NM_130786	1	A1BG	-22.8019	9.87E-05	1.83	97	A03	31883	-0.346	31756	-0.2275	8650	-2.187	8837	-2.0387
19	495	NM_006575	11183	MAP4K5	-4.56275	0.01617	1.8	6	B03	28553	-0.2745	30840	-0.1087	6585	-2.4827	12702	-1.4909
21	12188	NM_007372	11325	DDX42	-6.60219	0.0053	1.77	127	H08	19422	-1.1205	27561	-0.4535	7155	-2.4839	6141	-2.6263
22	15420	NM_020860	57620	STIM2	-12.0042	0.00079	1.73	161	E12	28806	-0.5106	32309	-0.2035	9682	-1.9912	7678	-2.1808
23	561	NM_033118	85366	MYLK2	-10.0229	0.00142	1.73	6	G09	18119	-0.9307	21047	-0.6599	5690	-2.6935	6988	-2.353
24	7373	NM_002265	3837	KPNB1	-4.28336	0.01942	1.69	77	G05	12662	-1.664	19515	-0.8943	6013	-2.6432	3911	-3.2944
25	16002	NM_023942	65999	MGC3036	-3.79145	0.02743	1.69	167	F06	30588	-0.4114	26554	-0.4877	13083	-1.5688	5326	-2.7042
26	9113	NM_014781	9821	RB1CC1	-6.64425	0.0052	1.68	95	H05	16493	-1.2779	11239	-1.6591	5212	-2.8886	3451	-3.4066
29	2081	NM_001834	1212	CLTB	-3.16229	0.04481	1.63	22	F05	26574	-0.4609	32372	-0.1049	6129	-2.553	14742	-1.2799
30	4485	NM_003348	7334	UBE2N	-11.7996	0.00084	1.63	47	F09	30734	-0.1809	24575	-0.4849	8878	-2.0478	9761	-1.8827
31	2688	NM_003278	7123	TNA	-3.42053	0.03637	1.62	28	H12	32084	-0.0645	29149	-0.2201	6907	-2.3691	15979	-1.1642
32	24515	XM_373466	0	LOC387690	-6.63473	0.00522	1.61	256	C11	37529	-0.1547	29501	-0.3295	13175	-1.5531	8303	-2.1434
33	17372	NM_032561	84645	C22ORF23	-9.48055	0.0017	1.61	181	H08	24123	-0.7051	26630	-0.4436	7559	-2.3486	9120	-2.011
34	24332	XM_372048	0	LOC389672	-13.241	0.00058	1.6	254	D08	27671	-0.5998	25112	-0.565	9649	-2.0353	7250	-2.3334
35	1757	NM_003301	7201	TRHR	-4.6986	0.01484	1.59	19	C05	19533	-0.8055	27288	-0.279	10686	-1.7908	6517	-2.4769
37	2079	NM_014718	9746	CLSTN3	-3.10435	0.04702	1.57	22	F03	21044	-0.7975	27858	-0.3215	5397	-2.7364	12397	-1.5298
38	21091	NM_175900	283897	FLJ35681	-4.93723	0.01282	1.57	220	F07	25515	-0.6978	22019	-0.6717	11025	-1.8518	5599	-2.6646
40	12750	NM_014338	23761	PISD	-4.12031	0.0217	1.57	133	G06	14885	-1.292	26609	-0.4086	8341	-2.2156	5746	-2.6248

41	1270	NM_012152	23566	EDG7	-8.52883	0.00237	1.56	14	B10	26485	-0.3743	33095	0.02478	10077	-1.8475	11694	-1.616
42	2684	NM_001063	7018	TF	-5.29569	0.0104	1.53	28	H08	20149	-0.7356	21883	-0.6337	5993	-2.5738	9957	-1.8466
44	4580	NM_001776	953	ENTPD1	-11.1029	0.00102	1.52	48	F08	22449	-0.6995	17134	-0.9665	6528	-2.4571	7523	-2.2441
45	15437	NM_020882	57642	KIAA1510	-4.80806	0.01386	1.52	161	G05	30215	-0.4417	26683	-0.4795	12926	-1.5743	6699	-2.3775
46	4763	NM_000937	5430	POLR2A	-4.91556	0.01299	1.52	50	E11	8667	-2.0926	13338	-1.382	3528	-3.4205	4056	-3.0842
48	4471	NM_003329	7295	TXN	-33.5783	2.78E-05	1.5	47	E07	32510	-0.0999	30283	-0.1836	11718	-1.6474	11541	-1.6411
49	5550	NM_018438	26270	FBXO6	-3.07078	0.04837	1.5	58	G06	31800	-0.3004	29045	-0.3211	16857	-1.1871	6772	-2.4383
50	1290	NM_017986	55065	FLJ10060	-3.40139	0.03693	1.5	14	D06	32926	-0.0603	32083	-0.02	8429	-2.1051	18207	-0.9773
51	16762	NM_030651	80863	C6ORF31	-5.46438	0.00946	1.49	175	E10	32154	-0.3198	31191	-0.1851	14459	-1.4044	8697	-2.0875
52	5204	NM_006421	10565	BIG1	-11.8309	0.00083	1.49	55	B08	19208	-0.9811	17900	-0.9759	7441	-2.3082	5690	-2.6205
53	15423	NM_020861	57621	ZBTB2	-7.43645	0.00366	1.48	161	F03	23716	-0.7911	25807	-0.5277	10138	-1.9248	6805	-2.3549
54	4605	NM_004462	2222	FDFT1	-5.83648	0.00775	1.47	48	H09	15056	-1.2759	14198	-1.2377	4338	-3.0467	6720	-2.4069
56	16746	XM_290811	80816	KIAA1713	-5.74798	0.00811	1.45	175	D06	32220	-0.3169	30905	-0.1984	14604	-1.39	9116	-2.0196
60	6620	NM_000832	2902	GRIN1	-4.27151	0.01957	1.42	69	H08	26509	-0.6047	28254	-0.3771	13376	-1.5019	7163	-2.3192
61	6200	NM_014207	921	CD5	-4.23608	0.02005	1.42	65	E08	27300	-0.5623	31278	-0.2602	14213	-1.4297	7640	-2.2292
64	6227	NM_001318	1444	CSHL1	-3.85696	0.02615	1.39	65	G11	15690	-1.3614	26629	-0.4923	8537	-2.1651	6438	-2.4761
65	2764	NM_001153	307	ANXA4	-6.81487	0.0048	1.39	29	G04	33981	-0.1003	28336	-0.2535	10088	-1.8151	14648	-1.3209
66	19479	NM_014261	148022	TRIF	-3.34139	0.03873	1.37	203	H03	23427	-0.7735	23489	-0.613	13154	-1.5468	5914	-2.5845
67	9306	NM_001679	483	ATP1B3	-4.27153	0.01957	1.36	97	H06	26807	-0.5962	17477	-1.0891	10724	-1.8769	6333	-2.5193
70	13684	NM_016564	51286	BM88	-3.3516	0.03842	1.33	143	E04	34298	-0.1448	31768	-0.2003	19537	-0.9948	8984	-2.0059
71	10180	NM_021974	5435	POLR2F	-5.15747	0.01125	1.32	107	A04	21413	-0.9452	23646	-0.6137	10747	-1.8222	7182	-2.3855
75	9453	NM_016451	1315	COPB	-6.05762	0.00691	1.31	99	D09	18805	-1.1431	13796	-1.4212	7342	-2.3584	5124	-2.8333
76	2859	NM_018489	55870	ASH1L	-3.66637	0.0301	1.31	30	G03	15697	-1.1712	19219	-0.7891	5595	-2.7075	9703	-1.8771
78	2745	NM_016265	51711	ZNF325	-5.46898	0.00944	1.29	29	E09	19968	-0.8673	23587	-0.5181	7580	-2.2275	10958	-1.7396
80	19803	NM_197964	154791	HSPC268	-7.09941	0.00423	1.28	207	C03	26773	-0.5778	25471	-0.4726	13142	-1.5816	8886	-2.024
81	3502	NM_005649	6940	ZNF354A	-12.9747	0.00062	1.27	37	D10	32500	-0.2182	31789	-0.0924	14946	-1.3282	12236	-1.5319
82	23124	XM_047083	0	LOC92755	-5.22651	0.01082	1.27	241	G12	19559	-1.1112	21422	-0.799	10244	-1.9593	6604	-2.4932
83	15976	NM_023016	65124	C2ORF26	-4.58047	0.01599	1.26	167	D04	34933	-0.2197	31752	-0.2298	17654	-1.1365	9702	-1.8389
84	4451	NM_024080	79054	TRPM8	-5.6848	0.00839	1.26	47	C11	28174	-0.3064	26936	-0.3526	10029	-1.8719	14515	-1.3103
86	142	NM_024110	79092	CARD14	-4.38345	0.01817	1.26	2	D10	24987	-0.5383	21564	-0.6542	13939	-1.4946	7798	-2.2182
87	19206	NM_080622	140701	C20ORF135	-3.26488	0.04119	1.26	201	A06	32973	-0.2925	30899	-0.249	18602	-1.0381	8738	-2.0233
88	3488	NM_003412	7545	ZIC1	-5.69806	0.00833	1.26	37	C08	23995	-0.6559	31627	-0.0998	11791	-1.6703	11663	-1.6011
89	23512	XM_371488	0	LOC388939	-3.80605	0.02714	1.26	245	H04	37409	-0.1901	30052	-0.2923	18325	-1.0794	9824	-1.9159
92	20242	XM_116971	196993	LOC196993	-5.99522	0.00714	1.25	211	G10	33023	-0.3048	29103	-0.2844	15503	-1.2801	9895	-1.8082
94	18475	NM_018593	117247	SLC16A10	-19.4232	0.00017	1.24	193	D07	40140	0.00163	33150	-0.133	15056	-1.3287	14613	-1.2791
95	3663	NM_021251	11132	CAPN10	-9.91634	0.00147	1.24	39	B03	29405	-0.2845	30984	-0.1324	11931	-1.5794	14283	-1.3095
96	13823	NM_016202	51157	ZNF580	-4.24964	0.01986	1.23	144	H11	21546	-0.8135	25491	-0.4991	13157	-1.5554	7813	-2.2259
100	7772	NM_020348	26507	CNNM1	-5.85646	0.00766	1.21	81	H08	30116	-0.3985	30788	-0.2276	15706	-1.2793	11021	-1.7767
102	10182	NM_006233	5438	POLR2I	-3.79512	0.02736	1.21	107	A06	33888	-0.2829	27524	-0.3946	17191	-1.1445	9720	-1.949

103	2755	NM_003427	7629	ZNF76	-7.46438	0.00362	1.21	29	F07	25479	-0.5157	28814	-0.2294	10736	-1.7253	13529	-1.4355
107	3715	NM_004390	1512	CTSH	-9.7223	0.00156	1.21	39	F07	34381	-0.059	33880	-0.0035	13613	-1.3891	16678	-1.0858
109	3483	NM_014569	23660	ZFP95	-3.63809	0.03075	1.2	37	C03	16563	-1.1907	26603	-0.3493	9530	-1.9774	9085	-1.9615
110	3594	NM_000687	191	AHCY	-8.34814	0.00254	1.2	38	D06	27358	-0.45	31166	-0.1007	12675	-1.5136	13136	-1.4305
111	24033	XM_379501	0	LOC401367	-3.80278	0.02721	1.2	251	C09	38151	-0.1387	30250	-0.295	18982	-1.0189	10541	-1.8055
116	20445	NM_078483	206358	SLC36A1	-4.2596	0.01973	1.19	213	H09	22190	-0.8891	22489	-0.4376	12787	-1.5754	7915	-2.1222
118	12575	NM_015305	23357	KIAA0759	-4.51727	0.01665	1.18	131	H11	19229	-0.941	28780	-0.2826	11840	-1.7478	9925	-1.8306
119	3911	NM_001535	3275	HRMT1L1	-3.6387	0.03074	1.18	41	F11	14452	-1.3851	23607	-0.5595	8455	-2.1477	7847	-2.1512
120	21792	NM_198504	344838	PAQR9	-3.90084	0.02534	1.18	227	H12	23283	-0.8716	28939	-0.383	13592	-1.5064	8757	-2.0999
121	13623	NM_016305	51188	SS18L2	-3.46051	0.03525	1.17	142	H03	36309	0.01159	33923	-0.1231	22225	-0.7988	11572	-1.6507
124	10503	NM_002951	6185	RPN2	-4.27767	0.01949	1.15	110	D03	30137	-0.4445	28198	-0.3297	16460	-1.2	10190	-1.8754
126	13217	NM_020847	27327	TNRC6	-4.96676	0.01259	1.15	138	F05	30640	-0.3109	26995	-0.4568	16478	-1.2461	10391	-1.8141
129	12810	NM_014033	25840	DKFZP586A0522	-4.23025	0.02013	1.13	134	D06	28897	-0.3672	32024	-0.1473	18570	-1.0636	10761	-1.7058
132	16915	NM_031309	83482	SCRT1	-4.61942	0.01559	1.12	177	B07	29889	-0.3776	31961	-0.1822	17975	-1.1071	11184	-1.6916
133	2012	NM_001762	908	CCT6A	-10.3758	0.00127	1.12	21	H08	22722	-0.6896	23621	-0.5465	10006	-1.8446	11510	-1.6224
135	18508	NM_178858	118980	SFXN2	-5.20677	0.01094	1.11	193	G04	38189	-0.0703	31505	-0.2065	19037	-0.9902	12399	-1.5161
136	18692	NM_145255	124995	MRPL10	-4.27088	0.01958	1.11	195	F08	33051	-0.2984	26047	-0.4786	17118	-1.1825	10290	-1.8213
139	16371	NM_024763	79819	FLJ23129	-3.06811	0.04847	1.11	171	E03	27854	-0.4867	31886	-0.1675	19083	-1.0031	10045	-1.8699
140	18753	NM_130807	126308	MOBKL2A	-4.90361	0.01308	1.11	196	C09	22598	-0.8529	18855	-0.9209	11789	-1.7097	7500	-2.2794
144	24186	XM_380120	0	LOC402537	-3.91333	0.02511	1.1	252	H06	31330	-0.4228	28217	-0.3955	17864	-1.1518	10135	-1.8681
145	18956	NM_144639	131669	FLJ31300	-5.53304	0.00911	1.09	198	D08	38162	-0.1108	32336	-0.1169	19804	-0.9574	12991	-1.4581
146	1330	NM_002068	2769	GNA15	-4.3137	0.01903	1.09	14	G10	23858	-0.525	28815	-0.175	11080	-1.7106	15922	-1.1708
149	4479	NM_021009	7316	UBC	-8.39703	0.00249	1.09	47	F03	2603	-3.7425	3008	-3.5152	1292	-4.8284	1484	-4.6003
151	2371	NM_017534	4620	MYH2	-8.45971	0.00244	1.07	25	F07	20353	-0.7325	24256	-0.4358	12188	-1.6022	10721	-1.708
153	475	NM_002419	4296	MAP3K11	-4.25692	0.01977	1.07	5	H07	21259	-0.7783	27470	-0.2804	14381	-1.3977	10478	-1.7973
155	16015	NM_024031	78994	MGC3121	-3.09888	0.04724	1.06	167	G07	29102	-0.4832	26344	-0.4992	17890	-1.1174	8710	-1.9946
159	654	NM_002645	5286	PIK3C2A	-4.96451	0.01261	1.06	7	G06	22457	-0.675	23919	-0.45	14500	-1.3731	10200	-1.8635
162	22289	NM_207477	400931	FLJ27365	-3.74662	0.02836	1.05	233	B05	36937	-0.2164	35649	-0.0467	21664	-0.8337	12876	-1.5262
164	2084	NM_014325	23603	CORO1C	-3.36723	0.03794	1.04	22	F08	23616	-0.6312	32442	-0.1017	11068	-1.7003	16523	-1.1153
166	13126	NM_014402	27089	QP-C	-5.01909	0.01221	1.04	137	F10	28886	-0.3988	30791	-0.2608	18157	-1.1156	11955	-1.6221
168	3324	NM_004348	860	RUNX2	-3.5497	0.0329	1.04	35	E12	33741	-0.1429	29141	-0.2553	20887	-0.8682	11884	-1.6048
169	406	NM_005544	3667	IRS1	-7.95342	0.00296	1.04	5	B10	26144	-0.4799	26487	-0.333	15414	-1.2976	12122	-1.587
172	22980	XM_210826	0	LOC286404	-4.38408	0.01816	1.03	240	C12	38710	-0.1192	34113	-0.1111	21896	-0.8441	13649	-1.4392
173	13299	NM_014167	29080	HSPC128	-5.99143	0.00715	1.02	139	E03	27292	-0.4409	30217	-0.2969	17246	-1.1884	12190	-1.5939
177	3491	NM_006006	7704	ZBTB16	-3.79363	0.02739	1.01	37	C11	19983	-0.9199	27922	-0.2795	13284	-1.4983	10686	-1.7273
182	5287	NM_005489	10044	SH2D3C	-5.63525	0.00862	1	56	A07	29159	-0.4177	28601	-0.2763	12632	-1.5547	15882	-1.1314
183	19064	NM_174959	136306	LOC136306	-3.50527	0.03404	0.99	199	E08	23483	-0.8004	17254	-1.0453	12731	-1.5763	7635	-2.2557
190	15814	NM_022489	64423	FLJ22056	-12.2164	0.00075	0.98	165	F10	36568	-0.1654	32994	-0.1716	18846	-1.0503	14393	-1.2396
193	844	NM_014264	10733	PLK4	-3.16682	0.04464	0.97	9	G04	30634	-0.2921	28237	-0.2155	20930	-0.8369	11703	-1.617

198	14736	NM_017842	55652	FLJ20489	-3.30231	0.03997	0.97	154	D12	26564	-0.5278	27930	-0.3879	18997	-1.059	10063	-1.7934
202	5375	NM_001783	973	CD79A	-3.44028	0.03581	0.96	56	H11	37277	-0.0634	32531	-0.0906	14131	-1.3929	21686	-0.682
204	15611	NM_021817	60484	HAPLN2	-5.58957	0.00883	0.96	163	E11	31899	-0.3546	31680	-0.2343	18680	-1.0459	12851	-1.4619
205	1507	NM_000865	3354	HTR1E	-3.35092	0.03844	0.96	16	F07	25055	-0.3984	28182	-0.1802	19794	-0.8983	11798	-1.5917
207	3184	NM_004739	9219	MTA2	-5.05503	0.01195	0.95	34	B04	25080	-0.6343	31149	-0.1595	15270	-1.3254	14080	-1.3769
208	19205	NM_080621	140700	C20ORF136	-10.2378	0.00133	0.95	201	A05	35160	-0.1999	33863	-0.1168	19021	-1.006	15298	-1.2154
209	10740	NM_004610	6953	TCP10	-4.10325	0.02196	0.95	112	G12	30153	-0.4148	27859	-0.3448	18497	-1.0382	12004	-1.6229
210	3604	NM_012067	22977	AKR7A3	-11.8407	0.00083	0.95	38	E04	32316	-0.2098	32866	-0.0241	17525	-1.0462	16656	-1.088
212	5220	NM_001493	2664	GDI1	-3.8431	0.02642	0.94	55	C12	40748	0.1039	32235	-0.1272	23279	-0.6628	14812	-1.2402
215	2442	NM_018903	56137	PCDHA12	-3.44046	0.03581	0.94	26	D06	23248	-0.5101	20584	-0.7082	15986	-1.2142	9703	-1.8799
216	3130	NM_015995	51621	KLF13	-4.06053	0.02262	0.94	33	E10	34511	-0.0601	31862	-0.0878	22654	-0.7186	14657	-1.3048
218	16121	NM_024322	79172	MGC11266	-3.07974	0.048	0.93	168	H05	28099	-0.5167	28879	-0.3387	19538	-0.9849	10370	-1.7369
221	4592	NM_004100	2070	EYA4	-5.29861	0.01038	0.93	48	G08	24628	-0.5659	27697	-0.2737	12572	-1.5116	15720	-1.1808
222	4460	NM_004623	7268	TTC4	-6.80386	0.00483	0.93	47	D08	31272	-0.1559	31460	-0.1286	15561	-1.2382	19302	-0.8991
223	3959	NM_024075	79042	LENG5	-3.07564	0.04817	0.93	42	B11	27502	-0.4827	24058	-0.5512	18194	-1.0607	9957	-1.8257
225	5324	NM_001376	1778	DNCH1	-13.6657	0.00052	0.92	56	D08	29857	-0.3836	25728	-0.429	15527	-1.257	13138	-1.405
226	2423	NM_006194	5083	PAX9	-6.73487	0.00498	0.92	26	B11	19601	-0.7563	23660	-0.5072	13694	-1.4375	11200	-1.6729
227	2492	NM_000296	5310	PKD1	-7.16407	0.00411	0.92	26	H08	22199	-0.5767	27665	-0.2816	13906	-1.4153	14612	-1.2892
228	3572	NM_000666	95	ACY1	-5.05904	0.01192	0.92	38	B08	28819	-0.375	31912	-0.0666	14571	-1.3125	18062	-0.9711
230	1266	NM_005226	1903	EDG3	-9.28695	0.00181	0.92	14	B06	26818	-0.3563	28549	-0.1884	14938	-1.2796	16656	-1.1057
231	4147	NM_005622	6296	SAH	-3.05612	0.04897	0.92	44	B07	17351	-1.1042	27141	-0.3643	12634	-1.552	10677	-1.7555
232	18478	NM_054114	117289	TAGAP	-4.28267	0.01943	0.92	193	D10	31675	-0.3401	30247	-0.2653	19544	-0.9523	12609	-1.4919
235	19391	NM_152908	146802	FLJ31196	-3.51124	0.03389	0.91	202	H11	23287	-0.8255	27162	-0.414	15765	-1.2743	10360	-1.7944
236	13111	NM_014388	27042	MGC29875	-9.48086	0.0017	0.91	137	E07	38238	0.0058	34389	-0.1014	21713	-0.8576	17575	-1.0662
240	3976	NM_002372	4124	MAN2A1	-4.0068	0.02349	0.91	42	D04	33401	-0.2024	34079	-0.0488	22484	-0.7553	14244	-1.3091
241	1192	NM_001716	643	BLR1	-3.81406	0.02698	0.91	13	D04	25724	-0.3989	26749	-0.3408	11728	-1.5755	17992	-0.9749
242	3927	NM_000203	3425	IDUA	-3.24991	0.0417	0.9	41	H03	18013	-1.0673	20808	-0.7416	13303	-1.4938	7999	-2.1235
244	3598	NM_003739	8644	AKR1C3	-7.48847	0.00358	0.9	38	D10	19820	-0.915	21686	-0.624	11074	-1.7084	11373	-1.6384
247	568	NM_025233	80347	COASY	-9.36483	0.00176	0.9	6	H04	28036	-0.3009	31386	-0.0834	16728	-1.1377	17234	-1.0507
248	9452	NM_004371	1314	COPA	-3.87917	0.02573	0.9	99	D08	6092	-2.7692	5239	-2.8181	3565	-3.4006	2300	-3.989
257	908	NM_003318	7272	TTK	-3.25604	0.04149	0.89	10	D08	23891	-0.5862	28836	-0.251	18720	-1.0057	11739	-1.6197
258	1409	NM_005281	2827	GPR3	-6.44518	0.00571	0.89	15	F05	24765	-0.5297	28380	-0.1887	15685	-1.2214	14679	-1.2843
262	19543	NM_152496	149175	FLJ31434	-3.29394	0.04024	0.89	204	E07	34272	-0.2588	29777	-0.2698	21808	-0.81	12987	-1.4979
265	1383	NM_018949	2837	GPR14	-3.49464	0.03433	0.89	15	D03	23810	-0.5864	32495	0.00662	17677	-1.0489	14478	-1.3042
269	5956	NM_014387	27040	LAT	-10.0413	0.00141	0.88	63	A04	32245	-0.3111	31585	-0.2056	18710	-1.0503	14532	-1.2338
270	1984	NM_018429	55814	BDP1	-3.18092	0.04412	0.88	21	F04	23745	-0.6261	29344	-0.2335	11827	-1.6033	17507	-1.0174
272	17505	NM_032810	84896	ATAD1	-27.9684	5.06E-05	0.88	183	C09	36459	-0.1024	34042	-0.0873	20058	-0.9787	18458	-0.9668
273	2804	NM_032595	84687	PPP1R9B	-4.02074	0.02326	0.88	30	B08	27859	-0.3436	32692	-0.0227	15005	-1.2842	19996	-0.8339
274	1975	NM_005872	10286	BCAS2	-11.9779	0.0008	0.88	21	E07	36106	-0.0215	34683	0.00769	18387	-0.9667	20370	-0.7989

275	15512	NM_021177	57819	LSM2	-3.48863	0.03449	0.87	162	E08	21637	-0.9243	24713	-0.5944	15220	-1.3604	9558	-1.9056
277	2205	NM_021170	57801	HES4	-6.68468	0.0051	0.87	23	H09	13697	-1.3815	15390	-1.1318	9147	-2.0238	7683	-2.2313
280	3828	NM_001680	486	FXYD2	-4.7131	0.0147	0.87	40	G12	17445	-1.0947	20123	-0.749	9491	-1.9431	11245	-1.6328
281	5304	NM_001101	60	ACTB	-11.6782	0.00087	0.86	56	B12	34060	-0.1936	29037	-0.2545	16495	-1.1697	17302	-1.0078
282	3825	NM_000150	2528	FUT6	-10.1676	0.00136	0.86	40	G09	35265	-0.0793	31428	-0.1058	20166	-0.8558	16755	-1.0575
283	20319	NM_144994	200539	ANKRD23	-4.01876	0.02329	0.86	212	F03	32101	-0.3243	28010	-0.3286	21170	-0.9174	12801	-1.4627
287	1269	NM_003775	8698	EDG6	-3.68767	0.02963	0.86	14	B09	26034	-0.3991	29774	-0.1278	13857	-1.388	19743	-0.8604
289	1678	NM_002831	5777	PTPN6	-7.53513	0.00351	0.86	18	D10	21382	-0.6952	23637	-0.5105	14767	-1.3555	12151	-1.568
290	5226	NM_015071	23092	ARHGAP26	-3.67456	0.02992	0.86	55	D06	35995	-0.075	32202	-0.1287	23268	-0.6634	14677	-1.2534
292	4144	NM_001034	6241	RRM2	-6.78081	0.00488	0.85	44	B04	8053	-2.2116	7999	-2.1269	5056	-2.8732	3991	-3.1752
293	2891	NM_005187	863	CBFA2T3	-5.7016	0.00832	0.85	31	A11	17990	-0.9899	21192	-0.6301	11171	-1.7195	11775	-1.6098
300	20595	NM_145115	221785	ZNF498	-4.61298	0.01566	0.85	215	E03	37987	-0.071	32674	0.11219	24766	-0.6143	16492	-1.0419
304	19233	NM_080827	140870	WFDC6	-5.20067	0.01098	0.85	201	C09	31153	-0.3745	27060	-0.4404	18428	-1.0517	12946	-1.4562
305	12174	NM_007242	11269	DDX19	-5.66003	0.0085	0.85	127	G06	28852	-0.5495	32414	-0.2195	16030	-1.3202	17187	-1.1416
306	18862	NM_144628	128637	C20ORF140	-3.27342	0.04091	0.84	197	D10	38282	-0.097	34360	-0.0656	25192	-0.5974	15318	-1.2528
307	1947	NM_001157	311	ANXA11	-6.21497	0.00639	0.84	21	C03	31212	-0.2316	30523	-0.1766	15486	-1.2145	19255	-0.8801
311	19139	NM_148178	138716	C9ORF23	-3.36384	0.03804	0.84	200	C11	36815	-0.128	33373	-0.0745	24708	-0.6242	15666	-1.2567
312	3320	NM_000538	5994	RFXAP	-15.7958	0.00033	0.84	35	E08	31957	-0.2213	30697	-0.1803	19226	-0.9878	16963	-1.0914
314	1470	NM_020400	57121	GPR92	-9.77043	0.00154	0.83	16	C06	27581	-0.2598	26571	-0.2652	18531	-0.9934	15506	-1.1975
315	2650	NM_152860	121340	SP7	-5.3267	0.01022	0.83	28	E10	17546	-0.9352	22996	-0.5622	11425	-1.643	12492	-1.5194
317	3707	NM_001908	1508	CTSB	-10.9675	0.00106	0.83	39	E11	37975	0.08446	34282	0.01351	21929	-0.7012	19443	-0.8645
321	17717	NM_033085	89885	FATE	-4.69845	0.01484	0.83	185	E05	25533	-0.647	31010	-0.2503	14928	-1.3788	16073	-1.1761
322	5958	NM_002309	3976	LIF	-5.15891	0.01125	0.83	63	A06	21525	-0.8942	22140	-0.7182	14154	-1.4529	9700	-1.817
326	2800	NM_003024	6453	ITSN1	-10.0395	0.00141	0.83	30	B04	32762	-0.1097	34913	0.0721	20865	-0.8086	19340	-0.882
328	3119	NM_001572	3665	IRF7	-4.04351	0.02289	0.82	33	D11	36165	0.00747	31880	-0.087	24441	-0.6091	16705	-1.1162
329	15526	NM_021196	57835	SLC4A5	-3.69803	0.0294	0.82	162	F10	33707	-0.2847	30578	-0.2871	22041	-0.8262	13653	-1.3911
330	3671	NM_001266	1066	CES1	-12.8052	0.00065	0.82	39	B11	28362	-0.3366	28016	-0.2777	15607	-1.1919	16975	-1.0604
331	20283	NM_182532	199964	LOC199964	-3.13965	0.04566	0.82	212	C03	37968	-0.0821	34349	-0.0343	27387	-0.546	15270	-1.2083
332	12129	NM_007177	11170	TU3A	-18.0985	0.00021	0.82	127	C09	42163	-0.0022	37698	-0.0016	23343	-0.778	20838	-0.8637
333	20529	NM_194247	220988	HNRNPA3	-3.74812	0.02832	0.82	214	G09	33838	-0.2744	23706	-0.3331	21146	-0.845	13134	-1.3944
335	11532	NM_014792	9834	KIAA0125	-6.26202	0.00624	0.81	121	A12	34801	-0.2563	32994	-0.1617	21411	-0.8681	16783	-1.178
339	60	NM_016248	11215	AKAP11	-4.39041	0.01808	0.81	1	E12	14848	-1.3048	14136	-1.3441	10449	-1.9012	7006	-2.3653
347	21527	XM_370995	333929	SNAI3	-4.40112	0.01796	0.8	225	B11	34659	-0.2871	31109	-0.2851	20941	-0.8592	14876	-1.3209
354	1695	NM_003702	8601	RGS20	-3.26393	0.04123	0.8	18	F03	10663	-1.699	14797	-1.1862	9029	-2.0652	6733	-2.4198
356	5296	NM_003254	7076	TIMP1	-4.29297	0.01929	0.8	56	B04	35790	-0.1221	33614	-0.0433	23662	-0.6492	16088	-1.1128
359	2622	NM_003017	6428	SFRS3	-5.24009	0.01073	0.8	28	C06	12347	-1.4422	15813	-1.1024	8011	-2.1551	9068	-1.9815
363	2564	NM_002916	5984	RFC4	-16.8733	0.00026	0.79	27	F08	21614	-0.6203	22207	-0.5377	14081	-1.3512	13062	-1.3902
367	15676	NM_022091	63921	DJ467N11.1	-3.92313	0.02493	0.79	164	C04	34895	-0.2361	28322	-0.3935	21634	-0.8608	13624	-1.3447
368	18096	XM_057296	116064	LOC116064	-3.31009	0.03972	0.79	189	D12	15841	-1.2755	21928	-0.7558	12577	-1.6486	9497	-1.9584

369	14598	NM_197958	55323	FLJ11196	-3.39591	0.03709	0.79	153	A06	35505	-0.1168	33881	-0.0928	25888	-0.598	15055	-1.1869
370	4930	NM_004574	5414	PNUTL2	-3.13129	0.04598	0.79	52	C10	34045	-0.1213	32529	-0.1011	25166	-0.5789	14928	-1.2186
371	3736	NM_016216	51163	DBR1	-9.35615	0.00177	0.79	39	H04	30284	-0.242	26374	-0.3648	15844	-1.1701	17566	-1.011
373	2063	NM_003663	8545	CGGBP1	-4.01101	0.02342	0.79	22	D11	32042	-0.191	33476	-0.0565	16213	-1.1495	22477	-0.6714
375	1704	NM_000327	6094	ROM1	-5.59594	0.0088	0.79	18	F12	19673	-0.8154	24292	-0.471	13701	-1.4636	13709	-1.394
376	1935	NM_016453	51517	NCKIPSD	-3.79816	0.0273	0.79	21	B03	29060	-0.3347	29217	-0.2397	14291	-1.3303	20147	-0.8147
379	3869	NM_012203	9380	GRHPR	-3.07613	0.04815	0.78	41	C05	25053	-0.5914	28705	-0.2774	19606	-0.9343	12312	-1.5013
384	3844	NM_001482	2628	GATM	-5.39212	0.00985	0.78	41	A04	25190	-0.5835	27659	-0.331	17378	-1.1083	13490	-1.3695
385	15507	NM_172231	57794	SF4	-3.35535	0.0383	0.78	162	E03	37532	-0.1297	34342	-0.1197	25607	-0.6099	15574	-1.2012
386	1240	NM_001841	1269	CNR2	-3.12298	0.04629	0.78	13	H04	16646	-1.0268	25602	-0.4041	11905	-1.5539	13088	-1.434
388	13036	NM_014356	26238	C6ORF123	-3.99032	0.02377	0.78	136	G04	37111	0.0868	34057	-0.0841	27166	-0.5445	17827	-1.0071
389	5019	NM_006325	5901	RAN	-3.83962	0.02648	0.78	53	C03	7874	-2.2857	10020	-1.823	5663	-2.7208	4523	-2.9421
393	703	NM_017431	53632	PRKAG3	-4.31244	0.01904	0.77	8	C07	14111	-1.2484	14641	-1.0907	8453	-2.153	11678	-1.7294
394	5298	NM_000362	7078	TIMP3	-8.2275	0.00266	0.77	56	B06	36065	-0.1111	32774	-0.0798	22013	-0.7534	17661	-0.9782
402	2395	NM_004148	4814	NINJ1	-3.78743	0.02751	0.76	25	H07	19454	-0.7976	21933	-0.581	15889	-1.2196	10932	-1.6799
403	3647	NM_000709	593	BCKDHA	-3.46016	0.03526	0.76	38	H11	18833	-0.9887	18916	-0.8211	13724	-1.3989	9288	-1.9306
415	896	NM_022445	27010	TPK1	-4.07589	0.02238	0.75	10	C08	21109	-0.7648	26806	-0.3563	16372	-1.199	13477	-1.4205
419	19359	XM_375359	146227	BEAN	-10.0959	0.00139	0.75	202	F03	29652	-0.4769	29268	-0.3063	17486	-1.1248	16161	-1.1529
425	526	NM_006343	10461	MERTK	-4.36439	0.0184	0.74	6	D10	35834	0.05315	33317	0.00272	25972	-0.503	18733	-0.9304
429	12004	NM_032102	10929	SRP46	-4.03741	0.02299	0.74	126	A04	40694	-0.0615	36649	-0.0343	26943	-0.5591	18334	-1.024
433	4461	NM_003320	7275	TUB	-11.6822	0.00087	0.74	47	D09	31060	-0.1657	30222	-0.1865	20467	-0.8428	18214	-0.9828
434	3664	NM_012114	23581	CASP14	-6.71935	0.00502	0.74	39	B04	34814	-0.0409	34472	0.02149	19404	-0.8777	23113	-0.6151
436	17484	NM_032786	84872	FLJ14451	-4.68074	0.015	0.74	183	A12	24520	-0.6747	29779	-0.2803	16855	-1.2297	15725	-1.198
437	4528	NM_001889	1429	CRYZ	-3.2387	0.04208	0.74	48	B04	32898	-0.1482	29551	-0.1802	23456	-0.6118	15642	-1.188
441	5370	NM_004244	9332	CD163	-8.72588	0.00221	0.73	56	H06	25639	-0.6033	26112	-0.4077	15463	-1.2629	14971	-1.2166
443	4470	NM_003323	7288	TULP2	-5.737	0.00816	0.73	47	E06	20425	-0.7704	25028	-0.4586	14126	-1.3778	14455	-1.3163
445	2865	NM_007348	22926	ATF6	-7.09682	0.00423	0.73	30	G09	31757	-0.1546	32980	-0.0101	19365	-0.9162	21793	-0.7097
446	16296	NM_024675	79728	FLJ21816	-3.29847	0.04009	0.73	170	F12	27565	-0.5068	30166	-0.2348	21295	-0.855	14222	-1.3467
454	16311	NM_024688	79741	C10ORF68	-7.90711	0.00302	0.72	170	H03	30857	-0.3441	32016	-0.149	18962	-1.0224	19143	-0.918
456	198	NM_004766	9276	COPB2	-5.90822	0.00746	0.72	3	A06	10083	-1.8246	9244	-1.8822	7367	-2.427	5588	-2.7251
458	8470	NM_006353	10473	HMGN4	-3.31176	0.03966	0.72	89	B10	27692	-0.5482	29447	-0.3085	20386	-0.901	14329	-1.3998
459	2863	NM_001675	468	ATF4	-5.74754	0.00812	0.72	30	G07	29145	-0.2784	30429	-0.1262	17521	-1.0606	20644	-0.7879
460	5322	NM_005552	3831	KNS2	-6.47795	0.00562	0.72	56	D06	33317	-0.2254	32311	-0.1004	21880	-0.7622	17316	-1.0067
464	4371	NM_004607	6902	TBCA	-3.91418	0.02509	0.72	46	E03	22389	-0.7062	28032	-0.2546	15603	-1.2497	16102	-1.1461
466	19833	NM_182525	157376	FLJ32770	-4.90429	0.01307	0.72	207	E09	34659	-0.2053	29369	-0.2672	23022	-0.7728	16464	-1.1343
471	1973	NM_004742	9223	BAIAP1	-3.89046	0.02553	0.71	21	E05	33612	-0.1247	35091	0.02456	18178	-0.9832	24302	-0.5442
475	18935	NM_182501	130916	MGC61716	-3.36537	0.038	0.71	198	B11	37878	-0.1215	31332	-0.1624	25619	-0.5859	16416	-1.1205
476	3620	NM_017584	55586	ALDRL6	-4.37275	0.01829	0.71	38	F08	24427	-0.6135	27980	-0.2563	15277	-1.2443	17154	-1.0455
482	3607	NM_000693	220	ALDH1A3	-4.04741	0.02283	0.7	38	E07	27860	-0.4238	31571	-0.0821	20509	-0.8194	16571	-1.0954

485	9220	NM_001088	15	AANAT	-3.1044	0.04702	0.7	97	A04	22826	-0.8281	26157	-0.5073	17970	-1.1322	11894	-1.61
486	669	NM_006875	11040	PIM2	-5.23323	0.01077	0.7	7	H09	20906	-0.7783	21926	-0.5755	15831	-1.2464	12999	-1.5136
488	4480	NM_006398	10537	UBD	-3.51272	0.03385	0.7	47	F04	33869	-0.0408	33849	-0.023	18510	-0.9878	25785	-0.4813
489	16316	NM_021819	79748	LMAN1L	-4.28829	0.01935	0.7	170	H08	33224	-0.2374	33451	-0.0857	24173	-0.6721	17401	-1.0557
491	2289	NM_031918	83855	KLF16	-3.32619	0.03921	0.7	24	G09	18377	-0.9692	22388	-0.5321	15624	-1.298	12078	-1.6065
500	1320	NM_004122	2693	GHSR	-7.70726	0.00327	0.7	14	F12	30976	-0.1484	30016	-0.1161	18915	-0.939	21722	-0.7226
501	12128	NM_007086	11169	WDHD1	-3.52599	0.0335	0.7	127	C08	36194	-0.2224	35909	-0.0717	26293	-0.6063	17876	-1.0848
506	6056	NM_016224	51429	SNX9	-7.95444	0.00296	0.7	64	A08	32296	-0.3206	33538	-0.1154	20789	-0.8914	18373	-0.9378
508	175	NM_025197	80279	CDK5RAP3	-4.77257	0.01417	0.7	2	G07	21595	-0.7488	24253	-0.4847	17257	-1.1865	13377	-1.4396
510	19114	NM_205545	137797	UNQ430	-7.27382	0.00392	0.7	200	A10	30764	-0.3871	30674	-0.1961	20119	-0.9207	18046	-1.0527
512	18681	NM_178860	124925	SEZ6	-9.20612	0.00186	0.69	195	E09	33935	-0.2603	30979	-0.2285	21544	-0.8507	17878	-1.0243
521	19155	NM_144657	139324	FLJ30678	-4.36112	0.01844	0.69	200	E03	27251	-0.562	24548	-0.5175	18617	-1.0326	13907	-1.4286
522	21359	NM_198281	285513	LOC285513	-4.38577	0.01814	0.69	223	D11	35851	-0.2099	31332	-0.2367	23192	-0.7162	16991	-1.1113
525	195	NM_004073	1263	PLK3	-4.13325	0.02151	0.69	3	A03	16310	-1.1308	19301	-0.8201	13791	-1.5224	10580	-1.8042
531	3936	XM_290331	2679	GGT2	-5.13942	0.01137	0.69	41	H12	31555	-0.2585	31616	-0.1381	22602	-0.7291	16953	-1.0398
538	3536	NM_003752	8663	EIF3S8	-6.22717	0.00635	0.68	37	G08	10118	-1.9017	10802	-1.6496	7064	-2.4094	6239	-2.5037
539	19493	NM_138813	148229	ATP8B3	-7.83902	0.0031	0.68	204	A05	34699	-0.241	31087	-0.2077	21928	-0.8021	18240	-1.0079
544	520	NM_002376	4140	MARK3	-6.02923	0.00701	0.68	6	D04	30446	-0.1819	24184	-0.4595	18504	-0.9921	17757	-1.0076
552	18480	NM_080864	117579	RLN3	-4.49347	0.01691	0.67	193	D12	40207	0.00403	35747	-0.0242	26794	-0.4971	19362	-0.8731
553	1588	NM_000911	4985	OPRD1	-5.28454	0.01046	0.67	17	E04	38007	0.1627	35939	0.09242	28126	-0.3914	22386	-0.7009
554	1616	NM_012369	26211	OR2F1	-3.10354	0.04705	0.67	17	G08	14674	-1.2103	18581	-0.8593	13079	-1.4961	9612	-1.9206
560	2192	NM_002092	2926	GRSF1	-7.50644	0.00355	0.67	23	G08	27914	-0.3544	30499	-0.145	19997	-0.8954	18732	-0.9455
562	4397	NM_006288	7070	THY1	-4.39083	0.01808	0.67	46	G05	31901	-0.1954	32299	-0.0502	24213	-0.6158	18182	-0.9708
563	928	NM_003390	7465	WEE1	-4.53968	0.01641	0.67	10	F04	10784	-1.7338	13301	-1.3674	7926	-2.2456	7880	-2.1947
565	1235	NM_000740	1131	CHRM3	-4.5704	0.01609	0.67	13	G11	22266	-0.6072	28447	-0.252	16854	-1.0524	16002	-1.144
569	4506	NM_022553	6293	VPS52	-3.45046	0.03553	0.67	47	H06	25838	-0.4312	29428	-0.2249	21480	-0.7731	15488	-1.2167
572	15201	NM_018226	57140	RNPEPL1	-3.58421	0.03204	0.67	159	C09	40559	0.04058	36975	0.00064	28816	-0.4112	19179	-0.8793
575	4553	NM_004401	1676	DFFA	-6.85824	0.00471	0.66	48	D05	37225	0.03008	35489	0.08398	25486	-0.4921	21617	-0.7213
576	13197	NM_014471	27290	SPINK4	-4.01356	0.02338	0.66	138	D09	27157	-0.485	29854	-0.3116	21352	-0.8723	15354	-1.2508
578	3672	NM_016280	51716	CES4	-6.82034	0.00479	0.66	39	B12	27356	-0.3887	27001	-0.3309	16204	-1.1377	18863	-0.9082
581	18491	NM_145202	118471	PRAP1	-7.2007	0.00405	0.66	193	E11	26084	-0.6202	26167	-0.4743	17328	-1.1259	14463	-1.2939
585	2591	NM_002968	6299	SALL1	-4.13876	0.02143	0.66	27	H11	12861	-1.3693	16484	-0.9676	10127	-1.8267	9619	-1.8316
594	2443	NM_018904	56136	PCDHA13	-3.35062	0.03845	0.66	26	D07	34808	0.07219	32925	-0.0305	28247	-0.393	19426	-0.8784
597	23944	XM_371843	0	LOC389425	-3.29288	0.04027	0.65	250	D04	19518	-1.1056	16298	-1.197	13119	-1.5561	8989	-2.0483
598	13896	NM_016310	51728	POLR3K	-5.75421	0.00809	0.65	145	F12	31497	-0.2531	32027	-0.2034	23395	-0.7415	17392	-1.0161
602	12730	NM_012322	23658	LSM5	-3.89554	0.02543	0.65	133	E10	26365	-0.4672	25566	-0.4663	20694	-0.9047	14162	-1.3234
603	4520	NM_000754	1312	COMT	-6.14853	0.0066	0.65	48	A08	29681	-0.2967	27891	-0.2636	17248	-1.0554	20480	-0.7992
607	898	NM_021643	28951	TRIB2	-3.09008	0.04759	0.65	10	C10	27339	-0.3917	32357	-0.0848	23658	-0.6679	16831	-1.0999
612	2313	NM_012090	23499	MACF1	-8.0764	0.00282	0.64	25	A09	32571	-0.0541	32413	-0.0176	21667	-0.7721	23319	-0.5869

616	4545	NM_014881	9937	DCLRE1A	-12.5465	0.00069	0.64	48	C09	36881	0.01668	35229	0.07337	23003	-0.64	24316	-0.5515
617	3643	NM_007255	11285	B4GALT7	-6.55035	0.00543	0.64	38	H07	30059	-0.3142	30908	-0.1127	20929	-0.7901	18756	-0.9167
622	3708	NM_001814	1075	CTSC	-4.2611	0.01971	0.64	39	E12	24415	-0.5528	27531	-0.3029	18772	-0.9255	15345	-1.206
623	5171	NM_006225	5333	PLCD1	-3.73767	0.02854	0.64	54	G11	40617	0.11862	34885	0.02004	29625	-0.3583	20117	-0.7765
625	2848	NM_014795	9839	ZFHX1B	-17.9567	0.00022	0.64	30	F04	38271	0.11455	34854	0.06966	24965	-0.5498	24539	-0.5385
626	424	NM_025164	23387	KIAA0999	-4.34372	0.01865	0.63	5	D04	37167	0.02761	30541	-0.1275	26446	-0.5188	20194	-0.8507
627	1683	NM_000322	5961	RDS	-5.22352	0.01083	0.63	18	E03	19210	-0.8497	22836	-0.5602	15373	-1.2975	13836	-1.3807
632	20502	NM_153451	220064	ORAOV1	-3.07634	0.04814	0.63	214	E06	37567	-0.1236	30735	0.04152	28257	-0.4268	18225	-0.9218
646	18499	NM_144587	118663	C10ORF87	-12.1647	0.00076	0.63	193	F07	37815	-0.0845	34279	-0.0847	23964	-0.6581	20874	-0.7646
650	2664	NM_006372	10492	SYNCRIP	-3.66496	0.03014	0.62	28	F12	26649	-0.3322	28740	-0.2405	16421	-1.1197	22038	-0.7004
661	332	NM_024619	79672	FN3KRP	-4.467	0.0172	0.62	4	D08	37087	0.03254	31408	-0.0861	27276	-0.4827	21417	-0.8081
662	3675	NM_016044	51011	CGI-105	-4.97994	0.01249	0.62	39	C03	34475	-0.055	33630	-0.0142	20414	-0.8045	25045	-0.4992
666	10649	NM_004175	6634	SNRPD3	-4.172	0.02094	0.62	111	H05	16830	-1.3044	14237	-1.3395	8022	-1.7538	8649	-2.1226
668	4484	NM_003969	9040	UBE2M	-5.08703	0.01173	0.62	47	F08	33993	-0.0355	32536	-0.0801	20767	-0.8218	25017	-0.5249
669	1232	NM_001407	1951	CELSR3	-5.20058	0.01098	0.62	13	G08	22517	-0.591	27461	-0.3029	16431	-1.089	17253	-1.0354
674	20442	XM_291062	205717	KIAA2018	-3.75824	0.02811	0.61	213	H06	39894	-0.0429	31781	0.06137	28815	-0.4033	19811	-0.7985
675	3150	NM_002357	4084	MAD	-5.45235	0.00952	0.61	33	G06	33440	-0.1056	27123	-0.3201	22381	-0.7361	19276	-0.9096
676	9222	NM_001606	20	ABCA2	-5.52225	0.00916	0.61	97	A06	34905	-0.2153	35160	-0.0806	25296	-0.6388	19802	-0.8746
677	2541	NM_002874	5887	RAD23B	-5.67122	0.00845	0.61	27	D09	31020	-0.0991	30655	-0.0725	24312	-0.5633	19317	-0.8257
679	3190	XM_034274	4603	MYBL1	-7.78991	0.00316	0.61	34	B10	29577	-0.3964	29872	-0.2199	20653	-0.8898	19023	-0.9428
680	388	NM_000875	3480	IGF1R	-5.28422	0.01046	0.61	5	A04	29448	-0.3082	30943	-0.1087	20060	-0.9175	22186	-0.715
683	19015	NM_153216	134187	FLJ25680	-3.79427	0.02738	0.61	199	A07	33305	-0.2963	31369	-0.1828	24137	-0.6534	17736	-1.0397
688	3774	NM_001406	1949	EFNB3	-4.4026	0.01794	0.6	40	C06	30367	-0.295	32334	-0.0648	19395	-0.9121	22111	-0.6573
689	3833	NM_000817	2571	GAD1	-3.0574	0.04891	0.6	40	H05	30775	-0.2757	29989	-0.1734	17345	-1.0733	23270	-0.5836
691	24096	XM_379508	0	LOC401386	-3.75126	0.02826	0.6	251	H12	33610	-0.3215	27724	-0.4208	22446	-0.777	16396	-1.1681
696	18502	NM_178832	118812	C10ORF83	-5.5072	0.00924	0.6	193	F10	35938	-0.1579	31900	-0.1885	20202	-0.9045	22775	-0.6389
697	16920	NM_031426	83543	C9ORF58	-7.93756	0.00298	0.6	177	B12	31494	-0.3022	33237	-0.1257	22013	-0.8147	20622	-0.8088
698	324	NM_152649	197259	FLJ34389	-6.34386	0.006	0.6	4	C12	36374	0.00453	32259	-0.0475	26808	-0.5077	22607	-0.7301
703	5189	NM_001092	29	ABR	-3.84483	0.02638	0.59	55	A05	30178	-0.3293	29828	-0.2392	22844	-0.69	16688	-1.0682
704	2363	NM_005823	10232	MSLN	-4.11376	0.0218	0.59	25	E11	20421	-0.7276	24738	-0.4074	17533	-1.0775	14759	-1.2468
706	2073	NM_015282	23332	CLASP1	-10.3408	0.00128	0.59	22	E09	32499	-0.1705	31971	-0.1228	22411	-0.6825	20594	-0.7976
708	5208	NM_014697	9722	CAPON	-6.4831	0.00561	0.59	55	B12	33565	-0.1759	31076	-0.1801	23331	-0.6595	19012	-0.8801
711	9316	NM_001686	506	ATP5B	-7.448	0.00364	0.59	98	A04	29193	-0.4913	27319	-0.4132	19908	-0.9581	16700	-1.1289
712	2819	NM_001756	866	SERPINA6	-7.42665	0.00367	0.59	30	C11	27428	-0.366	28786	-0.2063	19220	-0.9271	20089	-0.8272
716	3004	NM_005250	2300	FOXL1	-3.42275	0.03631	0.59	32	C04	30521	-0.1802	32701	0.0113	26362	-0.4791	19335	-0.8694
718	9036	NM_003169	6829	SUPT5H	-3.32291	0.03931	0.59	95	A12	34381	-0.2182	33520	-0.0826	26798	-0.5264	18899	-0.9533
719	7048	NM_000268	4771	NF2	-4.38797	0.01811	0.59	74	D04	36550	-0.0965	34573	-0.0787	27098	-0.5095	19174	-0.8443
721	19954	NM_173527	161253	FLJ38964	-3.80219	0.02722	0.59	208	G10	31826	-0.3363	28386	-0.3134	23120	-0.7196	16775	-1.1085
730	4293	NM_014272	11173	ADAMTS7	-7.25094	0.00396	0.59	45	F09	27159	-0.4374	27919	-0.2636	20173	-0.8958	18101	-0.9769

734	2103	NM_004392	1602	DACH1	-5.31902	0.01026	0.58	22	H03	32168	-0.1853	33038	-0.0755	20133	-0.8371	23775	-0.5904
735	22336	NM_203453	403313	LOC403313	-7.57216	0.00346	0.58	233	F04	42119	-0.027	37222	0.01558	27287	-0.5007	23197	-0.677
745	3845	NM_000157	2629	GBA	-4.94556	0.01275	0.58	41	A05	25019	-0.5934	27609	-0.3336	19014	-0.9785	16174	-1.1077
748	3690	NM_001871	1360	CPB1	-9.17883	0.00188	0.58	39	D06	34432	-0.0568	34807	0.03544	22854	-0.6416	24434	-0.5349
753	4548	NM_006773	8886	DDX18	-5.79332	0.00792	0.58	48	C12	31173	-0.2259	27692	-0.2739	18615	-0.9453	21827	-0.7073
758	4025	NM_012343	23530	NNT	-3.11932	0.04644	0.57	42	H05	28494	-0.4316	27458	-0.3605	22715	-0.7405	15355	-1.2008
767	17898	NM_144581	112849	C14ORF149	-6.82264	0.00479	0.57	187	D06	33642	-0.2185	32427	-0.1731	24419	-0.6704	20202	-0.8654
768	4401	NM_012461	26277	TINF2	-3.47708	0.0348	0.57	46	G09	14958	-1.2881	15814	-1.0805	12438	-1.5768	9318	-1.9352
781	18892	NM_174898	129530	LOC129530	-3.08322	0.04786	0.57	197	G04	30690	-0.4159	28994	-0.3105	23384	-0.7048	16345	-1.1592
785	4591	NM_001990	2140	EYA3	-7.68257	0.0033	0.57	48	G07	33058	-0.1412	28191	-0.2482	22152	-0.6943	20054	-0.8295
793	3259	NM_002584	5081	PAX7	-6.62393	0.00525	0.57	34	H07	38594	-0.0125	34622	-0.007	27574	-0.4728	22870	-0.6771
794	514	NM_004635	7867	MAPKAPK3	-10.2288	0.00133	0.57	6	C10	32276	-0.0977	33272	0.00077	24605	-0.581	22811	-0.6463
796	22710	XM_117266	0	LOC200726	-3.26103	0.04132	0.56	237	E06	40978	-0.0633	36173	-0.0417	29969	-0.3989	20669	-0.8351
799	5327	NM_021223	58498	MYL7	-9.56319	0.00165	0.56	56	D11	34209	-0.1873	29116	-0.2506	22435	-0.726	19454	-0.8387
801	3748	NM_001360	1717	DHCR7	-3.70697	0.0292	0.56	40	A04	32047	-0.2173	33224	-0.0256	20268	-0.8486	24331	-0.5193
808	12291	NM_014972	22980	KIAA1049	-3.11422	0.04663	0.56	129	A03	34177	-0.1289	33183	-0.0886	28615	-0.4413	19346	-0.892
811	1254	NM_006564	10663	CXCR6	-3.78189	0.02763	0.56	14	A06	27954	-0.2965	30219	-0.1064	19200	-0.9175	23643	-0.6004
812	16080	NM_024104	79086	MGC2747	-14.3581	0.00045	0.56	168	D12	34915	-0.2034	31909	-0.1947	23378	-0.726	20032	-0.787
814	4450	NM_014555	29850	TRPM5	-6.01699	0.00706	0.56	47	C10	35744	0.03696	33137	-0.0537	23119	-0.667	26125	-0.4624
817	1390	NM_024980	80045	GPR157	-5.42135	0.00969	0.55	15	D10	31143	-0.1991	30502	-0.0847	24374	-0.5854	20418	-0.8082
819	19699	NM_153044	150291	FLJ35155	-3.65295	0.03041	0.55	205	B07	40310	-0.0202	34724	-0.0437	29338	-0.3963	20994	-0.7769
824	19386	XM_378712	146713	LOC146713	-7.1078	0.00421	0.55	202	H06	36794	-0.1655	33423	-0.1147	25066	-0.6053	20901	-0.7818
825	15383	NM_020817	57577	KIAA1407	-10.3294	0.00129	0.55	161	B11	39945	-0.0389	36162	-0.041	26536	-0.5366	22193	-0.6495
827	1942	NM_014391	27063	ANKRD1	-4.50623	0.01677	0.55	21	B10	27778	-0.3998	29231	-0.239	17954	-1.0011	21180	-0.7426
832	4113	NM_000309	5498	PPOX	-3.82096	0.02685	0.55	43	G09	26204	-0.4644	28038	-0.3364	21977	-0.7824	16803	-1.1202
839	17759	NM_033199	90226	UCN2	-14.3224	0.00045	0.55	185	H11	37515	-0.0918	35054	-0.0735	25551	-0.6034	22985	-0.6601
841	4476	NM_018955	7314	UBB	-4.47703	0.01709	0.55	47	E12	1844	-4.2398	2051	-4.0677	1294	-4.8262	1509	-4.5762
842	1672	NM_000958	5734	PTGER4	-4.38541	0.01814	0.55	18	D04	32204	-0.1043	33239	-0.0186	27475	-0.4598	21304	-0.758
849	3694	NM_000098	1376	CPT2	-3.15309	0.04515	0.55	39	D10	34863	-0.0389	30542	-0.1531	19756	-0.8518	26264	-0.4307
851	1171	NM_000025	155	ADRB3	-3.42782	0.03617	0.54	13	B07	27937	-0.2798	31895	-0.087	18690	-0.9032	24103	-0.553
854	12102	NM_007056	11129	SFRS16	-5.73054	0.00819	0.54	127	A06	37300	-0.179	35914	-0.0715	23468	-0.7702	25599	-0.5668
862	19902	NM_144967	158763	FLJ30058	-3.45277	0.03547	0.54	208	C06	36017	-0.1578	30152	-0.2263	26198	-0.5393	19015	-0.9276
864	2619	NM_005066	6421	SFPQ	-3.61057	0.0314	0.54	28	C03	16402	-1.0324	21146	-0.6832	14202	-1.3291	12946	-1.4679
865	20537	XM_167709	221061	C10ORF38	-3.09558	0.04737	0.54	214	H05	34699	-0.2382	27155	-0.1371	26603	-0.5138	17960	-0.9429
866	23884	XM_371736	0	LOC389286	-4.33619	0.01874	0.54	249	G04	37954	-0.1295	33554	-0.1597	27933	-0.5308	20714	-0.8391
869	3377	NM_005643	6882	TAF11	-3.74412	0.02841	0.54	36	B05	39045	0.05472	36803	0.10789	30345	-0.2798	23207	-0.637
870	1954	NM_014278	22824	APG-1	-5.88225	0.00756	0.54	21	C10	32309	-0.1818	29621	-0.2199	23220	-0.6301	19690	-0.8478
872	1313	NM_031866	8325	FZD8	-3.89121	0.02551	0.54	14	F05	33646	-0.0291	33526	0.04345	22346	-0.6986	27906	-0.3612
875	19966	NM_130901	161725	C15ORF16	-10.6889	0.00115	0.54	208	H10	34920	-0.2024	32621	-0.1127	23945	-0.6691	21995	-0.7176

878	1977	NM_000633	596	BCL2	-6.46525	0.00566	0.53	21	E09	29095	-0.3329	27183	-0.3438	21008	-0.7745	18077	-0.9712
882	550	NM_001932	4356	MPP3	-7.37904	0.00375	0.53	6	F10	32804	-0.0743	33673	0.01805	26185	-0.4912	23045	-0.6315
883	13132	NM_014407	27094	KCNMB3	-3.06632	0.04855	0.53	137	G04	30973	-0.2982	33547	-0.1371	26935	-0.5467	18985	-0.9548
895	3899	NM_017902	55662	HIF1AN	-3.23282	0.04228	0.53	41	E11	34795	-0.1175	32188	-0.1122	27666	-0.4375	19349	-0.8491
896	24527	XM_378219	0	LOC399737	-4.21095	0.02039	0.53	256	D11	36494	-0.1951	32239	-0.2014	26031	-0.5706	19896	-0.8826
898	2128	NM_001941	1825	DSC3	-5.81439	0.00784	0.53	23	B04	32709	-0.1257	30465	-0.1466	25317	-0.5551	21106	-0.7734
899	16099	NM_024123	79136	LY6G6E	-3.07118	0.04835	0.53	168	F07	36868	-0.1249	34302	-0.0904	28912	-0.4195	19151	-0.8519
901	6128	NM_001138	181	AGRP	-4.79501	0.01398	0.53	64	G08	34217	-0.2373	29663	-0.2925	24407	-0.6599	18532	-0.9253
902	1709	NM_002980	6344	SCTR	-3.09207	0.04751	0.53	18	G05	28041	-0.304	32123	-0.0679	26114	-0.5331	19419	-0.8916
905	2428	NM_020418	57060	PCBP4	-5.02666	0.01215	0.53	26	C04	36300	0.13275	34027	0.017	29371	-0.3367	24127	-0.5657
910	5182	NM_004264	9412	SURB7	-8.25911	0.00263	0.52	54	H10	32743	-0.1923	28614	-0.2658	23498	-0.6926	19586	-0.8151
913	15846	NM_032461	64649	SPANXB1	-3.1712	0.04448	0.52	166	A06	32423	-0.3229	34420	-0.0937	26285	-0.5584	18811	-0.9056
933	15262	NM_020657	57343	ZNF304	-3.18325	0.04404	0.52	159	H10	26940	-0.5497	25753	-0.5212	21272	-0.8491	14751	-1.258
954	859	NM_015690	27148	STK36	-3.25937	0.04138	0.51	9	H07	24303	-0.6261	25611	-0.3563	20612	-0.859	16203	-1.1476
967	2873	NM_023005	9031	BAZ1B	-5.5026	0.00926	0.51	30	H05	24180	-0.5479	26299	-0.3367	18425	-0.988	18914	-0.9141
969	7571	NM_006409	10552	ARPC1A	-3.43642	0.03592	0.51	79	G11	25148	-0.6314	28450	-0.3217	20380	-0.8828	17794	-1.0874
971	5188	NM_000308	5476	PPGB	-5.99708	0.00713	0.51	55	A04	39906	0.07377	35519	0.01273	28553	-0.3681	23713	-0.5613
972	899	NM_016388	50852	TRIM	-3.05973	0.04882	0.51	10	C11	28695	-0.3219	33399	-0.0391	25957	-0.5341	20126	-0.842
976	7049	NM_005008	4809	NHP2L1	-4.20237	0.02051	0.51	74	D05	7248	-2.4307	8298	-2.1375	5687	-2.7619	4883	-2.8176
981	18500	NM_153336	118672	C10ORF89	-4.12548	0.02162	0.5	193	F08	32190	-0.3168	32418	-0.1653	20596	-0.8766	23174	-0.6138
982	2165	NM_001457	2317	FLNB	-3.13642	0.04578	0.5	23	E05	33601	-0.0869	34616	0.03768	29472	-0.3358	21901	-0.72
983	15575	NM_021242	58526	MIG12	-5.38278	0.0099	0.5	163	B11	35686	-0.1928	32023	-0.2187	25508	-0.5965	20031	-0.8216
991	18561	NM_175054	121504	HIST4H4	-3.71849	0.02895	0.5	194	C09	34715	-0.2393	30416	-0.2191	26506	-0.5619	19463	-0.8973
998	552	NM_006039	9902	MRC2	-6.69003	0.00509	0.5	6	F12	26267	-0.3949	28507	-0.2222	20844	-0.8204	20576	-0.795
1011	2519	NM_004705	5612	PRKRIR	-4.23884	0.02001	0.5	27	B11	25226	-0.3974	29181	-0.1436	22161	-0.6969	19164	-0.8372
1013	3414	NM_000458	6928	TCF2	-3.81022	0.02706	0.5	36	E06	33017	-0.1872	29886	-0.1925	25622	-0.5239	20043	-0.8485
1018	196	NM_006314	10256	CNKSR1	-10.0308	0.00142	0.49	3	A04	16281	-1.1333	15955	-1.0948	13411	-1.5627	11739	-1.6542
1023	13176	NM_014447	27236	ARFIP1	-3.24442	0.04189	0.49	138	B12	35847	-0.0844	35841	-0.0479	30266	-0.369	21750	-0.7484
1024	7320	NM_001316	1434	CSE1L	-3.39844	0.03701	0.49	77	B12	23189	-0.791	25727	-0.4956	18393	-1.0302	16229	-1.2415
1025	510	NM_012324	23542	MAPK8IP2	-4.37284	0.01829	0.49	6	C06	25763	-0.4229	27619	-0.2679	22307	-0.7225	18440	-0.9531
1028	1583	NM_001708	611	OPN1SW	-4.14987	0.02126	0.49	17	D11	13282	-1.3541	16024	-1.0729	11649	-1.6631	10839	-1.7473
1029	496	NM_002745	5594	MAPK1	-4.30413	0.01915	0.49	6	B04	31878	-0.1156	31425	-0.0816	22190	-0.7301	26134	-0.4501
1031	12167	NM_007230	11253	MAN1B1	-4.37073	0.01832	0.49	127	F11	39674	-0.09	35625	-0.0832	29523	-0.4391	23080	-0.7162
1032	435	NM_144624	127933	KIS	-3.22854	0.04243	0.49	5	E03	34702	-0.0714	33543	0.00774	30040	-0.335	22307	-0.7072
1042	18364	NM_172347	93107	KCNG4	-3.70623	0.02922	0.49	192	C04	34328	-0.1894	36058	-0.0792	28333	-0.4669	21303	-0.7754
1046	3581	NM_138430	113622	ADPRHL1	-3.26584	0.04116	0.49	38	C05	34550	-0.1133	33927	0.02172	22186	-0.706	27630	-0.3578
1047	13211	NM_014487	27309	ZNF330	-4.63171	0.01547	0.49	138	E11	34631	-0.1342	32994	-0.1673	27463	-0.5092	21510	-0.7644
1053	17946	NM_052880	113791	MGC17330	-3.70252	0.0293	0.48	187	H06	28335	-0.4662	31237	-0.227	23597	-0.7198	19175	-0.9407
1057	24463	XM_373471	0	LOC387706	-3.61323	0.03134	0.48	255	G07	41269	-0.0178	33906	-0.1157	29287	-0.3901	22522	-0.709

1058	3802	NM_016594	51303	FKBP11	-5.69263	0.00836	0.48	40	E10	37286	0.00113	30894	-0.1305	23678	-0.6242	25175	-0.4701
1066	7080	NM_003380	7431	VIM	-5.51175	0.00922	0.48	74	F12	32707	-0.2567	33993	-0.1031	23223	-0.7321	22877	-0.5896
1069	615	NM_018216	55229	PANK4	-6.76301	0.00492	0.48	7	D03	29756	-0.269	29275	-0.1585	24217	-0.6331	21995	-0.7549
1072	10183	NM_006234	5439	POLR2J	-3.25355	0.04158	0.48	107	A07	31881	-0.371	26639	-0.4417	23324	-0.7043	17914	-1.0669
1076	2662	NM_003174	6840	SVIL	-3.69992	0.02936	0.48	28	F10	25834	-0.377	31175	-0.1232	20102	-0.8279	23149	-0.6294
1079	17471	NM_032762	84848	MGC16121	-15.2321	0.00037	0.48	182	H11	36899	-0.0893	34344	-0.0801	27082	-0.5704	25353	-0.554
1080	17976	NM_052891	114771	PGLYRP3	-3.86769	0.02595	0.48	188	B12	36977	-0.0883	34151	-0.0798	29262	-0.408	22097	-0.7143
1096	6516	NM_002007	2249	FGF4	-3.36586	0.03798	0.47	68	G12	34990	-0.2342	33998	-0.107	27363	-0.4791	20245	-0.8062
1100	24141	XM_380098	0	LOC402475	-3.62967	0.03095	0.47	252	D09	38586	-0.1223	31334	-0.2444	27976	-0.5047	21189	-0.8041
1108	3699	NM_001888	1428	CRYM	-3.757	0.02814	0.47	39	E03	31505	-0.185	30619	-0.1495	20611	-0.7907	25342	-0.4822
1110	1223	NM_006641	10803	CCR9	-5.44078	0.00958	0.47	13	F11	35856	0.08019	34588	0.02995	24486	-0.5135	28460	-0.3133
1115	3573	NM_000022	100	ADA	-3.64874	0.03051	0.47	38	B09	33532	-0.1565	32299	-0.0492	27056	-0.4197	21502	-0.7195
1120	16036	NM_024051	79017	C7ORF24	-3.44404	0.03571	0.47	168	A04	28757	-0.4833	29418	-0.312	23509	-0.718	17174	-1.0091
1123	3822	NM_002569	5045	FURIN	-9.8483	0.0015	0.46	40	G06	39536	0.08567	34559	0.03122	26832	-0.4438	26999	-0.3692
1126	2071	NM_001280	1153	CIRBP	-14.8568	0.0004	0.46	22	E07	37479	0.03516	35896	0.04421	26657	-0.4322	26810	-0.4171
1129	19553	NM_182517	149466	MGC52423	-3.73151	0.02867	0.46	204	F05	39536	-0.0527	35335	-0.0229	30046	-0.3477	23294	-0.655
1130	24220	XM_379935	0	LOC402601	-13.6855	0.00052	0.46	253	C04	40551	-0.0329	35848	-0.0468	27427	-0.4858	25857	-0.521
1132	7884	NM_199336	151313	DKFZP434N062	-5.85489	0.00767	0.46	83	A12	36801	-0.1493	34696	-0.0649	24243	-0.6539	26864	-0.4868
1136	19120	NM_144651	137902	FLJ25471	-13.0045	0.00061	0.46	200	B04	41364	0.04005	36253	0.04496	27998	-0.4439	28429	-0.397
1138	4356	NM_001230	843	CASP10	-3.91287	0.02512	0.46	46	C12	26284	-0.4748	27772	-0.268	19375	-0.9374	21481	-0.7302
1139	5334	NM_000257	4625	MYH7	-3.87478	0.02582	0.46	56	E06	34307	-0.1832	32782	-0.0795	27069	-0.4551	20947	-0.732
1141	3738	NM_016286	51181	DCXR	-3.70859	0.02917	0.46	39	H06	31396	-0.19	31801	-0.0949	21179	-0.7514	25790	-0.457
1147	5242	NM_007066	11142	PKIG	-6.44555	0.00571	0.46	55	E10	31619	-0.262	32254	-0.1264	22660	-0.7016	22975	-0.6069
1149	13235	NM_031890	27439	CECR6	-3.34638	0.03858	0.46	138	G11	35730	-0.0892	33979	-0.1248	29705	-0.3959	21916	-0.7375
1153	24274	XM_379541	0	LOC401441	-6.46398	0.00566	0.46	253	G10	39894	-0.0565	34239	-0.113	27796	-0.4665	24128	-0.6208
1158	19257	NM_152427	142913	CFLP1	-4.18036	0.02082	0.46	201	E09	35620	-0.1811	33656	-0.1257	27402	-0.4793	21222	-0.7432
1159	3340	NM_003077	6603	SMARCD2	-4.05867	0.02265	0.46	35	G04	37209	-0.0017	32586	-0.0941	29413	-0.3744	23244	-0.6369
1160	4948	NM_000673	131	ADH7	-3.12194	0.04634	0.46	52	E04	25973	-0.5117	27104	-0.3643	22708	-0.7272	16620	-1.0637
1166	19396	XM_375404	146850	C17ORF38	-3.60649	0.0315	0.46	203	A04	34831	-0.2013	31216	-0.2027	27170	-0.5003	20171	-0.8144
1167	3574	NM_014237	8749	ADAM18	-4.55626	0.01624	0.46	38	B10	32320	-0.2096	28716	-0.2189	24760	-0.5476	20458	-0.7914
1178	2616	NM_006802	10946	SF3A3	-3.2817	0.04064	0.45	28	B12	13789	-1.2828	15353	-1.145	10062	-1.8263	12581	-1.5092
1185	2483	NM_004426	1911	PHC1	-3.19156	0.04374	0.45	26	G11	33626	0.02235	32799	-0.036	30448	-0.2847	22989	-0.6354
1188	572	NM_002498	4752	NEK3	-3.2631	0.04125	0.45	6	H08	23223	-0.5726	27987	-0.2488	21123	-0.8012	18797	-0.9255
1189	13759	NM_016257	51440	HPCAL4	-6.7014	0.00506	0.45	144	C07	34930	-0.1164	34203	-0.075	27845	-0.4739	23738	-0.6227
1200	1966	NM_021813	60468	BACH2	-6.54661	0.00544	0.45	21	D10	33806	-0.1164	30754	-0.1658	22637	-0.6667	24774	-0.5165
1204	19734	NM_178495	150771	MARLIN1	-3.41898	0.03642	0.45	205	E06	33332	-0.2945	31937	-0.1644	21721	-0.83	24935	-0.5287
1208	22376	NM_004698	9129	PRPF3	-4.17726	0.02087	0.45	234	A08	31200	-0.4563	32083	-0.2098	24079	-0.7344	20963	-0.8296
1209	2843	NM_004219	9232	PTTG1	-3.88229	0.02568	0.45	30	E11	28467	-0.3124	32112	-0.0485	22749	-0.6839	23938	-0.5743
1213	19271	NM_175733	143425	LOC143425	-6.95668	0.00451	0.45	201	F11	38475	-0.0699	33754	-0.1215	27467	-0.4759	23243	-0.6119

1214	1419	NM_001508	2863	GPR39	-3.61678	0.03125	0.45	15	G03	27735	-0.3663	30999	-0.0614	23459	-0.6406	22263	-0.6834
1215	18879	NM_152906	128989	DKFZP761P1121	-3.36343	0.03806	0.45	197	F03	36147	-0.1798	27423	-0.3909	25058	-0.6051	20084	-0.862
1216	519	NM_004954	2011	MARK2	-4.53994	0.01641	0.45	6	D03	32760	-0.0762	28375	-0.2289	22759	-0.6935	25112	-0.5076
1217	5355	NM_003357	7356	SCGB1A1	-4.34434	0.01864	0.45	56	G03	38887	-0.0024	32685	-0.0838	28690	-0.3712	22796	-0.61
1218	14096	NM_018364	54665	FLJ11220	-3.50047	0.03417	0.45	147	G08	38106	0.07616	35451	-0.0445	32642	-0.2842	23658	-0.5784
1226	294	NM_139021	225689	ERK8	-3.94159	0.02461	0.45	4	A06	36821	0.02216	34286	0.04043	31501	-0.275	25554	-0.5534
1227	23783	XM_374095	0	LOC389242	-6.30578	0.00611	0.44	248	F11	41071	-0.0437	35368	-0.0428	30717	-0.4066	24804	-0.5698
1246	19572	NM_053041	149951	COMMD7	-3.60201	0.03161	0.44	204	G12	36609	-0.1637	33062	-0.1188	28348	-0.4316	22084	-0.732
1248	23992	XM_374163	0	LOC389372	-8.01359	0.00289	0.44	250	H04	37000	-0.1829	32370	-0.207	23879	-0.692	24915	-0.5775
1250	15188	NM_020404	57124	CD164L1	-4.97916	0.0125	0.44	159	B08	33191	-0.2486	31816	-0.2162	25877	-0.5664	20605	-0.7758
1251	12191	NM_007272	11330	CTRC	-3.09771	0.04728	0.44	127	H11	32692	-0.3693	31401	-0.2653	26656	-0.5865	19965	-0.9254
1257	3696	NM_021151	54677	CROT	-3.12845	0.04608	0.44	39	D12	22485	-0.6716	21578	-0.6544	18766	-0.9259	14622	-1.2756
1259	2062	NM_005507	1072	CFL1	-4.18864	0.02071	0.44	22	D10	28933	-0.3382	32703	-0.0902	23407	-0.6197	22281	-0.684
1264	18492	NM_145806	118472	ZNF511	-3.56076	0.03262	0.44	193	E12	36137	-0.1499	33183	-0.1316	28155	-0.4256	21385	-0.7297
1265	502	NM_002746	5595	MAPK3	-3.60784	0.03147	0.44	6	B10	23868	-0.5331	28006	-0.2478	21429	-0.7804	19497	-0.8727
1276	2685	NM_022037	7072	TIA1	-6.99886	0.00442	0.43	28	H09	28138	-0.2538	29848	-0.1859	21772	-0.7127	23747	-0.5927
1278	8026	NM_004450	2079	ERH	-3.73843	0.02853	0.43	84	E10	36818	-0.138	31658	-0.1928	27964	-0.4576	22745	-0.7385
1281	20695	NM_153248	253150	MGC14276	-3.57668	0.03222	0.43	216	E07	36511	-0.1754	32545	0.01099	28910	-0.3968	22654	-0.6313
1284	17339	NM_032112	84545	MRPL43	-3.10559	0.04697	0.43	181	E11	36923	-0.091	35427	-0.0318	30806	-0.3216	23201	-0.664
1285	10668	NM_006943	6666	SOX12	-3.14441	0.04548	0.43	112	A12	34313	-0.2283	29905	-0.2425	26946	-0.4954	20683	-0.8379
1286	536	NM_152619	166614	MGC45428	-4.23427	0.02007	0.43	6	E08	25695	-0.4267	26174	-0.3454	22668	-0.6993	18679	-0.9346
1287	570	NM_024800	79858	NEK11	-6.61803	0.00526	0.43	6	H06	21828	-0.662	23152	-0.5224	17819	-1.0466	17860	-0.9993
1292	2549	NM_007182	11186	RASSF1	-3.60986	0.03142	0.43	27	E05	34359	0.04839	33439	0.05287	30596	-0.2316	23769	-0.5265
1301	20170	NM_153183	170685	NUDT10	-5.76744	0.00803	0.43	211	A10	38801	-0.0722	36016	0.0231	28930	-0.38	24084	-0.5249
1309	15	NM_032630	51550	CINP	-3.37553	0.03769	0.43	1	B03	40064	0.12728	36593	0.02807	33982	-0.1998	25557	-0.4982
1310	3111	NM_004516	3609	ILF3	-11.4873	0.00092	0.43	33	D03	24780	-0.538	23225	-0.544	19425	-0.9405	18175	-0.9945
1311	3264	NM_002636	5252	PHF1	-7.37042	0.00376	0.43	34	H12	23526	-0.7266	22153	-0.6512	18293	-1.0649	16297	-1.1659
1322	4455	NM_139073	130560	SPATA3	-5.57195	0.00892	0.42	47	D03	23558	-0.5645	26307	-0.3866	19577	-0.907	19404	-0.8915
1325	391	NM_054111	117283	IHPK3	-4.02265	0.02323	0.42	5	A07	30324	-0.2659	28389	-0.2329	25978	-0.5446	20910	-0.8005
1326	1338	NM_000172	2779	GNAT1	-11.1549	0.00101	0.42	14	H06	33363	-0.0413	31158	-0.0622	26588	-0.4478	25317	-0.5017
1328	1762	NM_003382	7434	VIPR2	-4.91311	0.013	0.42	19	C10	33628	-0.0218	31449	-0.0742	28595	-0.3708	24437	-0.5701
1330	7416	NM_000349	6770	STAR	-6.0684	0.00687	0.42	78	B12	33560	-0.2208	32447	-0.1627	25907	-0.5393	23213	-0.6887
1331	23604	XM_379145	0	LOC401020	-7.05962	0.0043	0.42	246	G12	39055	-0.1182	33960	-0.1278	28089	-0.4791	24408	-0.6105
1332	1281	NM_004767	9283	GPR37L1	-3.21318	0.04297	0.42	14	C09	33600	-0.0311	35494	0.12574	25333	-0.5176	30550	-0.2306
1333	19414	XM_378680	147080	LOC147080	-4.08168	0.02229	0.42	203	B10	39104	-0.0344	35838	-0.0035	30898	-0.3148	23965	-0.5657
1336	13380	NM_013349	29937	SPUF	-5.18851	0.01105	0.42	140	C12	34855	-0.0824	34963	-0.0779	29154	-0.4049	24304	-0.5977
1339	2343	NM_018848	8195	MKKS	-3.16631	0.04466	0.42	25	D03	24608	-0.4586	29645	-0.1464	23299	-0.6673	20402	-0.7797
1340	5506	NM_013367	29945	ANAPC4	-4.52872	0.01652	0.42	58	C10	36081	-0.1182	36080	-0.0082	29377	-0.3857	24521	-0.5819
1341	7348	NM_004975	3745	KCNB1	-3.10449	0.04702	0.42	77	E04	38970	-0.0421	34362	-0.0781	30249	-0.3125	24471	-0.649

1344	3642	NM_001497	2683	B4GALT1	-6.45095	0.0057	0.42	38	H06	28367	-0.3978	27666	-0.2726	20864	-0.7946	21549	-0.7164
1347	23328	XM_372749	390975	LOC390975	-4.62237	0.01557	0.42	243	H12	38589	-0.1105	33056	-0.1529	28477	-0.4438	23372	-0.6588
1352	2361	NM_002441	4439	MSH5	-6.85853	0.00471	0.42	25	E09	28459	-0.2488	30200	-0.1196	24016	-0.6236	23392	-0.5824
1353	3682	NM_001303	1352	COX10	-3.43919	0.03584	0.42	39	C10	25188	-0.5079	25085	-0.4371	17364	-1.038	21133	-0.7443
1354	24163	XM_379986	0	LOC402633	-3.18488	0.04398	0.42	252	F07	41324	-0.0234	36616	-0.0196	32777	-0.2762	24346	-0.6038
1355	4467	NM_016437	27175	TUBG2	-3.32891	0.03912	0.42	47	E03	34447	-0.0164	32512	-0.0811	29529	-0.314	23431	-0.6194
1369	20491	NM_152716	219988	FLJ36874	-3.54664	0.03297	0.42	214	D07	37422	-0.1292	33364	0.15993	28991	-0.3898	25983	-0.4101
1373	15005	NM_019606	56257	FLJ20257	-3.35578	0.03829	0.41	157	C05	33356	-0.2399	32100	-0.1986	27650	-0.4819	20304	-0.7862
1374	2535	NM_021168	57799	RAB40C	-5.87438	0.00759	0.41	27	D03	33939	0.03065	34989	0.11824	29768	-0.2712	25791	-0.4087
1382	24215	XM_374526	0	LOC392793	-3.83824	0.02651	0.41	253	B11	37311	-0.1531	30233	-0.2926	26721	-0.5234	22090	-0.7481
1385	22811	XM_293570	0	LOC344741	-8.19434	0.00269	0.41	238	E11	39552	-0.1031	34931	-0.0882	29668	-0.4572	25183	-0.5587
1389	7487	NM_012111	10598	AHSA1	-5.84693	0.0077	0.41	78	H11	36674	-0.0927	34443	-0.0766	28226	-0.4156	25072	-0.5776
1402	19291	NM_175058	144100	LOC144100	-4.63278	0.01546	0.41	201	H07	35325	-0.1931	34535	-0.0885	27811	-0.4579	22744	-0.6432
1409	1267	NM_004720	9170	EDG4	-4.63363	0.01546	0.41	14	B07	33419	-0.0389	34183	0.07145	25957	-0.4825	29085	-0.3015
1410	403	NM_001569	3654	IRAK1	-4.49091	0.01693	0.41	5	B07	31658	-0.2038	30797	-0.1155	27405	-0.4674	22915	-0.6684
1414	18802	NM_182752	127262	LOC127262	-11.9681	0.0008	0.41	196	G10	37223	-0.1329	33417	-0.0952	26771	-0.5265	25448	-0.5169
1419	12430	NM_015141	23171	KIAA0089	-3.46108	0.03524	0.41	130	D10	39135	0.04451	35829	-0.0178	32893	-0.2512	24707	-0.5353
1420	24175	XM_379848	0	LOC402521	-3.15374	0.04513	0.41	252	G07	32974	-0.3491	32896	-0.1742	27425	-0.5334	21216	-0.8023
1428	4433	NM_033285	94241	TP53INP1	-7.23479	0.00399	0.4	47	B05	32253	-0.1113	32998	-0.0597	27136	-0.4359	24680	-0.5445
1429	2615	NM_005877	10291	SF3A1	-6.82142	0.00479	0.4	28	B11	12822	-1.3877	14187	-1.259	10692	-1.7387	10890	-1.7174
1431	2528	NM_002859	5829	PXN	-9.78421	0.00153	0.4	27	C08	34542	0.05605	32921	0.03034	28621	-0.3279	26044	-0.3947
1434	2061	NM_004365	1070	CETN3	-6.19827	0.00644	0.4	22	D09	35294	-0.0515	33208	-0.0681	27436	-0.3906	24663	-0.5375
1436	4601	NM_015002	23014	FBXO21	-4.76813	0.01421	0.4	48	H05	34919	-0.0622	32327	-0.0507	27943	-0.3593	24146	-0.5617
1440	12897	XM_032397	25974	DKFZP564I122	-3.21853	0.04278	0.4	135	C09	33209	-0.1454	33749	-0.0659	30415	-0.358	22688	-0.6587
1441	2638	NM_005496	10051	SMC4L1	-3.20319	0.04332	0.4	28	D10	30277	-0.1481	30339	-0.1624	27014	-0.4015	21840	-0.7134
1444	2419	NM_019619	56288	PARD3	-4.55636	0.01623	0.4	26	B07	29931	-0.1456	29423	-0.1927	26823	-0.4676	22376	-0.6744
1445	2291	NM_000425	3897	L1CAM	-7.16568	0.00411	0.4	24	G11	34157	-0.0749	32556	0.00815	29288	-0.3914	26390	-0.4789
1448	7235	NM_003060	6584	SLC22A5	-3.11029	0.04679	0.4	76	C11	36012	-0.1356	31251	-0.215	28029	-0.4207	22836	-0.732
1455	5176	NM_080744	136853	SRCRB4D	-4.1457	0.02132	0.4	54	H04	35039	-0.0945	33051	-0.0579	29579	-0.3606	22852	-0.5926
1456	5347	NM_006654	10818	FRS2	-4.74933	0.01438	0.4	56	F07	31778	-0.2936	32494	-0.0922	24581	-0.5942	23079	-0.5922
1457	3126	NM_002229	3726	JUNB	-3.13984	0.04565	0.4	33	E06	39282	0.12674	33621	-0.0103	32479	-0.1989	25873	-0.485
1466	7188	XM_029962	57582	KCNT1	-5.34913	0.01009	0.4	75	G12	31187	-0.3412	29270	-0.3006	24592	-0.6349	20079	-0.8046
1471	24272	XM_378044	0	LOC402354	-3.14131	0.04559	0.4	253	G08	34581	-0.2627	29748	-0.3159	26562	-0.532	20686	-0.8429
1475	2523	NM_004697	9128	PRPF4	-4.98585	0.01245	0.4	27	C03	26307	-0.3369	29079	-0.1487	23173	-0.6325	21852	-0.6478
1482	24372	XM_378064	0	LOC402367	-3.82688	0.02673	0.4	254	G12	39861	-0.0732	29623	-0.3267	26294	-0.589	24035	-0.6043
1483	1423	NM_005305	2866	GPR42	-4.84949	0.01352	0.4	15	G07	31316	-0.1911	31491	-0.0387	26754	-0.451	24055	-0.5718
1491	2817	NM_000541	6295	SAG	-4.44844	0.01741	0.39	30	C09	29205	-0.2755	31631	-0.0703	24170	-0.5965	24549	-0.5379
1493	2399	NM_002516	4858	NOVA2	-4.6249	0.01554	0.39	25	H11	34795	0.04118	32523	-0.0127	30443	-0.2815	25143	-0.4783

B. Synthetic rescue genes

19877	16506	NM_024922	79984	FLJ21736	3.1258	0.04619	-0.1	172	H06	38138	-0.0543	34928	-0.0683	39809	0.03726	37813	0.03391
19888	3063	NM_000522	3209	HOXA13	3.16973	0.04453	-0.1	32	H03	33948	-0.0267	31503	-0.0425	38469	0.06614	36877	0.06209
19912	15175	NM_020367	57097	PARP11	3.13981	0.04565	-0.1	159	A07	37343	-0.0786	34626	-0.0941	38395	0.00284	36133	0.0345
19921	16320	NM_024701	79754	ASB13	3.25259	0.04161	-0.11	170	H12	35076	-0.1592	31085	-0.1916	36663	-0.0712	34599	-0.0641
19943	82	NM_020639	54101	ANKRD3	3.10322	0.04707	-0.11	1	G10	31406	-0.224	30949	-0.2136	36875	-0.0819	32967	-0.1309
19964	14988	NM_018897	56171	DNAH7	3.54834	0.03293	-0.12	157	A12	35639	-0.1444	33579	-0.1336	37642	-0.0369	35029	0.00059
19966	473	XM_042066	4214	MAP3K1	3.44267	0.03575	-0.12	5	H05	28835	-0.3386	26772	-0.3175	33341	-0.1846	31125	-0.2266
20001	1164	NM_000681	150	ADRA2A	3.58347	0.03206	-0.14	13	A12	31591	-0.1025	31826	-0.0901	36997	0.08195	35734	0.01507
20006	3659	NM_130767	134526	CACH-1	3.91047	0.02516	-0.15	39	A11	29888	-0.261	29408	-0.2077	33337	-0.0969	33569	-0.0766
20009	9312	NM_000705	496	ATP4B	3.15498	0.04508	-0.15	97	H12	35298	-0.1992	31429	-0.2424	38550	-0.031	33580	-0.1127
20010	15192	NM_020408	57128	C6ORF149	4.10137	0.02199	-0.15	159	B12	33503	-0.2352	32526	-0.1843	36647	-0.0644	33951	-0.0554
20011	3138	NM_006562	10660	LBX1	3.62652	0.03102	-0.15	33	F06	29831	-0.2703	28190	-0.2645	35224	-0.0818	32564	-0.1532
20016	16222	NM_024589	79641	FLJ22386	3.41518	0.03653	-0.15	169	H10	22293	-0.8347	14835	-0.9169	23221	-0.7281	22161	-0.7205
20026	15264	NM_020155	56834	C11ORF4	3.38126	0.03752	-0.15	159	H12	36410	-0.1151	32344	-0.1924	38854	0.01999	34807	-0.0194
20031	15180	NM_020378	57106	KLP1	3.17601	0.0443	-0.16	159	A12	33085	-0.2533	33134	-0.1576	37383	-0.0357	33792	-0.0621
20035	4236	NM_003358	7357	UGCG	3.59249	0.03184	-0.16	45	A12	31622	-0.2179	30080	-0.156	36131	-0.0549	35623	-0.0001
20045	15948	NM_032478	64978	MRPL38	4.04009	0.02295	-0.17	167	A12	33664	-0.2731	32408	-0.2003	36854	-0.0747	33342	-0.058
20052	9408	NM_001803	1043	CDW52	3.32333	0.0393	-0.18	98	H12	29461	-0.4781	24569	-0.5662	31351	-0.3029	28093	-0.3786
20061	4679	NM_002426	4321	MMP12	3.7641	0.02799	-0.19	49	F11	26820	-0.418	26072	-0.444	33038	-0.1851	28520	-0.2886
20064	90	NM_031916	83853	ASP	4.47302	0.01713	-0.2	1	H06	33368	-0.1366	31100	-0.2066	39170	0.00517	37380	0.05032
20065	2016	NM_001773	947	CD34	4.17455	0.02091	-0.2	21	H12	33188	-0.143	29496	-0.226	36946	0.03999	35261	-0.0072
20068	17561	NM_032648	84734	MGC10820	4.88665	0.01321	-0.21	183	H05	30997	-0.3365	29711	-0.2836	37512	-0.0755	32974	-0.1297
20070	14506	NM_018188	55210	ATAD3A	3.21911	0.04276	-0.21	152	A10	28627	-0.384	30097	-0.2818	37383	-0.0689	31223	-0.1762
20072	1944	NM_007193	11199	ANXA10	5.23897	0.01074	-0.21	21	B12	30574	-0.2614	27643	-0.3196	34533	-0.0574	33164	-0.0957
20073	91	NM_138293	472	ATM	5.7533	0.00809	-0.22	1	H07	29157	-0.3312	29550	-0.2803	36372	-0.1018	34166	-0.0794
20077	10571	NM_006278	6484	SIAT4C	3.70046	0.02935	-0.23	111	A11	29763	-0.4819	25653	-0.49	23665	-0.193	30004	-0.328
20081	13920	NM_138284	53342	IL17D	7.11055	0.00421	-0.24	145	H12	31194	-0.2671	29787	-0.308	38004	-0.0416	34119	-0.044
20085	183	NM_003948	8999	CDKL2	4.69091	0.01491	-0.25	2	H03	29061	-0.3204	27601	-0.2981	36323	-0.1128	36242	-0.0017
20087	95	NM_000706	552	AVPR1A	4.14803	0.02129	-0.25	1	H11	29279	-0.3252	31442	-0.1908	39246	0.00797	35718	-0.0153
20088	192	NM_005192	1033	CDKN3	3.3023	0.03997	-0.26	2	H12	26424	-0.4576	27497	-0.3035	37251	-0.0764	32166	-0.1738
20089	3477	NM_003403	7528	YY1	4.28212	0.01943	-0.26	37	B09	29433	-0.3612	28964	-0.2267	36497	-0.0402	34765	-0.0254
20093	17656	NM_033401	85445	CNTNAP4	3.11073	0.04677	-0.28	184	H04	26989	-0.5326	28506	-0.3291	36458	-0.1233	32170	-0.1872
20095	2235	NM_004134	3313	HSPA9B	3.03709	0.04976	-0.28	24	C03	17897	-1.0074	18706	-0.7913	25407	-0.5965	23513	-0.6454
20101	2884	NM_001208	690	BTF3L1	5.91575	0.00743	-0.3	31	A04	24139	-0.5658	21256	-0.6258	30987	-0.2476	28485	-0.3353
20102	4620	NM_002053	2633	GBP1	3.17475	0.04435	-0.31	49	A12	22097	-0.6975	25823	-0.4578	31233	-0.2662	28995	-0.2647
20110	1347	NM_018841	55970	GNG12	5.32998	0.0102	-0.39	15	A03	24437	-0.5489	24845	-0.3806	34467	-0.0855	34069	-0.0696
20112	96	NM_000707	553	AVPR1B	9.59179	0.00163	-0.41	1	H12	22186	-0.7254	22712	-0.66	32624	-0.2586	29300	-0.301
20115	4126	NM_002798	5694	PSMB6	3.19936	0.04346	-0.53	43	H10	14342	-1.334	16221	-1.126	26387	-0.5186	19837	-0.8808